



Green leaf volatile Triggered Defense Signalling and Cell Death Mediated by *Vitis* Metacaspase 5

Zur Erlangung des akademischen Grades eines
DOKTORS DER NATURWISSENSCHAFTEN

(Dr. rer. nat.)

von der KIT-Fakultät für Chemie und Biowissenschaften
des Karlsruher Institut für Technologie (KIT)

genehmigte

DISSERTATION

von

Xin ZHU

aus

Jiangxi, China

Dekan: Prof. Dr. Reinhard Fischer

Referent: Prof. Dr. Peter Nick

Korreferent: Prof. Dr. Jörg Kämper

Tag der mündlichen Prüfung: 21.10.2020

Die vorliegende Dissertation wurde am Botanischen Institut des Karlsruher Instituts für Technologie (KIT), Botanisches Institut, Lehrstuhl 1 für Molekulare Zellbiologie, von August 2017 bis Oktober 2020 angefertigt.

Erklärung

Hiermit erkläre ich, dass ich die vorliegende Dissertation, abgesehen von der Benutzung der angegebenen Hilfsmittel, selbständig verfasst habe.

Alle Stellen, die gemäß Wortlaut oder Inhalt aus anderen Arbeiten entnommen sind, wurden durch Angabe der Quelle als Entlehnungen kenntlich gemacht.

Diese Dissertation liegt in gleicher oder ähnlicher Form keiner anderen Prüfungsbehörde vor.

Zudem erkläre ich, dass ich mich beim Anfertigen dieser Arbeit an die Regeln zur Sicherung guter wissenschaftlicher Praxis des KIT gehalten habe, einschließlich der Abgabe und Archivierung der Primärdaten, und dass die elektronische Version mit der schriftlichen übereinstimmt.

Karlsruhe, im September 2020

Xin ZHU

Acknowledgement

First and foremost, I would like to express my deepest gratitude to my awesome supervisor Prof. Dr. Peter Nick for providing me with full support throughout my research and thesis writing. I am deeply thankful to him for his wonderful personality, his patience and motivation for scientific research and the spirit of seeking the truth. He is the wise man who guides me how to think in the interdisciplinary perspectives and illuminates my path of science.

I would like to thank my group leader Dr. Michael Riemann for his continuous help and suggestions during my work and for critical appreciation of my thesis.

My sincere thanks also go to all colleagues and Azubis at Botanical Institute 1 for such a friendly and helpful working environment. I appreciate the excellent work of our lab technician Sabine Purper, Ernst Heene, and, Dr. Gabriele Jürges and Dr. Jan Maisch for resolving any technical troubles while I needed help. Many thanks to Dr. Wadhvani Parversh for providing me the peptide used in the thesis.

I appreciate all the help from all my friends, who accompany and help me in their thoughtful way during this four years no matter where they are. As the old saying said, among any three people meeting, I will find something to learn for sure. We make progress and pursue our dreams together. My sincere thanks to Dr. Juning Ma, Dr. Hao Wang, Dr. Gangliang Tang, Dr. Ruipu Wang, Dr. Pinying Guan, Dr. Kunxi Zhang, Dr. Huapeng Sun, Xinshuang Ge, Wenjing Shi and Xuan Liu, Daniela Rios, Karwan sofi, Dr. Sascha Wetters, Pallavi, Islam Khattab and Christian Metzger from

Acknowledgement

whom I always learned many things. I specially want to thank my friend Shan Xin for her unselfish support and relieving my pressure.

Also I would like to thank the authors who write the novels and create the characters I like, giving me some good distraction and entertainment during my PhD studying.

Last but not the least, the special and important appreciation to my family, especially my parents, my husband Can Cao and my dog for their unconditional love and supports in my life. I appreciate their all the contribution and encouragement to support me to pursue dream and life meaning.

This work was supported by the China Scholarship Council (CSC).

Karlsruhe, August 2020

Xin ZHU

Table of Contents

Acknowledgement	I
Abbreviations	VI
Zusammenfassung	VII
Abstract	IX
1 Introduction.....	1
1.1 Green Leaf Volatiles and Hydroperoxy lyase	1
1.1.1 GLVs biosynthesis and hydroperoxy lyase.....	1
1.1.2 Green leaf volatiles in plant defense	2
1.2 Plant immune system	5
1.2.1 PAMP-triggered immunity (PTI) and effector-triggered immunity (ETI)	5
1.2.2. Salicylic acid and jasmonate in plant immunity	7
1.3 Programmed cell death.....	8
1.3.1 Hypersensitive response (HR)	9
1.3.2 Executioners of hypersensitive response	10
1.4 Metacaspase	11
1.4.1 Structure of metacaspases	12
1.4.2 Activation mechanism of metacaspases.....	13
1.4.3 Roles of metacaspases in defense PCD	15
1.5 Cell penetrating peptides.....	16
1.5.1 Chemical engineering	16
1.5.2 Cell penetrating peptides (CPPs)	17
1.6 Scope of study	21
2 Materials and Methods.....	23

Contents

2.1 Cell culture	23
2.2 Construction of VrMC5 overexpressor variants	23
2.3 Stable transgenic tobacco BY-2 cell establishment.....	24
2.4 Stress and inhibitor treatments	26
2.5 Microscopy of VrMC5 localization and response to stresses.....	27
2.6 Determination of cell mortality.....	29
2.7 Western blot	29
2.8 EPC-affinity chromatography	31
2.9 Recombinant expression of VrMC5 and its variants.....	31
2.10 Enzymatic activity assay.....	33
2.11 RNA extraction and cDNA synthesis	34
2.12 Real-time PCR analysis	34
3 Results	36
3.1 Chapter 1: The role of VrMC5 in programmed cell death.....	36
3.1.1 Subcellular localization of VrMC5.....	36
3.1.2 The response of cytoskeleton and VrMC5 in Z-3-hexenal signalling	40
3.1.3 Expression and subcellular localization of VrMC5 variants	46
3.1.4 VrMC5 variants are deficient in the responses to Z-3-hexenal.....	49
3.1.5 SA-related signalling response is induced by Z-3-hexenal in VrMC5 but not in its variants	53
3.1.6 JA mitigates Z-3-hexenal-triggered cell death and SA-related response	56
3.1.7 Ca ²⁺ is required for VrMC5 self-processing and enzymatic activity	59
3.1.8 C139 and R226 are essential for VrMC5 self-processing and enzymatic activity	62
3.2 Chapter 2: Cell permeating peptide inhibits VrMC5 activity.....	65
3.2.1 Cellular uptake of LMTP-peptide in BY-2 cell	65
3.2.2 Subcellular localization of LMTP-peptide.....	66

Contents

3.2.3 LMTP-peptide is taken up into cell through endocytosis	69
3.2.4 Uptake of LMTP-peptide depends on microtubules, not actin	70
3.2.5 LMTP-peptide could relieve actin depolymerization to Z-3-hexenal	72
3.2.6 LMTP-peptide could decrease cell death induced by Z-3-hexenal and harpin	73
3.2.7 LMTP-peptide protects VrMC5 from autoproteolysis in the presence of Ca ²⁺	75
3.3 Summary of results	77
4 Discussion	79
4.1 Biological characterization of VrMC5	80
4.1.1 The heterologous expressed VrMC5 co-localizes with microtubules	80
4.1.2 Interaction between VrMC5 with cytoskeleton	81
4.2 VrMC5 acts as a positive regulator in Z-3-hexenal triggered HR cell death	82
4.3 Self-processing is essential for VrMC5 activation during cell death	85
4.4 Cell penetrating peptide manipulates VrMC5 activity	86
4.4.1 Cellular uptake mechanism of metacaspase inhibitory peptide	87
4.4.2 LMTP-peptide efficiently alleviates cellular stress responses	89
4.5 Conclusion	90
4.6 Outlook	92
4.6.1 Hunting the specific downstream events of Z-3-hexenal signal pathway	92
4.6.2 Functional features of VrMC5 in PCD	93
5 Appendix	95
Reference	101

Abbreviations

BY-2: Tobacco *Nicotiana tabacum* L. cv. bright yellow 2

CBB: coomassie Brilliant Blue

EGTA: ethylene-bis(oxyethylenitrilo)tetraacetic acid

EPC: Ethy-N-phenylcarbamate

ETI: effector-triggered immunity

GFP: green fluorescent protein

GLVs: green leaf volatiles

GRRase: Boc-GRR-AMC-hydrolyzing activity

HR: hypersensitive response

ICS: isochorismate synthase

JA: jasmonic acid

LMTP: lipid-membrane-translocating peptide

MC: metacaspase

MT: microtubule

NLS: nuclear localisation signal

PAL: phenylalanine ammonia lyase

PCD: programmed cell death

PR1: pathogenesis related 1

PTI: PAMP-triggered immunity

qRT-PCR: quantitative real-time PCR

ROS: Reactive oxygen species

SA: salicylic acid

VrMC5: *Vitis rupestris* metacaspase 5

Z-3-hexenal: *cis*-3-hexenal

Zusammenfassung

Es wird weitestgehend akzeptiert, dass Green Leaf Volatiles (GLVs) eine Schlüsselrolle im Priming Prozess und in der pflanzlichen Verteidigung gegen Schädlinge und Pathogene spielen. Ein Vertreter der GLVs, das *cis*-3-hexenal (*Z*-3-hexenal) aktiviert äußerst effizient den Abbau der Aktinfilamente gefolgt von Zelltod. Dies wurde sowohl in Weinblättern als auch in Tabak (BY-2) und *Vitis* Zellen, die einen fluoreszenten Aktin-Marker produzieren, beobachtet. Daher gehen wir davon aus, dass *Z*-3-hexenal einen spezifischen Signalweg aktiviert, der schlussendlich zu programmiertem Zelltod (engl. PCD) führt.

PCD ist ein unentbehrlicher Prozess, der durch stringente intrazelluläre Programme reguliert wird. Die Kontrolle von PCD ist ein ausschlaggebend für die Fitness der Pflanzen, sollten diese extrinsischem Stress ausgesetzt sein. Hierfür sind die Metacaspasen (MCs), eine Familie von cystein-abhängigen Proteasen mit Caspase-ähnlicher Aktivität potenzielle Regulatoren. Sie sind in die, bei Verteidigungsreaktionen auftretende Hypersensitive Response (HR) involviert.

In dieser Arbeit charakterisierten wir die *Vitis rupestris* Metacaspase 5 (VrMC5). Sie war nicht nur in Cytoplasma und Nukleus zu finden, sondern co lokalisierte sich spezifisch mit Mikrotubuli. Heterologe Überexpression von VrMC5 in der BY2 Tabak Zelllinie offenbarte eine dramatische Erhöhung des durch *Z*-3-hexenal ausgelösten, Verteidigung assoziierten Zelltods. VrMC5 wird der Metacaspase Typ II Familie zugeordnet, welche zwingend für ihre Aktivierung eine intermolekulare Spaltung benötigen. Hier konnten wir einige mögliche Stellen zur Auto-Lysis

identifizieren und entsprechende funktionelle Mutationen generieren, um die Rolle von VrMC5 in den von *Z*-3-hexenal aktivierten Signalwegen zu studieren. Durch die Beobachtung der Aktivität der Rekombinanten von VrMC5 und deren Mutationsvarianten konnten Abhängigkeiten von Kalzium, der katalytischen Cys-139 und Spaltungsproteinstelle Arg-226 festgestellt werden. Des Weiteren konnte die äußere Anwendung von Jasmonsäure (JA) den *Z*-3-hexenal induzierten Zelltod in den VrMC5 Überexpressions-Linien reduzieren, indem die Salicylsäure-Synthese und der dazugehörige Signalweg unterdrückt wurde. Zusammen implizieren die Ergebnisse, dass VrMC5 HR-assoziierten Zelltod, ausgelöst durch *Z*-3-hexenal positiv reguliert und in den SA-Crosstalk involviert ist.

Abstract

It is widely accepted that green leaf volatiles (GLVs) play a key role in plant defence responses to pathogens or herbivores and plants priming. One type of GLVs, *cis*-3-hexenal (*Z*-3-hexenal) is highly efficient in activating disassembly of actin followed by cell death. This has been observed both in tobacco BY-2 cells and *Vitis* cell expressing a fluorescent actin marker, as well as in real grape leaves. Therefore, we assumed that *Z*-3-hexenal triggers a specific signalling pathway leading to programmed cell death (PCD).

PCD is an indispensable process that is strictly controlled by an intracellular program. The regulation of PCD is crucial for the fitness of plants when encountering extrinsic stress. Here, potential regulators of this signalling, are metacaspases (MC), a family of cysteine-dependent proteases with caspase-like activity, which are involved in defence-related hypersensitive response (HR).

In this study, we characterized *Vitis rupestris* Metacaspase 5 (VrMC5). It not only locates in the cytoplasm and nucleus but specifically co-localizes with microtubules. Heterologous overexpression of *VrMC5* in the BY-2 tobacco cell line exhibits a dramatic increase in defence-triggered cell death induced by *Z*-3-hexenal. VrMC5 belongs to the metacaspase type II family, which requires intermolecular cleavage of itself for activation. Here we predict a few autolysis sites in VrMC5 and generate functional mutations to study the role of VrMC5 in the *Z*-3-hexenal triggered signalling pathway. Meanwhile, the activity of the recombinants of VrMC5 and its variant-proteins are analyzed *in vitro*, revealing calcium-dependent protease activity of VrMC5. The catalytic site Cys-139, as well as cleavage site Arg-226 are essential

Abstract

for VrMC5 autolysis and activity. Furthermore, exogenous jasmonic acid (JA) application could inhibit Z-3-hexenal triggered-cell death in *VrMC5* overexpressor by suppressing salicylic acid (SA) synthesis and responsive pathway. Taken together, these results indicate that VrMC5 positively regulates HR related cell death induced by Z-3-hexenal and is involved in SA crosstalk.

1 Introduction

1.1 Green Leaf Volatiles and Hydroperoxy lyase

Plants cannot move to avoid being attacked by pathogens and herbivores, thus they evolve to protect themselves with molecular weapons against enemies. Green leaf volatiles (GLVs) are metabolites which are commonly emitted by almost every green plant. GLVs consist of a family of C6 and C9 compounds, including alcohols, aldehydes and esters (Matsui, 2006). Unlike other volatiles, GLVs are released immediately upon various stresses challenge and function as an instant and priming signal for adaption in plant defense (Scala *et al.*, 2013a).

1.1.1 GLVs biosynthesis and hydroperoxy lyase

Green leaf volatiles are synthesized through the oxylipin pathway derived from C18 fatty acids (Matsui, 2006). Two polyunsaturated fatty acids (PUFAs) are formed from membrane lipids catalyzed by lipases, that is linoleic acid and α -linolenic acid, serve as the precursor of saturated and unsaturated (most abundant) C6 volatiles respectively. 13-lipoxygenases (LOXs) generates 13-hydroperoxides (13-HPOT) by introducing oxygen to α -linolenic acid (Matsui *et al.*, 2000). 13-hydroperoxides are the same substrate for the formation of GLVs and jasmonates converted by hydroperoxide lyase (HPL) and allene oxide synthase (AOS), respectively (Kombrink, 2012).

In the branch to synthesize GLVs, 13-hydroperoxides are cleaved into a C9 compound 9Z-raumatin and a C6 compound varies depending on its precursor α -linolenic acid and linoleic acid, leading to the formation is either unsaturated Z-3-hexenal or saturated n-hexanal (Scala *et al.*, 2013a). Z-3-hexenal is relatively

unstable and is converted to *E*-2-hexenal spontaneously or through the activity of (3*Z*):(2*E*)-enal isomerase (Allmann & Baldwin, 2010; Kunishima *et al.*, 2016). These C6 aldehydes can be reduced and further transformed to their corresponding alcohols and esters through the activity of alcohol dehydrogenase (ADH) and alcohol acyltransferase (AAT), or *E*-2-hexenal can be conjugated to glutathione (GSH) (Matsui, 2006; D'Auria *et al.*, 2007; ul Hassan *et al.*, 2015). Describing above is the widely accepted GLVs synthesis pathway that HPL utilizes the hydroperoxides as the substrates. In fact, it has been reported when *Arabidopsis* leaf tissues are damaged by mechanical wounding or herbivore attack, GLVs can also be formed without cleavage from membrane lipids via a lipase-independent pathway. In that case, the enzymes in the oxylipin pathway show a wider range of catalytic activity toward substrates, HPL is able to use lipid HPOs as substrates to form volatile C6 aldehydes to make quick response to stress (Nakashima *et al.*, 2013) (**Figure 1.1**).

1.1.2 Green leaf volatiles in plant defense

So far, GLVs have been reported as a key role in plant direct defense. In the early studies show that GLVs have antibacterial activity against both Gram-positive and Gram-negative bacteria (Nakamura & Hatanaka, 2002). *E*-2-hexenal is a C6 aldehyde with the highest antimicrobial activity among C6 GLVs, which is widely reported. For instance, *E*-2-hexenal emitted by *Arabidopsis* in response to herbivore damage is identified to increase resistance against a fungal pathogen *Botrytis cinerea* (Shiojiri *et al.*, 2006). Upon *Pseudomonas* infection, Lima bean leaves release sufficient amount of *E*-2-hexenal and *Z*-3-hexenol to suppress bacterial growth *in vitro* (Croft *et al.*, 1993). Moreover, the *n*-hexenal and *E*-2-hexenal extracted from wound cotton leaves inhibited completely the growth of the fungus *Aspergillus flavus* (Zeringue & McCormick, 1989).

Introduction

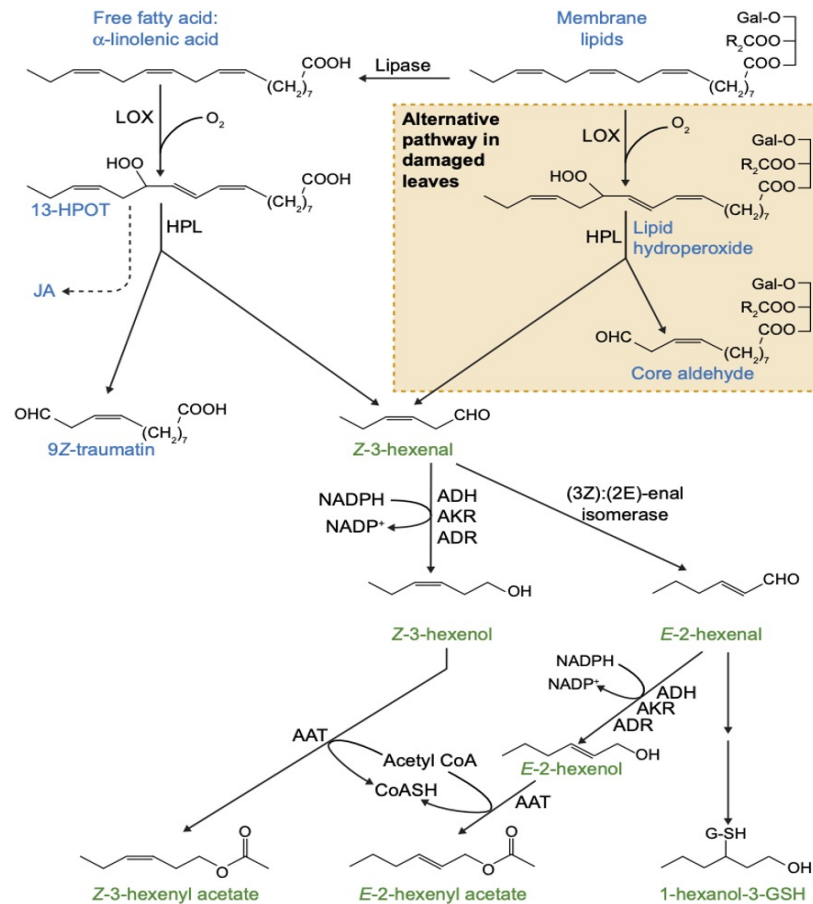


Figure 1.1 Overview of biosynthetic pathways leading to green leaf volatiles (GLVs). This pathway mainly shows the formation of the most abundant unsaturated C6 volatiles. GLVs and their derivatives are labeled in green. LOX, lipoxygenase; HPL, hydroperoxide lyase; ADH, alcohol dehydrogenase; AKR, aldo-keto reductase; ADR, aldehyde reductase; AAT, alcohol acetyl Transferase (Ameye *et al.*, 2018).

In order to respond to herbivores, plants produce GLVs to activate its own defense signalling pathway or attract the natural enemies of herbivores. The biosynthesis of GLVs is initiated at the site attacked by herbivores or mechanical wounding, the emission of GLVs induces indirect defense by activating defense-related gene expression and attracting predators to locate their prey on herbivore-attacked plants

(Halitschke *et al.*, 2007). When maize plants are exposed to *Z*-3-hexenol, a strong defense is elicited and numerous genes involved in direct and indirect defense has been up-regulated this effect is even more active than common defense signals like methyl jasmonate, methyl salicylate, and ethylene(Heil *et al.*, 2013). In addition, GLVs are effective in reducing tobacco aphid (*Myzus nicotianae*) population and act antagonistically on the attraction of insects to pheromones resulting in a repellent effect on insects searching for mating partners (Hildebrand *et al.*, 1993; Reddy & Guerrero, 2004).

GLVs participate in plant priming, serve as aerial messengers from a damaged or infected plant to warn neighbouring plants to defend themselves against upcoming challenges. Maize plants exposed with GLVs (*Z*-3-hexenal, *Z*-3-hexenol, and *Z*-3-hexenyl acetate) collected from maize plants infested by caterpillars, subsequently produced more JA than the control plants. While with the same volatiles from only mechanical wounding plants failed to induce more JA levels, indicating that maize plants recognize signals coming from plants in biotic stress and initiate signal transduction for priming itself (Engelberth *et al.*, 2004). A series of GLVs including *Z*-3-hexenol, *Z*-3-hexenyl acetate, *E*-2-hexenal from clipped sagebrush prime primed the tobacco trypsin proteinase inhibitor induction resulting high resistant against herbivory (Karban *et al.*, 2000; Kessler *et al.*, 2006).

GLVs have been shown direct influence on phytohormonal signalling pathway. Exogenous *E*-2-hexenal increases susceptibility of *Arabidopsis* to *Pseudomonas syringae* pv. *tomato* by activating the JA-dependent signalling pathway mediated by ORA59, a key transcription factor in the JA pathway (Scala *et al.*, 2013b). Volatile hormone ethylene is found that promotes the emission of volatiles induced by *E*-2-

hexenol and genes involved in ethylene biosynthesis expression are induced by GLVs in lima bean (Arimura *et al.*, 2001; Ruther & Kleier, 2005).

1.2 Plant immune system

Plants as sessile organisms have evolved multiple layers of defense strategies, called plant immunity, to prevent various invasion. The first layer is mechanical barriers, plant's structures such as waxy surface, thorns or spines, and thickened or lignified cell wall compose of the intact and impenetrable barrier (War *et al.*, 2014). Once pathogens overcome the first layer, they will face the second layer, plant innate immune system including at least two major layers, PAMP-triggered immunity (PTI) and effector-triggered immunity (ETI).

1.2.1 PAMP-triggered immunity (PTI) and effector-triggered immunity (ETI)

Plant pattern-recognition receptors (PRRs) on membrane surface recognize microbes via conserved pathogen- or microbial-associated molecular patterns (PAMPs and MAMPs), such as flagellin, leading to PAMP-triggered immunity (PTI) known as plant basal immunity (Ausubel, 2005; Zipfel & Felix, 2005). Meanwhile, pathogens secrete virulence molecules (effectors) and deliver in the extracellular matrix or into the plant cell in order to adapt plant basal immunity, effectors effectively interfere with PTI resulting in effector-triggered susceptibility (ETS) of host plants (Abramovitch *et al.*, 2006; Cook *et al.*, 2015).

Plants also have co-evolved strategy to recognize introduced effectors by resistance (R) proteins, such as one of the NB-LRR (nucleotide-binding site-leucine-rich repeat) receptor (NLR), and deploy the second level immunity referred to as effector-triggered immunity (ETI) (Dodds & Rathjen, 2010). ETI accelerates and amplifies

PTI response to enhance diseases resistance and generally accompanied with programmed cell death, hypersensitive response (HR) at the infection site to prevent pathogens further colonization (Greenberg & Yao, 2004; Truman *et al.*, 2006). To avoid ETI, the pathogens either eliminate or diversify the recognized effector or acquire additional effectors that inhibit ETI under natural selection. Natural selection drives new NLR alleles that respond to new effectors so that ETI could be rapidly activated again. The well-known zig-zag model provides the interaction between pathogens and plant immune system (Jones & Dangl, 2006).

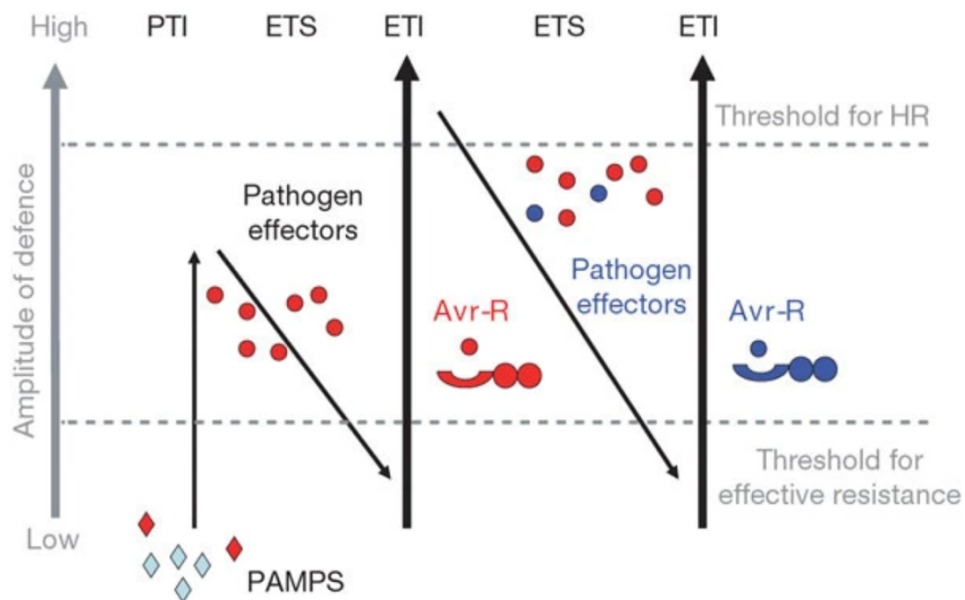


Figure 1.2 A zigzag model illustrates the quantitative output of the plant immune system. PAMPs, pathogen-associated molecular patterns; PTI, PAMP-triggered immunity; ETS, effector-triggered susceptibility; ETI, effector-triggered immunity, R, NLR-type resistance (R) proteins (Jones & Dangl, 2006).

1.2.2. Salicylic acid and jasmonate in plant immunity

Downstream of pathogens perception, diverse phytohormones are extensively upregulated and deployed to modulate plant immune signalling network (De Vos *et al.*, 2005; Bari & Jones, 2009; Dodds & Rathjen, 2010). Salicylic acid (SA) and jasmonic acid (JA) with its derivatives (jasmonates) are the major hormones that regulate defense responses (Vlot *et al.*, 2009; Robert-Seilaniantz *et al.*, 2011). SA typically plays a role in defense against biotrophic or hemibiotrophic pathogens while JA signalling commonly is involved in basal immunity against necrotrophs (Glazebrook, 2005). Many studies support a conception over the years that antagonism between SA and JA pathways in plant immune signalling network (Koornneef & Pieterse, 2008; Diezel *et al.*, 2009; Van der Does *et al.*, 2013), however a study using quadruple mutant defected in SA, JA and ET pathway showed the synergistic interaction among SA, JA, and ET signalling pathways, which contribute positively to flg22-triggered immunity response (Tsuda *et al.*, 2009).

Following pathogen perception, SA is produced from primary metabolite chorismate via two pathway: the Isochorismate synthase (ICS) pathway and the Phenylalanine Ammonia Lyase (PAL) pathway (Garcion & Métraux, 2007). Once SA is synthesized, the downstream signalling is tightly controlled by regulatory protein NON-EXPRESSION OF PR GENES1 (NPR1) (Moore *et al.*, 2011). Redox change occurred in NPR1 results in its translocation to the nucleus and activates the expression of SA-responsive genes, like *PR* (*Pathogenesis-Related*), leading to cell death or cell survival depending on SA level (Dong, 2004; Tada *et al.*, 2008; Yan & Dong, 2014).

JA biosynthesis starts with the release of α -linolenic acid (α -LA) via oxylipin pathway catalyzed by AOS in the plastid. JA can be readily converted to methyl

jasmonate (MeJA) or conjugated with isoleucine to generate the bioactive form JA-Ile (Seo *et al.*, 2001; Fonseca *et al.*, 2009). Although JA is prominent in defense against necrotrophs and herbivores, some virulence factors produced by biotrophic or hemibiotrophic pathogens could suppress host defense by utilizing the antagonism between JA and SA pathways and activate JA signalling (Gimenez-Ibanez *et al.*, 2014; Fyans *et al.*, 2015). For instance, the virulence factor coronatine (COR) produced by *P. syringae pv. tomato* strain DC3000 (*PtoDC3000*), showing much more effective in inducing JAZ (Jasmonate ZIM domain, transcriptional repressors of JA signalling) degradation and activating JA signalling (Katsir *et al.*, 2008).

1.3 Programmed cell death

Programmed cell death (PCD) is a fundamental process of living organisms. This process commonly occurs during growth and development, as well as in the response to various environmental stresses and pathogens infection (Jones, 2001). PCD is a genetically programmed cell suicide process occurring in a sequence of organized destructive events (Lockshin & Zakeri, 2004). In animal cells, apoptosis, autophagy and necroptosis are main forms of PCD (Lockshin & Zakeri, 2004; Degtarev *et al.*, 2005). Apoptosis is the most well-understanding PCD in mammals, characterized by some typical morphological changes such as membrane blebbing, cell shrinkage, chromatin condensation and DNA fragmentation, and eventually the breakup of the cell into apoptotic bodies that will be subsequently hydrolyzed by lysosomal enzymes (Adrain & Martin, 2001). Various types of PCD in plants are classified into two groups of PCD in plants: autolytic and non-autolytic PCD, differ in that rapid cytoplasm clearance after tonoplast rupture occurs in former while not accompanies with the latter (van Doorn, 2011).

1.3.1 Hypersensitive response (HR)

Hypersensitive response (HR) usually occurs at the site of pathogens infection following with rapid cell death and prevents pathogens further spread (Levine *et al.*, 1996; Mittler *et al.*, 1997). It is one example of non-autolytic PCD, instead of rapid clearance of cytoplasm, it undergoes swelling of organelles and without an increase in vacuolar volume (van Doorn, 2011). Morphological hallmarks of HR include reorganization of cytoskeleton, cytoplasmic shrinkage, chromatin condensation, mitochondrial swelling, and vacuolar collapse as well as chloroplast disruption during the final stages (Mur *et al.*, 2008; Higaki *et al.*, 2011) (**Figure 1.3 A**).

In the initiation of plant ETI processing, the “(R)gene-for-(Avr)gene” concept was proposed that described the avirulence (Avr) pathogen effector was recognized by Resistant (R) protein of host plant leading to HR (Flor, 1971). Ca²⁺ influx is one of the earliest response triggered by pathogenic signal (Seybold *et al.*, 2014). Following signal events such as reactive oxygen species (ROS), reactive nitrogen species (RNS) and the downstream defense hormones SA and JA are produced in chloroplast and mitochondria and induce defense-related genes expression (Torres *et al.*, 2005; Coll *et al.*, 2011)(**Figure 1.3 A**).

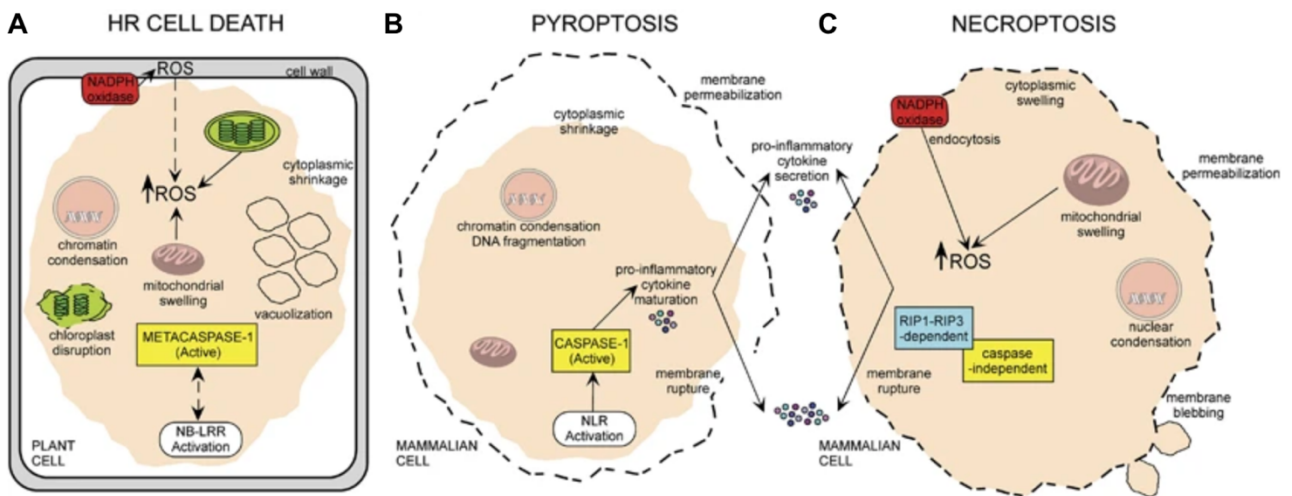


Figure 1.3 Characteristic features comparison of different types of PCD between plants and mammals. A, HR cell death in plants. B, Pyroptosis in mammalian cells. C, Necroptosis in mammalian cells (Coll *et al.*, 2011).

1.3.2 Executioners of hypersensitive response

During the apoptosis in mammals, cellular destruction is driven by a family of cysteine-dependent proteases known as caspases. They could activate other caspases and activate degradative enzymes or proteins to amplify the apoptotic signalling resulting in PCD morphological changes (Cohen, 1997). For instance, pyroptosis is caspase-1-dependent cell death in macrophages (Brennan & Cookson, 2000) (**Figure 1.3 B**). However, plants do not possess any caspase, while some proteases with caspase-like activities have been identified to be involved in the execution of PCD, including vacuolar processing enzyme (VPE), phytaspase and proteasome subunit $\beta 1$ (PBA1).

VPE localizes in the vacuole and it has been confirmed has the ability to cleave the caspase-1 substrate YVAD. The YVADase activity of VPE has been clearly

associated with the regulation of PCD during stresses and development via vacuolar collapse (Hatsugai *et al.*, 2004). VPEs function in activating other hydrolases and inducing further disruption of tonoplast and degradation of the cellular components (Hatsugai *et al.*, 2006). During the ER stress-induced PCD in *Arabidopsis* triggered by mutualistic fungi *Piriformospora indica*, VPE positively regulates this processing by causing vacuole collapse and a reduced vacuolar membrane collapse is displayed in VPE-null mutant line (Qiang *et al.*, 2012). On the other hand, phytaspase is a serine protease of the subtilisin-like family which was first isolated from tobacco. Phytaspase has been reported it is synthesized as a zymogen and generate the mature enzyme after autocatalytical processing. Mature phytaspase localizes in the apoplast but it is reimported into the cell when PCD is occurring (Chichkova *et al.*, 2010). Forward genetic analysis shows that phytaspase with caspase-6-like activity is essential for PCD-related responses to tobacco mosaic virus (TMV) and abiotic stresses (Chichkova *et al.*, 2010). Proteasome subunit β 1 (PBA1) is identified to be a positive regulator of ROS generation during HR and specifically required for tonoplast fusion with the plasma membrane at the early stage of the process (Lequeu *et al.*, 2005; Hatsugai *et al.*, 2009).

1.4 Metacaspase

Another type of caspase-like protease with similar caspase catalytic domains called metacaspases (MCs) have been identified in plants, fungi, protozoa and cyanobacteria (Uren, 2000). In the past several years, metacaspases have been reported as regulators of plants PCD.

1.4.1 Structure of metacaspases

Metacaspases are distantly related to animal caspases while they have a few common structural features. Caspases are synthesized as inactive zymogens form and undergo proteolytic cleavage to release two subunits around ~20 kD and ~10 kD (p20 and p10), after which become active mature enzymes. According to sequence similarities and structural properties, metacaspases are grouped into types I, II, and III, only type I and type II metacaspases exist in higher plants (**Figure 1.4A**).

Type I metacaspases are widespread in various organisms including plants, protozoan parasites, fungi, unicellular photosynthetic planktons and many species of cyanobacteria (Jiang *et al.*, 2010; Tsiatsiani *et al.*, 2011). In the higher plants, type I metacaspases have a N-terminal extension of 60-133 amino acids. This pro-domain usually contains a zinc-finger motif as well as a proline-rich repeat motif, while the pro-domain is much more variable in non-plant species, sometimes lack zinc-finger motif (Klemencic & Funk, 2019). The zinc-finger motifs of type I metacaspase AtMC1 and AtMC2 in *Arabidopsis* were found to be homologous to the negative cell death regulator LSD1 (Coll *et al.*, 2010).

In the contrast, a linker region ranging from 90 ~150 amino acids connects the catalytic p20 and the regulatory p10 domain in type II metacaspases. They do not contain any N-terminal extensions but a ~50 amino acids conserved central core region exists within linker region. Most of metacaspases contain the major catalytic cysteine near the C-terminal of the p20 subunit (Cys1-1 for type I metacaspases and Cys2-1 for type II metacaspases), and another conserved cysteine residue near the N-terminus (Cys1-2 for type I metacaspases and Cys2-2 for type II metacaspases) (Lam & Zhang, 2012). (**Figure 1.4B**).

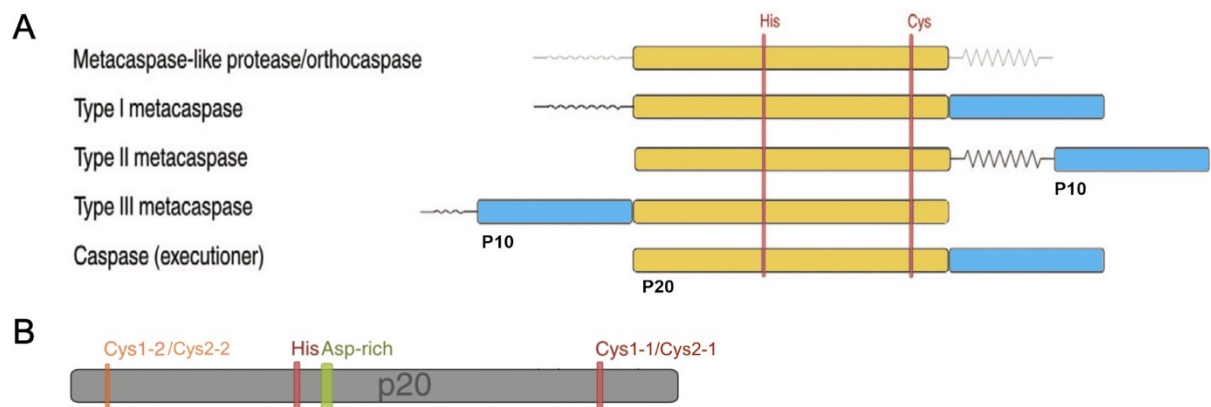


Figure 1.4 Structural comparison between caspase and metacaspase. **A**, The p20 subunits and p10 subunits of these proteases are represented in yellow and blue. The conserved His and Cys in the catalytic p20 region is indicated. Metacaspase-like proteases/orthocaspases contain an N-terminal linker or a C-terminal extension, but they lack p10 region. Type I metacaspases contain an N-terminal domain and without linker between the p20 and p10 domains. Type II metacaspases generally contain a long linker region between the p20 and p10 domains. In type III metacaspases, the p10 domain is located N-terminally to the p20 domain and shorter linker in front of the p10 domain. **B**, Most of metacaspases contain the catalytic His–Cys dyad in red and a conserved Cys residue in orange at the N-terminus of the p20 domain and the conserved repeat of Asp residues is in green (Klemencic & Funk, 2019).

1.4.2 Activation mechanism of metacaspases

Not like caspases, which cleave target proteins only after aspartate at the P1 position, metacaspases prefer to target substrates either lysine or arginine residue at the P1 position (Vercammen *et al.*, 2004; Watanabe & Lam, 2005). Both type metacaspases undergo proteolytic processing during activation. In type I pathway, experiments *in vitro* performed with recombinant zymogens indicate the N-terminal domain of type I and type III metacaspases is removed in the starting of activation, while this cleavage does not seem to be a prerequisite, it is required for their optimal activity

(**Figure 1.5**). The recombinant type I metacaspase TbMC2 from *Trypanosoma brucei*, pro-domain is cleaved after lysines 55 and 268 (Moss *et al.*, 2007). Although unprocessed TbMC2 can cleave synthetic substrates, only processed TbMC2 have activity towards large substrates such as asocasein (Gilio *et al.*, 2017).

Similar to type I, most of type II metacaspases are calcium-dependent and are capable of undergoing autocatalytic processing during activation. The presence of calcium facilitates the cleavage within the long linker region in order to form the proper dimer conformation and activate proteases. For example, upon calcium stimulation, AtMC4 zymogen can be rapidly cleaved into putative large p20 and small p10 fragments during activation (Watanabe & Lam, 2011b; Machado *et al.*, 2013), while the AtMC9, with a very short linker comprising essentially only the core region, exhibits the calcium independency for activation and so can rapidly convert to its active form *in vitro* (Vercammen *et al.*, 2004). In the Ca²⁺-dependent metacaspases, there are four conserved aspartic residues within the p20 domain and these Asp coordinate one Ca²⁺ binding site with high affinity (Machado *et al.*, 2013), and the other one in low-affinity Ca²⁺ binding site is assumed formed by two negatively charged regions, one each within the p20 and p10 domains (McLuskey *et al.*, 2012)(**Figure 1.5**).

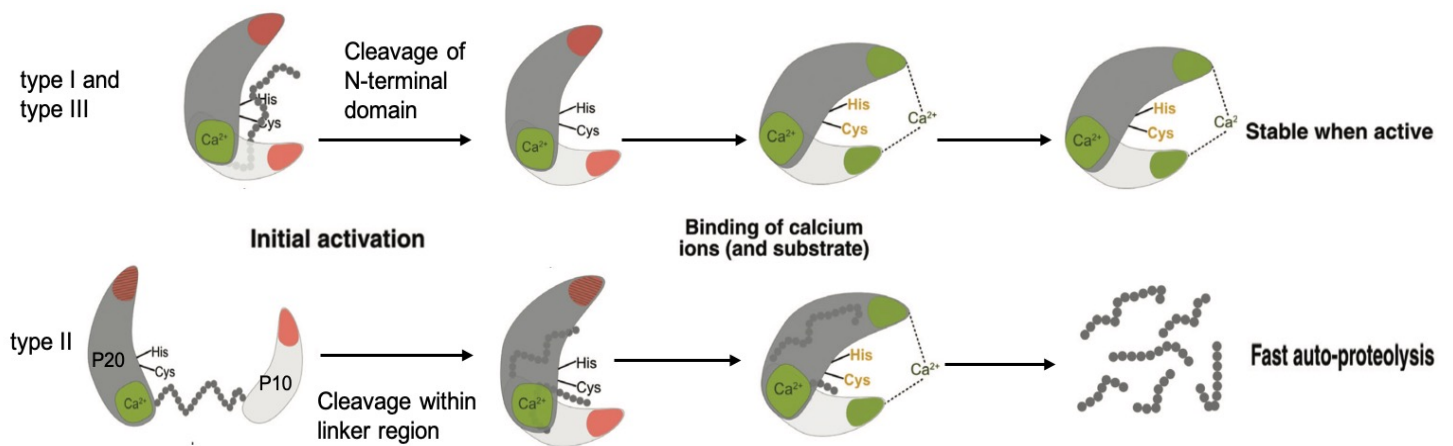


Figure 1.5 Proposed activation mechanism of metacaspases. Catalytic p20 domain (dark grey), which contains the two catalytic residues, a cysteine and a histidine, and a regulatory p10 domain (light grey) of metacaspases. The N-terminal pro-domain of type I and type III metacaspases indicated by the chain of grey dots. *In vitro*, this pro-domain is removed but this cleavage does not seem to be a prerequisite, it is required for their optimal activity. While the activity of type II metacaspases, strictly depends on cleavage within the linker region (also grey dots). In the Ca^{2+} -dependent activation, the green region labelled Ca^{2+} shows one calcium-binding site located in the p20 domain and most likely constantly occupied by one calcium ion. The second binding site is proposed to be formed by two loops, one each in the p20 and the p10 domains (shown as red regions) (Klemencic & Funk, 2019).

1.4.3 Roles of metacaspases in defense PCD

Numerous studies have demonstrated that metacaspases are multifunctional regulator during programmed cell death, stress response, protein aggregation and cell proliferation. In this thesis, we mainly focus on their function in defense related PCD.

In *Arabidopsis*, the nine metacaspases are well investigated. The first genetically dissected *Arabidopsis* metacaspase *in vivo* is AtMC8, a type II metacaspase acts as

a positive regulator in ROS induced cell death. It is specifically upregulated by UVC and oxidative stresses in *Arabidopsis* seedlings (He *et al.*, 2008). The other type II metacaspase in *Arabidopsis*, AtMC4, has been found that its-deficient mutant compromises in fumonisin B1 (FB1, a fungal toxin) induced-cell death whereas overexpressors exhibited heightened cell death responses. This work has further shown that the conversion of AtMC4 zymogen to active protease is accelerated during cell death activation by FB1 and during HR activation, contributing as a positive player to cell death (Watanabe & Lam, 2011a; Watanabe & Lam, 2011b). It has been previously reported among type I metacaspase that AtMC1 is a positive regulator of HR by interacting with negative regulator LSD1 with its N-terminal pro-domain, whereas AtMC2 was found to counteract the function of AtMC1 in an enigmatic mechanism, either interacts with LSD1 or AtMC1 (Coll *et al.*, 2010; Coll *et al.*, 2014).

Apart from defense related PCD, metacaspases also play the roles in developmental PCD. For instance, a Type II metacaspase in Norway spruce (*Picea abies*), McII-Pa, silencing of *mcII-Pa* suppresses terminal cell differentiation and programmed cell death in the early stage of embryogenesis (Bozhkov *et al.*, 2005). Moreover, *Arabidopsis AtMC9* was found to be upregulated in the developing xylem vessel and triggered cell death in the tracheary element (TE) during differentiation (Bollhoner *et al.*, 2013).

1.5 Cell penetrating peptides

1.5.1 Chemical engineering

Genetic engineering such as overexpression, gene knock-out, and knock-down, acts as a classical and widely used tool to control and manipulate protein function and

generates molecular diversity in living organisms. While this approach suffers from several flaws, like lack of temporal control, lethality, genetic redundancy or the modulation of target protein requires the correct folding and transports to the proper site. Another practical limitation is the transformation processing is much more complex in other plants than the models. Thus, chemical engineering is developed as an alternative method to unravel biological processes.

Chemical engineering is termed that the application of small bioactive molecules to alter protein function and thereby explore biological roles of target proteins in networks. Therefore, chemical engineering can be the tool to overcome genetic redundancy. Screened bioactive small molecules are used to identify novel signalling pathway and clarify redundant networks. The chemicals work in two way, either the compound inhibits multiple components in the network (Robert *et al.*, 2008; De Rybel *et al.*, 2009) or the compound activates a specific component of the network (Park *et al.*, 2009) (**Figure 1.6 C and D**) For example, a small molecule bikinin inhibits multiple GSK3-kinases (Glycogen synthase kinase 3) as an ATP competitor to activate BR (brassinosteroid) signalling downstream of the BR receptor. Inhibition of GSK3 is regarded as the only activation mode of BR signalling in *Arabidopsis*, that makes bikinin become a useful tool to reveal further BR regulatory mechanisms (De Rybel *et al.*, 2009).

1.5.2 Cell penetrating peptides (CPPs)

Cell membrane selective permeability plays an important function in molecular exchanges between the cytosol and the extracellular environment, which challenges the active uptake and transport of bioactive compounds to reach their targets within

the organism. Therefore, the specific carriers are essential for facilitating compounds pass through cell membrane, they are so called cell penetrating peptides (CPPs).

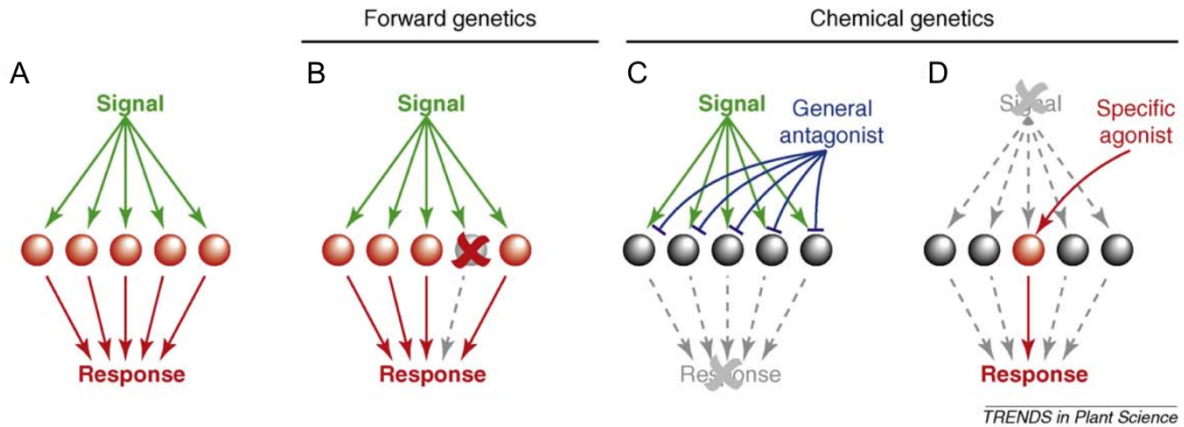


Figure 1.6 Chemical genetics overcomes genetic redundancy. **A**, General redundant signalling networks. **B**, Classical forward genetic screens to unravel redundant networks. **C**, General antagonists that inhibit multiple components can block redundant networks. **D**, Specific agonist activates only one of the components in the pathway to trigger the response in the absence of signal (Tóth & van der Hoorn, 2010).

Classification of CPPs

CPPs are short peptides composed 5–30 amino acids that are capable to deliver compounds including small molecule compounds, nucleic acids, proteins, viruses and drugs inside the cells (Heitz *et al.*, 2009). CPPs are classified into cationic, amphipathic and hydrophobic CPPs according to their physical and chemical properties (Pooga & Langel, 2015). Typical cationic CPPs are classified only peptides that contain a continuous stretch of basic amino acids. The polycationic regions are considered to be responsible for the cellular uptake of the peptide, and not contribute to a helical conformation of the peptide. For instance, the nuclear localization sequences (NLS) are a special group of short cationic CPPs containing rich lysine, arginine sequence (Ragin *et al.*, 2002). The amphipathic CPPs are most

abundant CPPs that possess both polar/ hydrophilic and nonpolar/ hydrophobic regions, are mainly participate the intracellular transport and accumulate preferentially in the nucleus (Milletti, 2012). Hydrophobic CPPs consist of either only nonpolar or very few cationic amino acids, and they are rarely used for cargo delivery but used to produce chemically modified hydrophobic, such as structurally stabilized α -helical peptide to increase resistance to proteolysis (Dietrich *et al.*, 2017).

The mechanism of cellular uptake

On the basis of the use of energy, single CPP enters into cell in two principal mechanisms: direct translocation without any energy consumption and endocytosis in an energy-dependent manner (**Figure 1.7**)(Kauffman *et al.*, 2015).

There are three proposed models explain the uptake of CPPs by direct penetration. The first one is called carpet-like model, When CPPs concentration reaches critical level, CPPs rotate themselves resulting in a phospholipids remodelling that elevates membrane fluidity and the formation of micelles and pores in it (Shai, 1999). In the second model “toroidal pore”, the CPP is orientated parallel to the bilayer at low levels. At high concentrations, the CPP is orientated perpendicularly to the bilayer and induce membrane to adopt a transient multi-pore state then translocate itself into inner monolayer (Zhao *et al.*, 2003). The last is barrel-stave pore model, in the model peptides first assemble in the surface of the outer membrane, then form a transient internal pore in the lipid of the membrane following recruitment of additional monomers (Shai, 1999).

CPPs internalized processing includes all major endocytosis routes: clathrin- or caveolin-dependent endocytosis and macropinocytosis.

Introduction

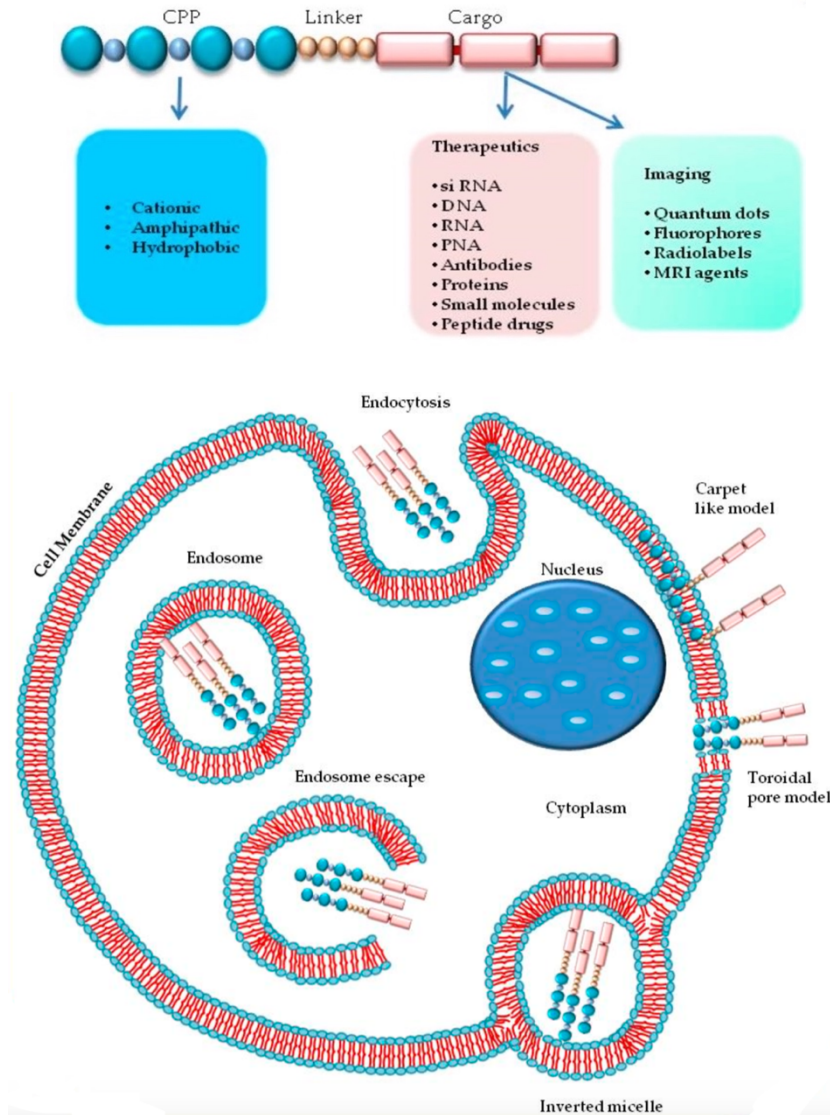


Figure 1.7 Schematic model for internalization of several cargo types delivered by CPPs. Mechanisms including endocytosis (clathrin mediated endocytosis, caveolae mediated endocytosis, clathrin/caveolae independent) and direct traslocation (carpet like model, toroidal pore model) (Borrelli *et al.*, 2018).

The major endocytic route for internalization CPPs is clathrin-mediated endocytosis. Clathrin-coated endocytic vesicles are transiently assembled on the inner surface of plasma membrane initiated by clathrin, the coated vesicles are separated from the membrane by the scission and release coat of clathrin proteins and fused with an

early endosome that can participate in intracellular membrane trafficking events (Kaksonen & Roux, 2018). In caveolin-dependent endocytosis, caveolae buds from invaginations of the plasma membrane binding with actin and trap CPP with its cargo, internalization of caveolae is facilitated by the actin depolymerization and GTPase activity (Le & Nabi, 2003). Macropinocytosis mediates a non-selective uptake of extracellular molecules and it is an actin-dependent process begins with formation and mature of macropinosomes, the large endocytic vacuoles (Lim & Gleeson, 2011).

1.6 Scope of study

As the metabolic weapon against various stresses, GLVs have been shown that are involved in physiological responses causing from complex signals network in plants. The previous work in our lab suggested that *Z*-3-hexenal is related to cytoskeleton depolymerization during cell death in suspension grapevine and tobacco cell. Meantime, a promising metacaspase VrMC5 isolated from *V. rupestris* has been identified as the potential target in defense-triggered cell death. Therefore, the general aim of this study is to characterize the role of VrMC5 in the response to *Z*-3-hexenal-induced PCD. To approach this objective, these specific questions are brought up:

1. What are the early signals mediating the *Z*-3-hexenal triggered responses?

The actin disassembly indicates a role for the NADPH oxidase Respiratory burst oxidase Homolog. This can be tested by specific inhibitors DPI, but also by measuring the level of reactive oxygen species (ROS) via fluorescent probes. Analysis of defense-related gene of the early stage will be also performed.

2. What is the role of VrMC5 in regulating plant PCD?

The tools to manipulate VrMC5 activity and test whether this allows manipulating defense-related PCD in response to different elicitors: gain of function by overexpression of VrMC5 in suspension BY-2 cell or loss of function by cell permeating peptides functionalised with a metacaspase-inhibiting functionality. Analysis of VrMC5 biological characterizations and cellular responses during various stress inductions will be performed.

3. The activation mechanism of VrMC5 during PCD activation.

Mutations in catalytic site and putative cleaved site will be generated and explore if these mutant overexpressors would have high PCD level in BY-2 under inducers. In addition, recombinant VrMC5 and its variants will be purified from *E.coli* and their enzymatic activity will be evaluated.

2 Materials and Methods

2.1 Cell culture

Suspension cells of *Nicotiana tabacum* L. cv. 'Bright Yellow 2' (BY-2, Nagata et al., 1992) were cultivated in liquid medium containing 4.3 g/L Murashige and Skoog salts (Duchefa, Haarlem, The Netherlands), 30 g/L sucrose, 200 mg/L KH_2PO_4 , 100 mg/L inositol, 1 mg/L thiamine, and 0.2 mg/L 2,4-dichlorophenoxyacetic acid (2,4-D), pH 5.8. Cells were subcultured weekly by inoculating 1.5 ml of stationary cells into 30 ml fresh medium in 100 ml Erlenmeyer flasks. The cells were then incubated on a horizontal shaker (KS250 basic, IKA Labortechnik, Staufen, Germany) at 150 rpm and 25°C in darkness. Transgenic suspension cells microtubule marker line *TuA3* (Kumagai *et al.*, 2001), actin marker line *GF11* (Sano *et al.*, 2005), overexpressing lines *VrMC5-GFP* and its variants lines were subcultivated in the same medium as mentioned above, but supplemented with either 25 mg/L Kanamycin or 30 mg/L Hygromycin (more details in Appendix).

2.2 Construction of VrMC5 overexpressor variants

Three mutant forms of VrMC5 (C139A, S190A, R226G) were constructed using site-directed mutagenesis method. The full plasmid amplification was carried out using Q5 Phusion High-Fidelity DNA polymerase (NEB, Germany) via PCR. A set of primers (Appendix table 5.1) containing the desired mutation was designed and a constructed plasmid *pH7FWG2.0/VrMC5* was used as template to create mutants. The PCR reaction mixture was optimally set as: 14.7 μL nuclease-free H_2O , 5 μL Q5 buffer, 1.0 μL dNTP (10 mM), 0.9 μL forward primer (10 μM), 0.9 μL reverse primer (10 μM), 1.5 μL DMSO and 0.5 μL Q5 Polymerase, and 0.5 μL template. PCR thermal program consisted one cycle of 98°C for 3 min and 17 cycles of 98°C

for 10 s, annealing at 55°C for 30 s, and prolongation at 72°C for 5 min. PCR products were digested by 1 µL of *Dpn I* restriction enzyme (10 U/µL, NEB, Germany) at 37°C for 3 hours to eliminate the non-mutated parental plasmid. Products were subsequently transformed into *Escherichia coli* DH5α for DNA sequencing (GATC Biotech, Cologne, Germany) and the verified amplicons were then used for stable transformation of tobacco BY-2 cells.

2.3 Stable transgenic tobacco BY-2 cell establishment

2.3.1 *Agrobacterium tumefaciens* transformation

Purified constructed plasmid was transformed into Chemo-competent *Agrobacteria* LBA4404 (Invitrogen Corporation, Paisley, UK) strain by using freeze-thaw method. The reaction mixture of 100 µL thawed LBA4404 competent cell and 500 ng plasmid was kept on ice for 30 minutes, freeze cells in liquid nitrogen for 5 minutes and heat shock cells at 37°C by water bath for 10 minutes. 1 mL LB medium was added into the mixture and incubate shaking for 4 hours at 28 °C. The culture was spread on LB agar plates containing 50 µg/mL rifampicin + 300 µg/mL streptomycin + 100 µg/mL spectinomycin and incubated at 28°C for 3 days. Positive transformants were verified using colony PCR.

2.3.2 *Agrobacterium*-mediated transformation of BY-2 cell

The BY-2 stable overexpressing VrMC5 variants lines were generated according to *Agrobacterium*-mediated transient transformation (Buschmann *et al.*, 2011) with slight modification.

A single transformants colony was inoculated into 5 mL of LB liquid medium supplied with antibiotics and incubated in a shaker (250 rpm) at 28°C overnight.

1mL overnight culture was inoculated into 5 mL of fresh LB-medium (without antibiotics) then cultivated for further 4-5 h at 28°C until the OD₆₀₀ had reached 0.8-1.0. 6 mL suspension Agrobacteria were harvested and spun down at 8000 g (Heraeus Pico 17 Centrifuge, 600 Thermo Scientific, Langenselbold, Germany) for 8 min in a 50 mL Falcon tube at room temperature. Removed the supernatant and resuspended the bacteria in 180 µL Paul's medium (4.3 g/L MS salts with 1% sucrose, pH 5.8) by vortexing vigorously to homogenize the suspension.

Normally during 3-4 days after subcultivation wild type (wt) tobacco BY-2 cells were used for transformation. 30mL cells were washed five times with 300 mL of Paul's medium using sterile filter holder (Scientific Nalgene® Filter Holder, Thermo Scientific, Langenselbold, Germany) combined with a sterilized Nylon mesh (Eggert Mehlsiebe, Waldkirch, Germany) with a mesh size of 70 µm. The washed cells were then resuspended in 6 mL of Paul's medium yielding a 5-fold concentrated cell suspension. 5 mL concentrated cell suspension was mixed with 180 µL of Agrobacteria prepared as above for cocultivation.

The mixture of bacteria and cell prepared in a Falcon tube on an orbital shaker (100 rpm) for 10 min. The mixture was inoculated onto Paul's agar (Paul's media with 0.5% Phytigel without any antibiotics) with sterile cut tips. The plates were then incubated for 3 days at 22°C in the dark. Cells were subsequently transferred onto MS agar plates (MS medium with 0.8% Danish agar) containing 60 µg/mL hygromycin to select transformed tobacco cells, and 300 µg/mL cefotaxime to eliminate Agrobacteria. After incubation at 26°C in the dark for 3 weeks, resistant calli had appeared and were transferred onto fresh MS agar plates (with antibiotics) for further growth. Finally, the sufficient size calli were inoculated into liquid medium to establish suspension culture.

2.4 Stress and inhibitor treatments

2.4.1 Z3HAL and harpin treatment

To activate cell-death related defence, the elicitor harpin derived from the phytopathogenic bacterium *Erwinia amylovora* was used at a final concentration of 30 µg/mL (stock solution of 300 mg/mL solved in water with 1% effective concentration, Pflanzenhilfsmittel, ProAct, Germany), this treatment was applied at the time of subcultivation. The samples for RNA extraction were collected after 6 h, the cell mortality and protein extraction were checked after 24 h.

The biological effect of cis-3-hexenal (50% purified in triacetin, Sigma-Aldrich), and trans-2-hexenal (98% purified, Sigma-Aldrich) were tested in signalling and defence responses. Cells were collected at day 3 after subcultivation and incubated with 12.5 µM volatiles. The samples for RNA extraction were collected after 30 min, the cell mortality and protein extraction were checked after 15 min.

2.4.2 Inhibitor treatment

In some experiments, inhibitors were pretreated on cell for proper time. An inhibitor of actin polymerisation Latrunculin B (Lat B, Sigma-Aldrich, Germany), which can disrupt actin filament organisation, was applied on *GF11* for 1 h with 10 µM concentration (stock solution 1 mM in DMSO). Phalloidin (Sigma-Aldrich, Germany), which has a strong affinity with microfilaments, but does not bind to actin monomers, so it can facilitate microfilaments remains stable. Like Latrunculin B, the suspension cells were pretreated with phalloidin at a concentration of 1 µM (stock solution 1mM in ethanol) for 1 h.

To test the role of microtubules, oryzalin (Sigma-Aldrich, Germany) acts as an inhibitor of microtubules organization. Microtubule-marker line *TuA3* was tested by

pretreatment with 10 μM of oryzalin (stock solution 1 mM in DMSO) over 1 h. Taxol (Sigma-Aldrich, Germany) is a microtubule-stabilizing agent binding to the β -tubulin subunits. Suspension cells were pretreated with taxol at a concentration of 10 μM (stock solution 1mM in DMSO) for 1 h.

All the tests were set up with solvent control to eliminate the side effect of the solvent.

2.4.3 Anti-metacaspase peptide treatment

To measure the time course of uptake, the cells were incubated with 1 μM LMTP-peptide conjugated rhodamine B for 15, 30, 60, 120, 180 min in the dark under continuous shaking and then washed three times before observation.

To assess the localization of peptide in relation to cytoskeleton and VrMC5 in vivo, the conjugated peptides were incubated with the 3-day old transgenic tobacco TuA3, *GF11* and *VrMC5* cell line for 2 h, washed as described above and viewed under a microscope immediately. Ikarugamycin (IKA, Sigma-Aldrich, Germany) specifically inhibited clathrin-dependent endocytosis, 10 μM IKA was pre-incubated on cells for 30 min before peptide application to test if the uptake of peptide depended on endocytosis.

2.5 Microscopy of VrMC5 localization and response to stresses

All the confocal files were recorded with an AxioObserver Z1 (Zeiss, Jena, Germany) inverted microscope equipped with a laser dual spinning disc scan head from Yokogawa (Yokogawa CSU-X1 Spinning Disk Unit, Yokogawa Electric Corporation, Tokyo, Japan), and a cooled digital CCD camera (AxioCamMRm; Zeiss), using a 63 \times LCI-Neofluar Imm Corr DIC objective (NA 1.3). Two filter

channels were used: EGFP (excitation 488 nm, emission 509 nm) and RFP (excitation 561 nm, emission 610 nm). The images were processed with the ZEN 2012 (Bule edition) software to generate orthogonal projections from the recorded stacks and to export in TIFF format.

2.5.1 Microtubule visualization

Microtubules were stained by indirect immunofluorescence using a monoclonal antibody against α -tubulin (ATT, Sigma, Germany), and a secondary anti-mouse IgG antibody conjugated to Tetramethylrhodamine (TRITC; Sigma; Germany) following the protocol published by Eggenberger et al. (2007). Cells were fixed in 3.7 % (w/v) paraformaldehyde in microtubule stabilising buffer (MSB: 50 mM PIPES, 2 mM EGTA, 2 mM MgSO₄, 0.1% Triton X-100, pH 6.9) in custom-made micro-staining chambers (Nick et al., 2000) for 30 min, and then washed with MSB three times for 5 min. The cell wall was perforated using 1 % (w/v) Macerozym (Duchefa, Haarlem, Netherlands) and 0.2 % (w/v) Pectolyase (Fluka, Taufkirchen, Germany) in MSB for 5 min, and unspecific binding sites were blocked with 0.5 % (w/v) bovine serum albumin (BSA) dissolved in PBS (150 mM NaCl, 2.7 mM KCl, 1.2 mM KH₂PO₄, 6.5 mM NaH₂PO₄) for 30 min. After blocking, primary antibody was added at a 1:500 dilution into PBS at 4°C overnight. To remove unbound primary antibodies, cells were rinsed three times with PBS and incubated with a secondary anti-mouse IgG conjugated with TRITC at 1:250 dilution for 1 h at 37°C in a moist chamber. Unbound antibodies were removed by washing with PBS and cells were observed under spinning disc confocal microscopy with excitation at 561 nm for imaging of TRITC signal.

2.5.2 Actin visualization

For actin filaments visualization, BY-2 cells were stained with TRITC-phalloidin as described previously with slight modification (Maisch and Nick, 2007). Cells were fixed in 1.85 % (w/v) paraformaldehyde in standard buffer (0.1 M PIPES, pH 7.0, supplemented with 5 mM MgCl₂ and 10 mM EGTA) for 10 min at room temperature and after a subsequent 10 min fixation in standard buffer containing 1% (v/v) glycerol. Then washed cells with standard buffer for 10 min twice. Subsequently, samples were stained with 0.66 μM TRITC-phalloidin (Sigma-Aldrich, Deisenhofen, Germany) for 30 min. Cells were then washed three times for 5 min in PBS and observed immediately using spinning disc microscope as described above.

2.6 Determination of cell mortality

Evans blue staining method was used To determine the cell viability (D.F.Gaff & O.Okong'O-Ogola, 1971). For each sample, aliquots of 250 μL cells were transferred into custom-made staining chambers with filtration mesh to remove the medium, incubated in 2.5% (w/v) Evans Blue solution for 3-5 min, and then washed with distilled water 3 times. Aliquots of 50 μL stained cells were microscopically observed using AxioImager Z.1 microscope (Zeiss, Jena, Germany), DIC illumination, 10 × objective. The membrane-impermeable dye can penetrate only into dead cells resulting in blue staining of the dead cell. Mortality was calculated as the ratio of dead cells over the total number of cells. Data represent a population of 1500 cells scored over three independent experiments.

2.7 Western blot

The expression pattern of MC5 and its variants response to stresses was verified by Western blotting. The cells were collected by short-time vacuum and shock-frozen in liquid nitrogen and ground with mortar and pestle (both sterilised and precooled)

before extracting protein. Protein was extracted as following: cells were homogenized on ice for 15 min with the same volume of extraction buffer (25 mM morpholine ethanesulfonic acid, 5 mM EGTA, 5 mM MgCl₂, pH 6.9) supplemented with 1 mM dithiothreitol (DTT), and 1 mM phenylmethylsulphonyl fluoride (PMSF). Cell lysates were centrifuged at 13000 g at 4°C for 15 min to isolate soluble extract containing cytosolic proteins. All samples were finally dissolved in loading buffer (50 mM Tris/HCl (pH 6.8), 30 % glycerol (v/v), 300 mM DTT, 6 % SDS (w/v), 0.01 % bromophenol blue) and heated at 95 °C for 5 min.

Proteins were separated by 10% SDS-PAGE gel (Table 2.1). Separated proteins were electrophoretically transferred to a PVDF membrane (0.45 µm, Roti[®]-PVDF, Carl Roth, Germany) with a semi-dry blotter (Trans-Blot[®] SD cell, Bio-Rad, Germany) followed as guide instruction. Non-specific binding was blocked using 5% w/v non-fat dry milk in TBST buffer (20 mM Tris/HCl, 300 mM NaCl, 0.1% w/v Tween-20, pH 7.4) for 1 h at room temperature. The target proteins were probed by monoclonal mouse antibodies against the GFP reporter (Anti-Green Fluorescent Protein antibody, Sigma-Aldrich, Germany) in a dilution of 1:1000 in TBS buffer (20 mM Tris/HCl, 300 mM NaCl, pH 7.4) and incubated at 4°C overnight, followed by washing three times with TBST buffer. For signal development, the secondary antibody, goat polyclonal anti-mouse IgG conjugated to alkaline phosphatase (Sigma-Aldrich, Germany) in a dilution of 1:25000 in TBS buffer was employed and incubated for 1.5 h at room temperature. After washing three times in TBS buffer, the protein bands were visualized on the PVDF membrane with BCIP/NBT liquid substrate reagent (Sigma-Aldrich, Germany).

Table 2.1 Formula of SDS-PAGE gels of different concentration

	Con	30%AA/ml	Separation gel buffer/ml	ddH ₂ O/ml	10%APs/ μ l	TEMED/ μ l
Separation gel	5%	4,2	6,2	14,3	215,9	108
	7,5%	6,2	6,2	12,3	215,9	108
	10%	8,2	6,2	10,3	215,9	108
	15%	12,3	6,2	6,2	215,9	108
Stacking gel			Stacking gel buffer/ml			
	4%	1,3	2,3	6,2	105,7	52,8

2.8 EPC-affinity chromatography

Carboxy-ethyl-N-phenylcarbamate (EPC) was synthesized as described in Mizuno (Koichi MIZUNO, 1981) and coupled to sepharose 4B (Sigma-Aldrich, Germany). EPC coupled sepharose 4B was filled onto glass wool and concentrated by centrifugation at 15000 g for 1 min into Eppendorf column. Total proteins were extracted as described above, then loaded through EPC-sepharose column pre-equilibrated with MT-stabilizing buffer (25 mM MES, 5 mM EGTA, 5 mM MgCl₂, 1 M glycerol, 1 mM DTT, 1 mM phenylmethylsulphonyl fluoride, pH 6.9) to bind α -tubulin to EPC and discarded the filtration containing α -tubulin unbound proteins by centrifugation at 15000 g for 1 min. Fractions containing proteins bound to α -tubulin were obtained through elution with KCl from low concentration to high concentration. The fractions were precipitated by trichloroacetic acid (Bensadoun & Weinstein, 1976) prior to processing for western blot and were probed by anti-GFP and ATT antibody.

2.9 Recombinant expression of VrMC5 and its variants

The coding sequence of the *VrMC5* was inserted into the pET21b expression vector (Appendix 5.3). The resulting construct encoding the VrMC5 protein fused with

successive 6 histidine residues tag was expressed in *E. coli* strain BL21(DE3) following heat-shock transformation. The site-directed mutagenic VrMC5 variants were generated as described above. A single positive colony was inoculated into 50 mL of LB liquid medium containing ampicillin (100 µg/mL) and grown at 37°C overnight. The entire volume of the pre-culture was inoculated into 3 L of LB medium complemented with 100 µg/mL of ampicillin at a starting OD₆₀₀ of 0.1 and cultivated at 37°C, 200 rpm for 3-4 hr to achieve the final OD₆₀₀ of 0.8-1.0. Cooled the culture in an ice-water bath for 15min and induce the expression with 80 µM isopropyl-β-D-thiogalactopyranoside (IPTG). The culture was subsequently incubated at 18°C, 200 rpm for 24 hr, the induced cell should have an OD₆₀₀ over 2. Cells were harvested by centrifugation at 10000 g for 20 min at 4°C (Sorvall LYNX 4000 Superspeed Centrifuge, Thermo Scientific, Germany). Proteins were extracted as following: The sedimented cells were suspended with 200 mL ground buffer (50 mM Tris, 5 mM EDTA, 300 mM NaCl, 10%w/v glycerol, pH 7.8) centrifuged at 10000 g for 10 min at 4°C again, and subsequently were resuspended in 60 mL ground buffer, then lysed twice using a French Press at 1000 bar/Psi. Cell debris was removed by first centrifugation at 15000 g for 30 min and second centrifugation for 15 min, 4°C, and the supernatant fraction contained the soluble recombinant VrMC5. Protein was precipitated from supernatant at 4°C overnight with 70% ammoniumsulfat buffer without EDTA (3.3 M ammoniumsulfat, 50 mM Tris, pH 7.8) and then added solid ammoniumsulfat to final concentration of 93%. For calculation of solid ammoniumsulfat amount, the online calculator could be used: <http://www.encorbio.com/protocols/AM-SO4.htm> .

Precipitated protein was obtained by centrifugation at 10000 g for 30 min at 4°C and dissolved sedimented protein in 40 mL store buffer (50 mM Tris, 300 mM NaCl, 10%w/v glycerol, pH 7.8). The solution containing soluble protein was applied onto

Ni-NTA agarose column, which was previously equilibrated with one volume of column distilled water and three-volume of column wash buffer (50 mM Tris, 300 mM NaCl, 10 mM imidazol, 10%w/v glycerol, pH 7.8). Unbound proteins were washed out from the column with 2 L washing buffer and the His-tagged recombinant MC5 was eluted with elution buffer (50 mM Tris, 300 mM NaCl, 250 mM imidazole, 10%w/v glycerol, pH 7.8). The eluted fractions were concentrated and precipitated by 70% ammoniumsulfat buffer with EDTA (3.3 M ammoniumsulfat, 5 mM EDTA, 50 mM Tris, pH 7.8) and used solid to get 93%, then centrifuged at 10000 g for 30 min at 4°C. Concentrated recombinant protein was dissolved with 2 mL ground buffer and stored at -80°C.

2.10 Enzymatic activity assay

Assessing the activity of VrMC5 and its mutants were achieved by measuring the release of the fluorescent group AMC from the hydrolysis of the peptide substrate Boc-GRR-AMC (Bachem) by the purified protein. The assays were carried out in 100 μ L total volume of reaction mixture which consists of 30 nM of purified recombinant protein, 100 μ M of Boc-GRR-AMC and reaction buffer (50 mM Tris, 100 mM NaCl, 5 mM DTT, 0 –50 mM CaCl₂, pH 7.5). Each assay was set up in triplicates in 96-well plate and the release of AMC was continuously monitored every minute for 30 min at room temperature with a microtiter plate reader (Synergy HT, BIO-TEK) at an excitation wavelength of 360 nm and an emission wavelength of 460 nm. Data were read-out as increases in relative fluorescence as a function of time. The specific enzyme activity was calculated as nmol of substrate hydrolyzed/mg of protein/min using a standard curve of AMC in the enzyme reaction buffer (RFU).

2.11 RNA extraction and cDNA synthesis

BY-2 cells were harvested at proper time point under various treatment condition using a Büchner funnel via short-time vacuum (10s), and shock-frozen immediately in liquid nitrogen. After homogenizing (TissueLyser, QIAGEN, Germany), total RNA was extracted using innuPREP RNA Mini Kit (Analytik Jena AG, Germany). The procedure followed as manual instruction and the potential genomic DNA contamination was removed by using the DNase (Invitrogen, Germany). These RNA quantity and quality were measured by Nanodrop spectrometer (Eppendorf BioSpectrometer basic, Germany), and were electrophoresed on a 1% agarose gel. The mRNA was transcribed into cDNA using the M-MuLV cDNA Synthesis Kit (New England BioLabs; Frankfurt am Main, Germany). 1 µg of purified RNA as template for reverse transcription. The two-step synthesis of cDNA are as follows: step one, 0.4 µL oligo-dT (100 µM) and 1 µL dNTP (10 mM) were mixed with 1 µg total RNA, and the final volume fill up with nuclease-free water was 16 µL. The reaction mixture was incubated at 70 °C for 5 min and put immediately on ice. Then step two, 2 µL 10×MULV buffer, 0.5 µL RNAase inhibitor (10 U/µL) and 0.25 µL MULV reverse transcriptase (200 U/µL) and 1.25 µL nuclease-free water was adequately mixed with reaction mixture from the first step and incubated at 42 °C for 1 hour, then 90 °C for 10 min to stop the reaction.

2.12 Real-time PCR analysis

Steady-state relative transcript abundance of the selected genes was measured by quantitative real-time PCR (qRT-PCR), reactions were performed using a CFX96™ real-time PCR cycler (Bio-RAD, USA). Primers and conditions of the genes *PALA*, *PALB*, *ICSI*, *PR1a*, *EF1α* were given in Appendix table 5.2.

The PCR condition was optimally set to 20 μL reaction mixture containing: 11.75 μL nuclease-free H_2O , 4 μL GoTaq buffer, 0.4 μL dNTP (10 mM), 0.4 μL forward primer (10 μM), 0.4 μL reverse primer (10 μM), 1 μL MgCl_2 (50 mM), 0.95 μL SybrGreen and 0.1 μL GoTaq Pol, and 1 μL cDNA diluted 1:10. PCR thermal conditions consisted of one cycle of 95 $^\circ\text{C}$ for 3 min and followed by 40 cycles of 95 $^\circ\text{C}$ for 15 sec, annealing at 60 $^\circ\text{C}$ for 45s. The homogeneity of the PCR products was confirmed by melting curve analyses. Quantification of the transcript level among different samples was conducted according to $2^{-\Delta\Delta\text{Ct}}$ method.

A tobacco housekeeping gene *Elongation factor 1 α* (*EF1 α*) was used as an internal reference, to normalize the relative level of target gene expression by calculating ΔCt , the difference in Ct value between the reference *EF1 α* products and the target gene products calculated as $\Delta\text{Ct}=\text{Ct}(\text{target})-\text{Ct}(\text{reference})$. The difference in target gene expression between control and treated samples was expressed as $2^{-\Delta\Delta\text{Ct}}$ ($\Delta\Delta\text{Ct} = \Delta\text{Ct treated}-\Delta\text{Ct control}$). The Final result was representative of three independent biological replicates, each was consist of three technical replicates.

3 Results

3.1 Chapter 1: The role of VrMC5 in programmed cell death.

A green leaf volatile *cis*-3-hexenal (*Z*-3-hexenal) plays as an important signal in the plant defence response and plants priming pathway. It has been reported that elicited a rapid response of actin filaments and HR-like cell death in BY-2 cells, which is one type of programmed cell death (PCD) (Akaberi *et al.*, 2018). Meanwhile, metacaspases are thought to be executioners of cellular suicide in plants in the past decade years. To better understand of the roles of metacaspases in HR process, a vitis metacaspase VrMC5 from *Vitis rupestris* was identified and considered to be a potential regulator in harpin (a bacterial elicitor) induced cell death (Gong *et al.*, 2019). Therefore, in the current study, we focus on the specific roles of VrMC5 plays in *Z*-3-hexenal signal pathway.

In the first part, work was started with the analysis of the subcellular localization of VrMC5 by microscopy and biochemical analysis, followed by cellular and molecular response of VrMC5 with *Z*-3-hexenal induction was investigated. Furthermore, the activation mechanism of VrMC5 was explored *in vivo* and *in vitro*. In the end, an assumptive link between *Z*-3-hexenal pathway and VrMC5 was established.

3.1.1 Subcellular localization of VrMC5

To test the subcellular localization of VrMC5, a C-terminal fusion of VrMC5 with green fluorescent protein (GFP) was expressed under the control of the CaMV 35S promoter in tobacco BY-2 suspension cells. Green fluorescence of the fusion protein

Results

was observed mainly in the cytoplasm and exhibited obvious morphological change in the nucleus during mitosis, the pattern observed reminded of microtubules.

To verify if VrMC5 co-localized with microtubules, α -tubulin was visualized in a *VrMC5-GFP* (*VrMC5*) overexpression line through immunofluorescence probing with anti-tyr- α -tubulin antibody (ATT). When cells were in the interphase of mitosis, the central microtubules were co-localized with VrMC5 and cortical microtubules partially overlapped with VrMC5 (**Figure 3.1 A**). During mitosis, cortical microtubules reorganized into a dense ring-shaped preprophase band (PPB), and pre-nuclear microtubules started with the formation of a mitosis spindle and ended with the metaphase plate, and then phragmoplast formed in cytokinesis to assemble cell plate and separate cytoplasm. Although VrMC5 did not perform specifically at PPB region in the preprophase, its expression in the nucleus showed the same pattern as microtubules (**Figure 3.1 B**) in the other phases, which suggested the VrMC5 was partially co-localized with microtubules.

Results

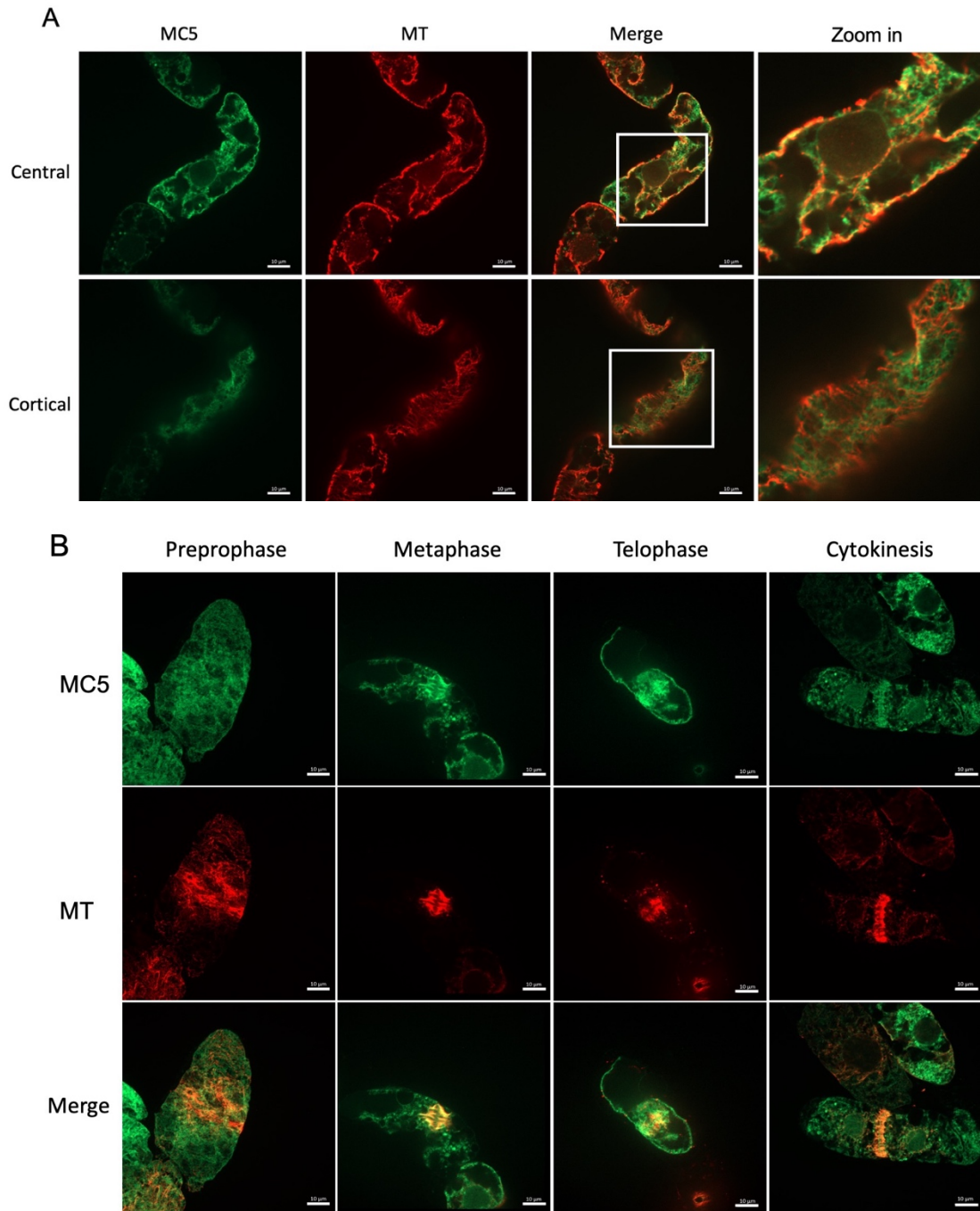


Figure 3.1 Immunofluorescence staining of microtubules (MTs) in *VrMC5-GFP* tobacco cell lines during the cell cycle. A, Central and cortical MTs were visualized in *VrMC5-GFP* in the interphase. B, MTs were visualized in *VrMC5-GFP* during different phases of mitosis. MTs are labelled using anti-tyr- α -tubulin antibody (ATT). Cells 3 days after subcultivation were stained. Scale bar=10 μ m.

It is possible that the microtubules localization of GFP is due to truncation of the fusion proteins by internal cleavage at the C-terminal portion of VrMC5, because VrMC5 can perform autocleavage. Therefore, it is necessary to use biochemical approach to verify the microscopical readout. To examine the physical binding between VrMC5 and microtubules, ethyl-N-phenylcarbamate (EPC) affinity chromatography was applied. EPC is a microtubule polymerization blocker which binds to α -tubulin and coupled to sepharose 4B. The proteins with low affinity to MTs would be removed by washing steps with increasing concentration of KCl while proteins binding to MTs would stick longer to MT-EPC-sepharose 4B and then eluted by KCl solution of higher stringency. The eluted proteins were probed with anti-GFP and ATT antibodies to detect VrMC5-GFP and tubulins respectively (**Figure 3.2**). Multiple bands corresponding to various forms of VrMC5 were detectable after EPC-affinity chromatography by anti-GFP (**Figure 3.2 A**). Upper bands around 80 kDa represented full-length VrMC5-GFP, and the other lower bands represented cleaved form of VrMC5-GFP. Tyrosinated α -tubulin detected by ATT had a lower affinity with EPC sepharose and could be eluted at lower ionic stringency, by lower concentrations of KCl (0-0.25 M), whereas detyrosinated α -tubulin could only be eluted by higher concentration of KCl (0.3-1.0 M). Both, tyrosinated α -tubulins and detyrosinated α -tubulins were detectable by ATT from EPC-affinity proteins (**Figure 3.2 B**). These results indicated that VrMC5 binds to microtubules, confirming its co-localization.

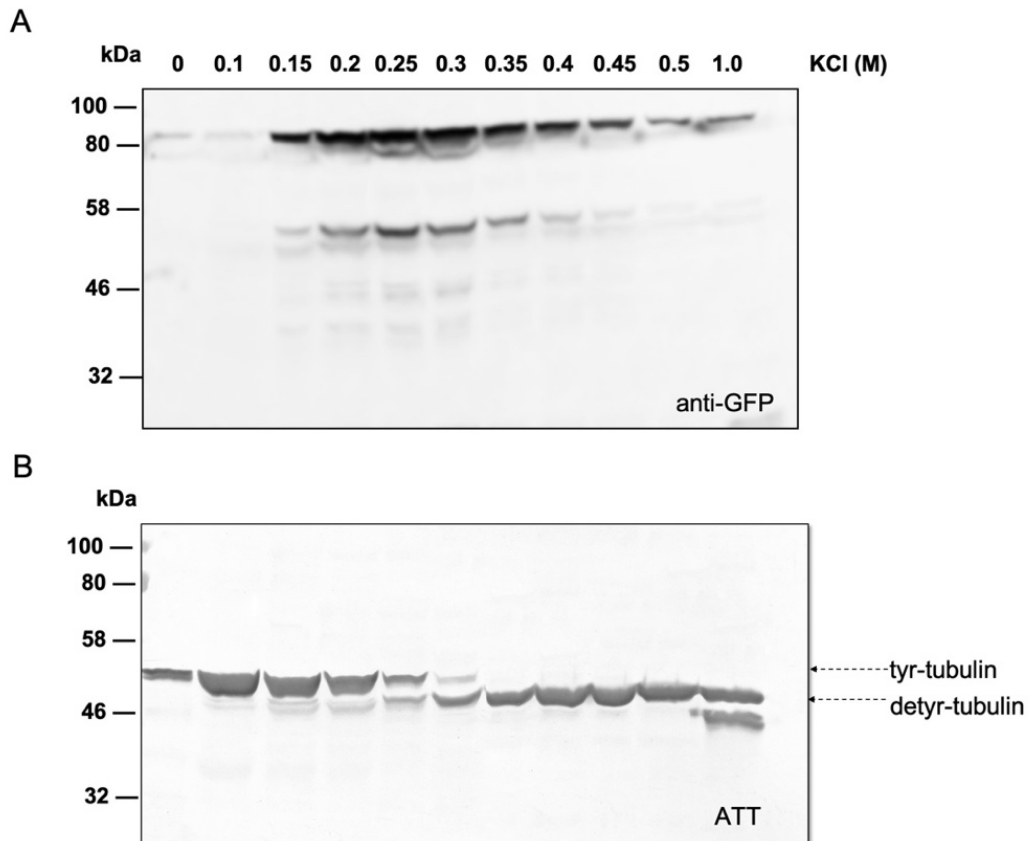


Figure 3.2 Isolation of MT-binding VrMC5. Total proteins were extracted from *VrMC5-GFP* cell line eluted with KCl from ethyl-N-phenylcarbamate (EPC) affinity chromatography column and were subjected to immunoblot analysis with anti-GFP and ATT antibody. **A**, Immunoblot analysis of VrMC5-GFP in *VrMC5-GFP* using anti-GFP antibody. **B**, Immunoblot analysis of α -tubulins in *VrMC5-GFP* using ATT antibody.

3.1.2 The response of cytoskeleton and VrMC5 in Z-3-hexenal signalling

VrMC5 has been found to be a candidate regulator in programmed cell death, it was assumed to make response to inducers or participate in cellular morphological changes. Cytoskeleton reorganization act as an indicator during the PCD processing. The rapid disruption of actin filaments caused by *cis*-3-hexenal (Z-3-hexenal) has been reported as an early hallmark of programmed cell death (Akaberi *et al.*, 2018), the reorganization of microtubules has also been reported in many studies, although

the effects of stresses on microtubule response were variable (Kobayashi I *et al.*, 1994; Takemoto *et al.*, 2006; Guan *et al.*, 2013).

To find out which response of microtubules would be evoked by *Z*-3-hexenal, microtubule response to *Z*-3-hexenal along with solvent control was investigated in the tobacco microtubule marker cell line *TuA3-GFP* using a spinning disc confocal microscopy. In the solvent control, the microtubules remained overall their integrity, in contrast, a rapid and strong disintegration of the microtubule network was developed at 10 min after start of the treatment (**Figure 3.3 A**), like actin response to *Z*-3-hexenal (**Figure 3.3 B**). However, this microtubules depolymerization could be relieved by taxol, a microtubule stabilizing agent which binds to β -tubulin subunits (**Figure 3.3 A**), while the actin stabilizer phalloidin could not suppress actin disintegrate to *Z*-3-hexenal (**Figure 3.3 B**). The cytoskeleton depolymerization caused by *Z*-3-hexenal indicated that *Z*-3-hexenal might induce programmed cell death.

Results

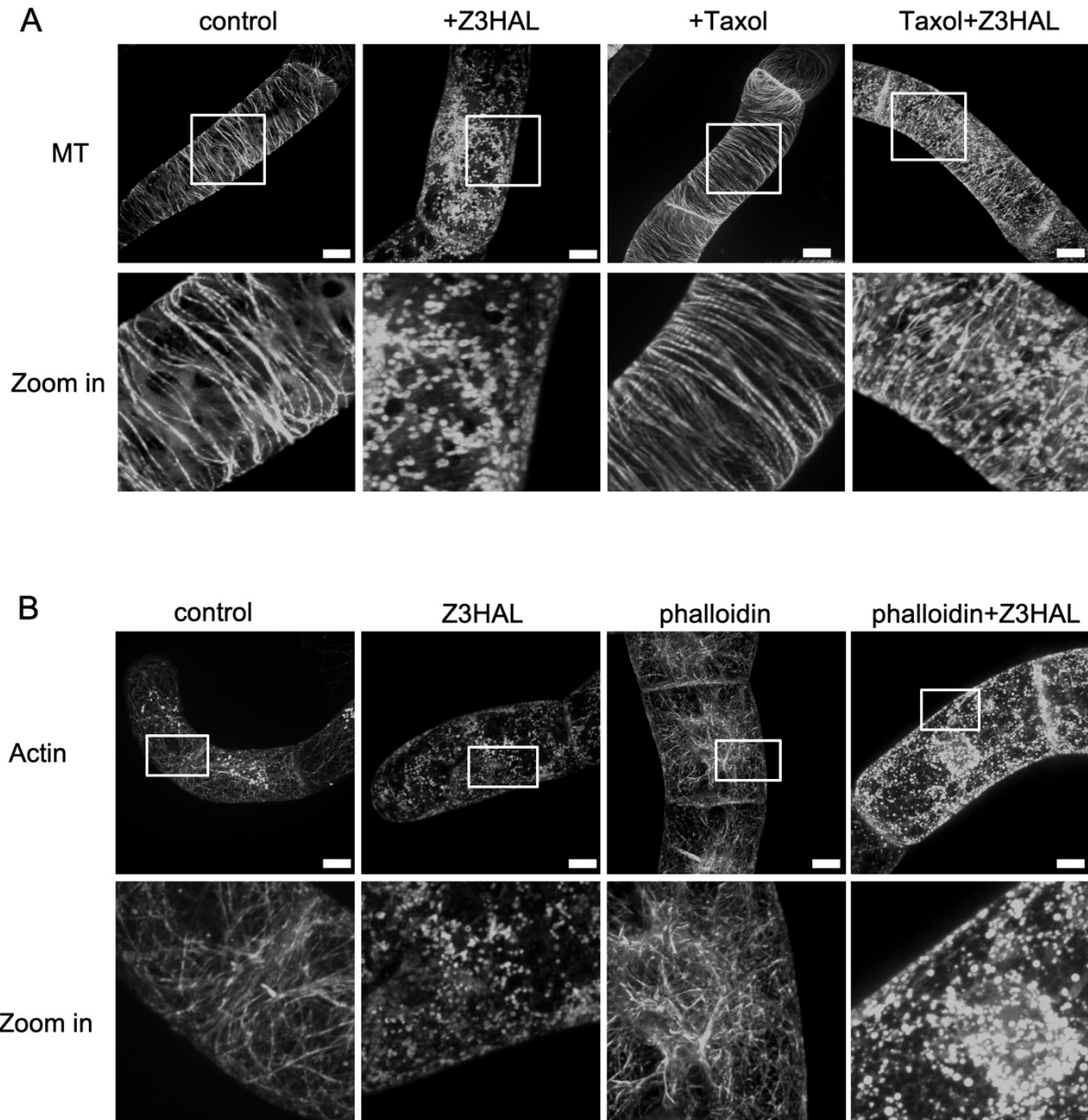


Figure 3.3 Microtubule and actin response to Z-3-hexenal were observed in cytoskeleton marker line *TuA3-GFP* and *GF11* respectively. A, 7-day-old *TuA3* cells were treated with 1) solvent control triacetin, 2) 12.5 μM Z-3-hexenal for 10 min, 3) 10 μM Taxol for 1 h, 4) pretreated with 10 μM Taxol for 1h then with 12.5 μM Z-3-hexenal for 10 min. **B**, 3-day-old *GF11* cells were treated with 1) solvent control triacetin, 2) 12.5 μM Z-3-hexenal for 10 min, 3) 1 μM phalloidin for 2h, 4) pretreated with 1 μM phalloidin for 2h then with 12.5 μM Z-3-hexenal for 10 min. Scale bar=10 μm .

To address the question whether VrMC5 is involved in Z-3-hexenal-induced signalling, *VrMC5-GFP* overexpression cell lines and wt were challenged with Z-3-hexenal. VrMC5-GFP response to Z-3-hexenal along with solvent control was monitored under a confocal microscopy. A short-term Z-3-hexenal treatment was employed on 3-day-old *VrMC5-GFP*, it became evident that integrated VrMC5 scattered as numerous spots throughout cell at early time (**Figure 3.4 A**), resembling microtubules depolymerization. This observation could be explained in two ways: (1) VrMC5 binds to microtubules and microtubules depolymerization induced by Z-3-hexenal makes an impact on VrMC5-GFP localization pattern. (2) Z-3-hexenal directly affects VrMC5-GFP expression pattern. Since a cell-death related immunity elicitor harpin could cause a radial microtubule elimination, but cortical microtubules remained integrated (Guan *et al.*, 2013), we treated *VrMC5-GFP* with saturated concentration harpin to observe the VrMC5 expression pattern. We found that VrMC5 lost the radial network structure when merging Z-stack of cell center sections in the majority of cells under saturated harpin treatment (**Figure 3.4 A**), but not the cortical VrMC5 that indicated the Z-3-hexenal affects VrMC5 localization pattern through depolymerizing microtubules.

An increase of HR-like cell death induced by harpin in *VrMC5-GFP* overexpression line has been reported (Gong *et al.*, 2019) and previous work implied Z-3-hexenal might induce cell death. *VrMC5-GFP* overexpression cells 3 days after subcultivation were treated with 12.5 μ M Z-3-hexenal for 15 min and cell mortality was determined using Evans blue assay. Compared with wt cells, cell death significantly increased in the *VrMC5-GFP* cell line under Z-3-hexenal, even higher than harpin induction (**Figure 3.4 B**), which suggested VrMC5 plays a role in the Z-3-hexenal signalling pathway.

As many studies in metacaspase have demonstrated that self-processing is required for activation of type II metacaspase (Vercammen *et al.*, 2004; Watanabe & Lam, 2005; Belenghi *et al.*, 2007; Watanabe & Lam, 2011a), we wondered if VrMC5 self-processing is correlated with induction of cell death by Z-3-hexenal. Cell samples were collected at time points challenged with Z-3-hexenal. In the *VrMC5-GFP* overexpression line, cleaved active forms of VrMC5 (approximately 57 and 52 kD) were detectable during Z-3-hexenal induction of HR cell death, although they were decreased during cell death processing, as well as the full-length form of VrMC5-GFP (**Figure 3.4 C**). It is possible that VrMC5 undergoes fast-proteolysis when activated like other type II metacaspases, having an efficient and rapid self-activation process suggests that activated VrMC5 will have a short functional half-life. For anti-GFP which could detect the full-length or fragments of VrMC5 fused with C-terminal GFP, the decreased intensities of full-length form of VrMC5 represents the more VrMC5 convert from the proenzyme form into catalytically active forms, and the decreased intensities of VrMC5 fragments suggested the activated VrMC5 go through fast-proteolysis.

Results

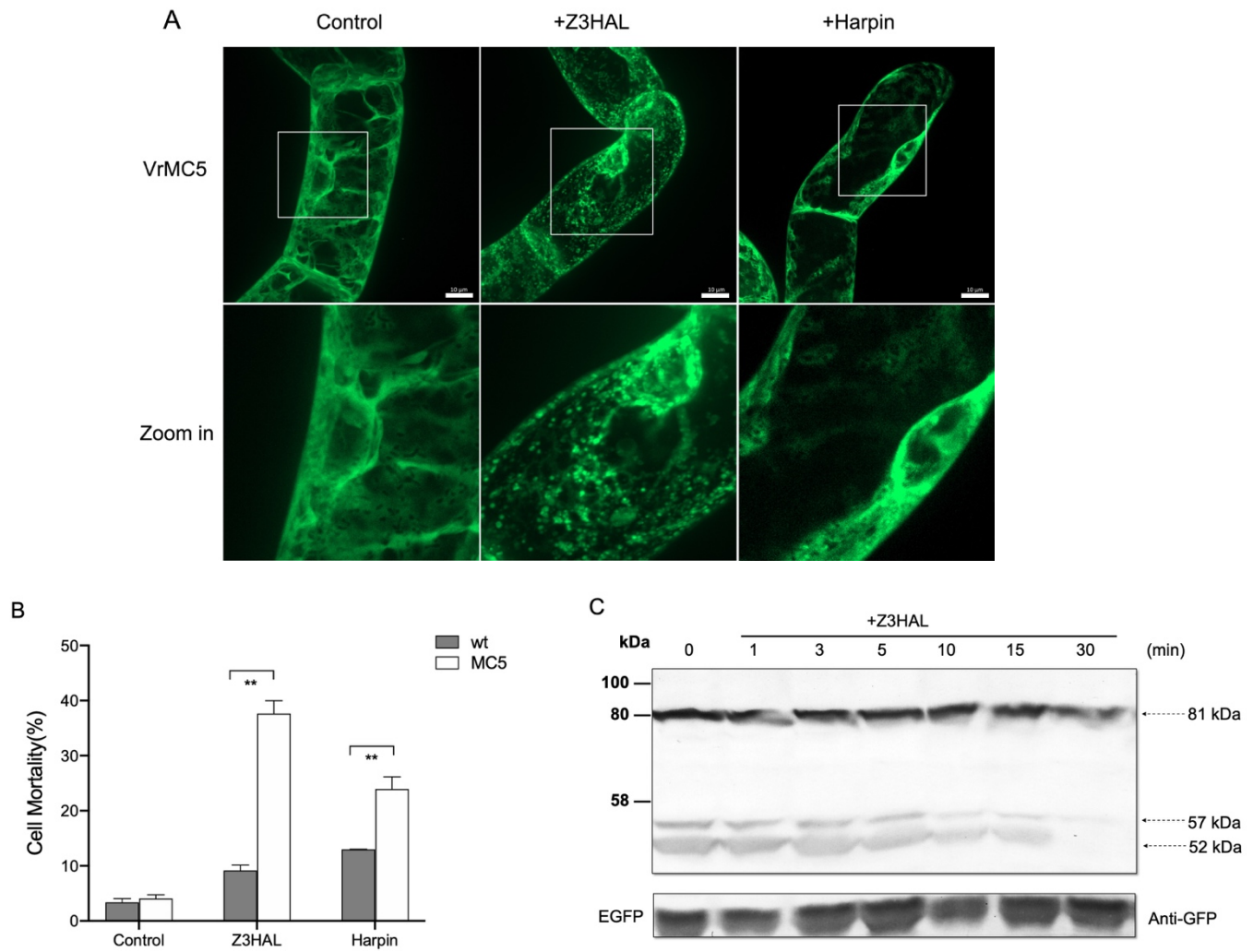


Figure 3.4 Z-3-hexenal induced cell death in *VrMC5* cell line. **A**, Responses of *VrMC5* to Z-3-hexenal (12.5 μ M, 10 min) and harpin (90 μ g/mL, 60 min) were visualized, disintegrated *VrMC5* were observed in the presence of Z-3-hexenal. Scale bar=10 μ m. **B**, Cell mortality of *VrMC5* cells under Z-3-hexenal (12.5 μ M, 15 min) and harpin (30 μ g/mL, 48 h) treatment. Data represent the mean \pm standard error (SE) of four independent biological replicates, ** indicates significant difference value $P < 0.01$ (Student's t-test). **C**, Self-processing of *VrMC5* proteins during 12.5 μ M Z-3-hexenal-induced cell death. Samples were collected at time point after incubation, immunoblot analysis using anti-GFP antibody.

3.1.3 Expression and subcellular localization of VrMC5 variants

VrMC5 belongs to the Type II metacaspase family that has a highly conserved catalytic cysteine residue within its p20 subunit domain at position 139. The mutation at this active site cysteine of AtMC4, AtMC8 and AtMC9 was reported to abolish cell death stimulation activity (Vercammen *et al.*, 2004; Watanabe & Lam, 2011a). Type II MCs have been reported to require autolytic cleavage of the zymogen for conversion into active enzymes. The peptide mapping has shown that a crucial arginine located within the Type II-specific linker region at site 183 (R183) is the key autolytic cleavage site in AtMC9 mutation at this site (R183A) would completely result in inactivation of recombinant zymogen (Vercammen *et al.*, 2004), and its analogous residues lysine at position 225 (K225) in the core region of the linker of AtMC4 is essential for its activation (Watanabe & Lam, 2011b). An additional cleavage site of AtMC4 is arginine 190 (R190), instead of affecting zymogen activation directly, this site might be secondary cleavage sites after activation of AtMC4 *in vitro* (Watanabe & Lam, 2011b).

Therefore, a set of primers to create corresponding analogous residues (C139, S190, R226) amino acid substitution were designed and the mutations were generated by site-directed mutagenesis technique. These constructs were named VrMC5^{C139A} (C139A), VrMC5^{S190A} (S190A) and VrMC5^{R226G} (R226G) (**Figure 3.5**).

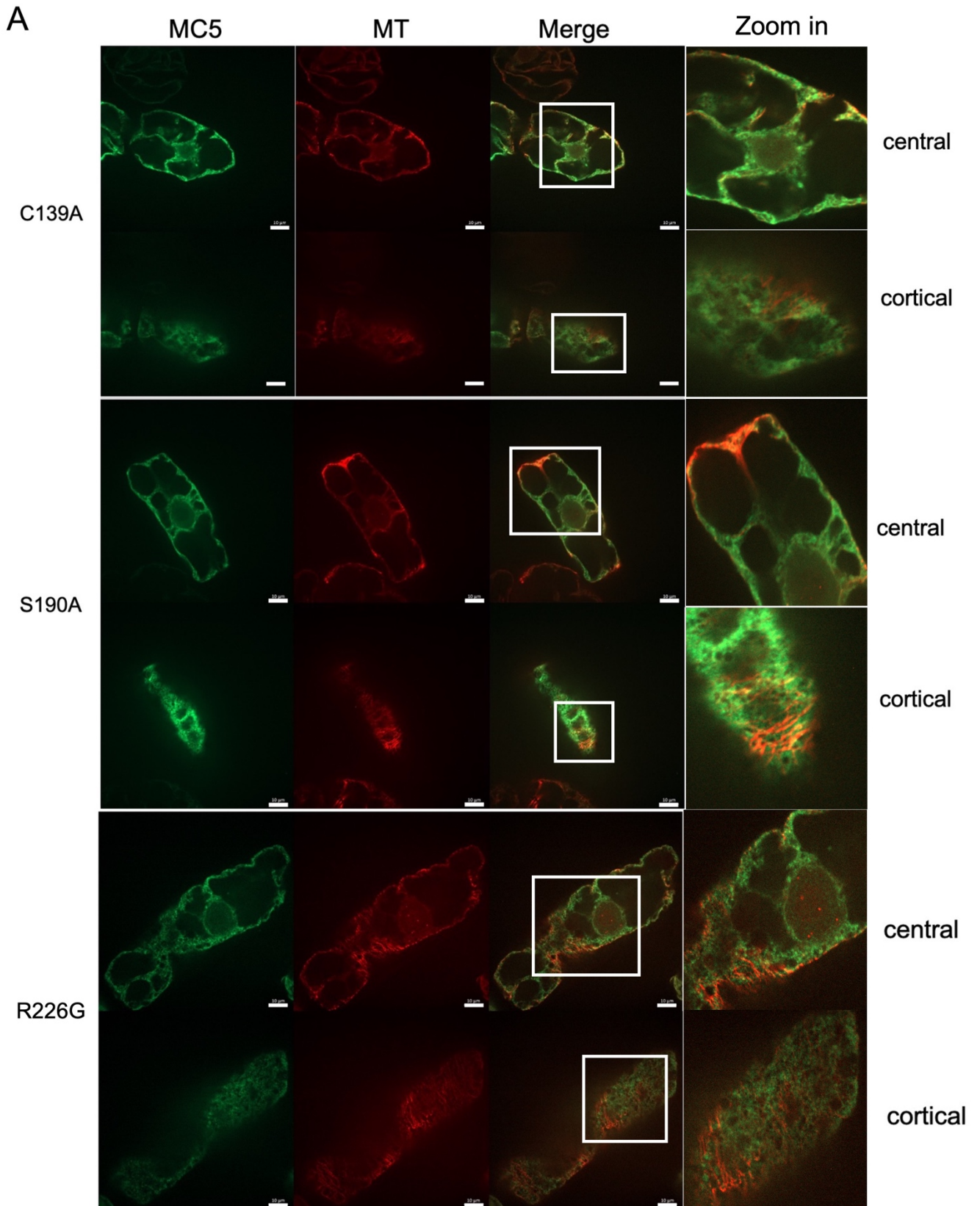
Results



Figure 3.5 Schematic drawing of the constructs for functional analysis of VrMC5 *in vivo* in this study.

To address the biological function of these sites, we overexpressed VrMC5 mutant constructs in BY-2 cell lines to create stable transgenic lines. We confirmed successful expression of these variants detecting the GFP signal using microscopy in suspension cells. The immunofluorescence assay of microtubules in *VrMC5* mutant lines indicated the VrMC5 mutants still bound to microtubules, the putative non-processed mutants did not exhibit any distinct localization, the mutated VrMC5 proteins specifically overlapped with microtubules, especially central microtubules (**Figure 3.6 A**). The self-processing of VrMC5 variants was examined through western blot using anti-GFP antibody (**Figure 3.6 B**). Compared to original VrMC5, the zymogen and cleaved products form maintained the same in VrMC5^{S190A}, the mutation at site S190 did not alter its autolysis pattern. In contrast, one of major cleaved bands could not be detected in VrMC5^{C139A} and VrMC5^{R226G}, as shown in Figure 3.6 B, specific self-processing of VrMC5 required both its catalytic active site (C139) and self-processing site (R225) because each mutant form exhibited similar non-specific degradation patterns.

Results



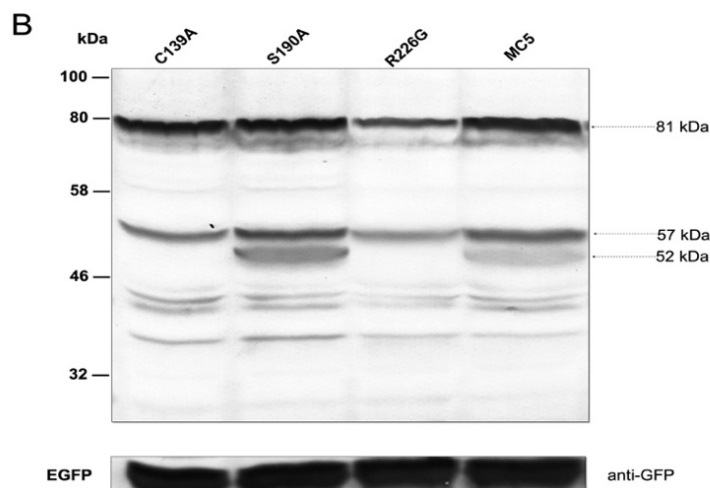


Figure 3.6 Expression and localization of VrMC5-GFP mutant proteins in transgenic BY-2 cells. **A**, Microtubule immunofluorescence images of VrMC5 mutants in stable overexpression transgenic cell lines. MTs are labelled using ATT. Cells 3 days after sub-cultivation were stained. Scale bar=10 μ m. **B**, Characterization of VrMC5 mutants in overexpression transgenic cell line. Total proteins were extracted from 3-day-old cells and subjected to immunoblot analysis using anti-GFP antibody. MC5, VrMC5; C139A, VrMC5^{C139A}; S190A, VrMC5^{S190A}; R226G, VrMC5^{R226G}.

3.1.4 VrMC5 variants are deficient in the responses to Z-3-hexenal

To determine whether the cleavage sites or catalytic site is functionally relevant for VrMC5 *in vivo*, the response of mutant cells to Z-3-hexenal and harpin was examined. Previously we found that Z-3-hexenal affected the subcellular expression pattern of VrMC5-GFP through microtubule depolymerization, therefore, we assumed the pattern of cells expressing VrMC5 variants to either Z-3-hexenal or harpin would be same as VrMC5-GFP. Consistent with VrMC5-GFP, a strong and rapid disintegration of its variants was observed early after Z-3-hexenal treatment and central radial structure was eliminated in the presence of harpin (**Figure 3.7**).

We further assessed the cell viability and autolytic processing of these mutants when Z-3-hexenal and harpin treatment were conducted. *VrMC5* variants overexpression cells were treated with 12.5 μ M Z-3-hexenal for 15 min 3 days after subcultivation and cell mortality was determined using an Evans blue assay. Mortality was drastically reduced in variant cell lines in presence of Z-3-hexenal compared to *VrMC5-GFP*, close to the wt level (**Figure 3.8 A**). Immunoblot analysis was employed to investigate the autolysis process of *VrMC5* variants induced by Z-3-hexenal *in vivo*. As **Figure 3.8 B** shows, self-processed products of variants were still detectable while they were lacking in *VrMC5* wild type form. That revealed the catalytic center C139, putative cleavage site R226 and site S190 are critical for cell death-inducing activity when challenged with Z-3-hexenal.

However, the variants cells presented an opposite response to harpin. The induction of cell death was greatly elevated in mutant cell lines when applied with 30 μ g/ml harpin for 48 h (**Figure 3.8 C**) and autolysis processing of proteins was not observed in response to harpin (**Figure 3.8 D**). Either *VrMC5* wild type form or mutant forms maintained similar self-processing pattern as control condition. It might exist other executers in harpin signalling pathway that complement *VrMC5* activity when its function is impaired.

Results

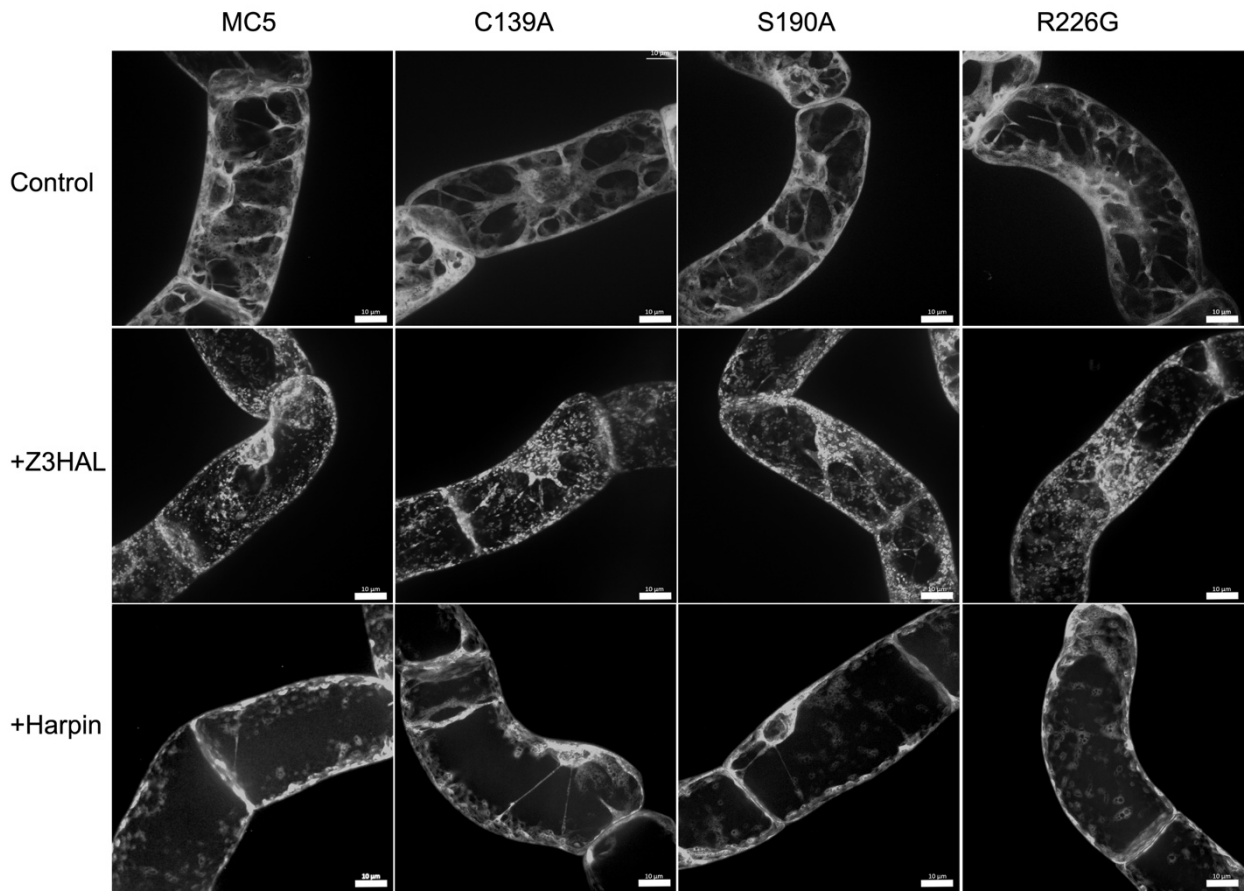


Figure 3.7 Subcellular response of VrMC5 mutants to Z-3-hexenal and harpin. Disintegrated VrMC5-GFP variants were observed in the presence of Z-3-hexenal, whereas central radial pattern disappeared under harpin, wild type VrMC5 was performed as control. Cells were visualized after 10 min and 60 min incubation with 12.5 μ M Z-3-hexenal and 90 μ g/ml harpin, respectively. MC5, VrMC5; C139A, VrMC5^{C139A}; S190A, VrMC5^{S190A}; R226G, VrMC5^{R226G}. Scale bar=10 μ m.

Results

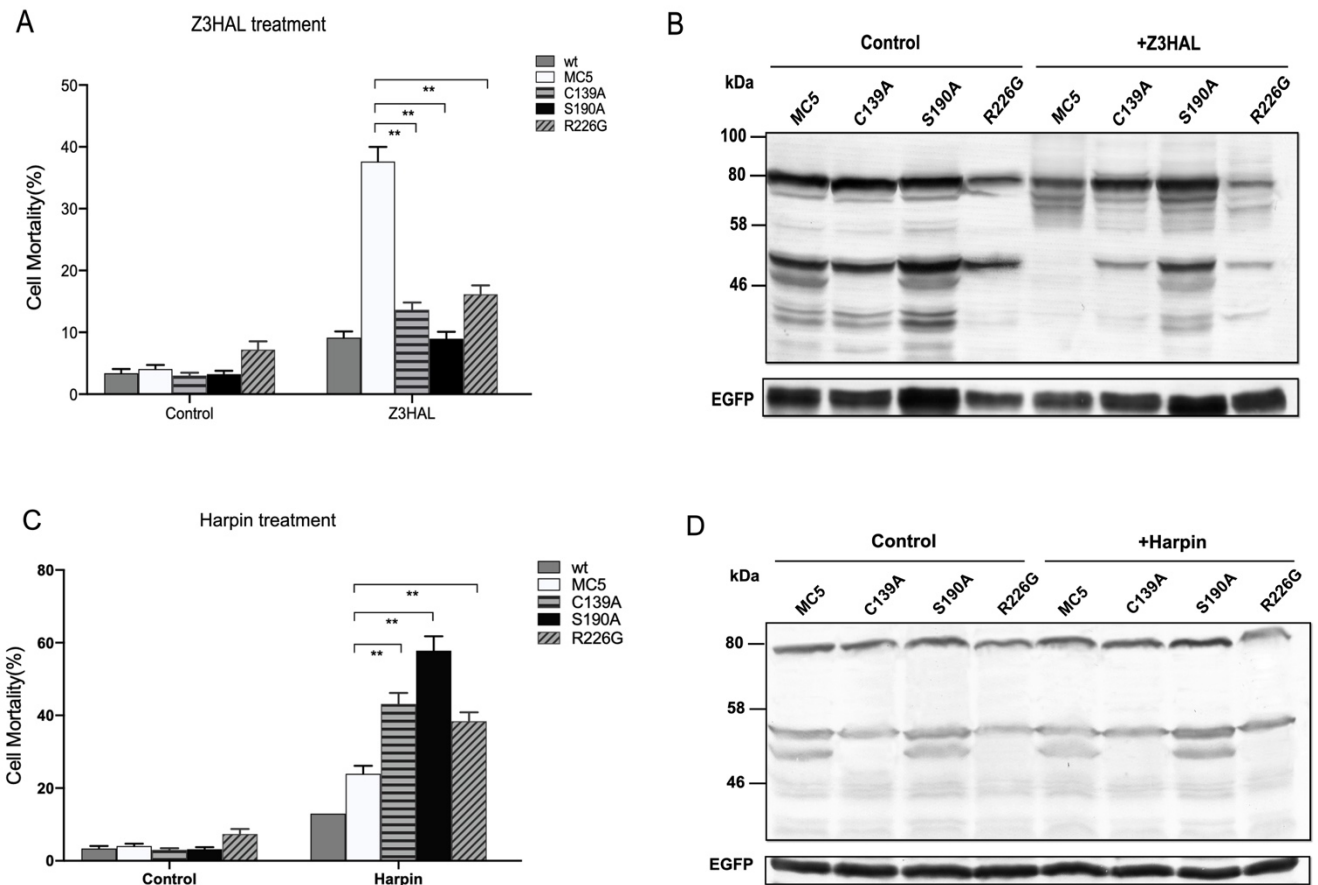


Figure 3.8 Response of VrMC5 mutant variants to Z-3-hexenal and harpin. **A, C,** Cell mortality of VrMC5 wild type and mutants challenged with Z-3-hexenal (12.5 μ M, 15 min) and harpin (30 μ g/ml, 48 h) treatment. Data represents the mean \pm standard error (SE) of four independent biological replicates, ** indicates significant difference value $P < 0.01$ (Student's t-test). **B, D,** Self-processing of VrMC5 variants during Z-3-hexenal (12.5 μ M, 30 min) and harpin-induced (30 μ g/ml, 6 h) cell death. Immunoblot analysis was performed using an anti-GFP antibody.

3.1.5 SA-related signalling response is induced by Z-3-hexenal in *VrMC5* but not in its variants

Since salicylic acid (SA) plays a key role in defense signalling, and commonly regulates cell death-related defense. Biotrophic pathogen infection would induce SA biosynthesis and accumulation, and SA accumulation is associated with hypersensitive response often induced during ETI (Vlot *et al.*, 2009). Two pathways of SA biosynthesis have been clarified, one pathway forms SA from cinnamate produced by phenylalanine ammonium lyase (PAL), in the other pathway SA is synthesized from isochorismate and catalyzed by isochorismate synthase (ICS) (Chen *et al.*, 2009). Therefore, the expression level of *PAL* and *ICS* transcripts can potentially indicate the accumulation of SA in response to stress. In addition we investigated the transcript levels of *PR-1a* (*pathogenesis related 1*) (Riviere *et al.*, 2008) as a readout for SA response.

Cells were treated with 12.5 μ M Z-3-hexenal for 30 min in parallel to a with solvent control, transcription of related genes was measured by qPCR. As shown in **Figure 3.9**, the transcription of SA synthesis genes in *VrMC5* was significantly upregulated by Z-3-hexenal, mainly in *PALA*, *PALB*, up to ~20 and ~10-fold, induction of *ICSI* was little weaker but activated up to ~6-fold. In comparison, transcription of SA synthesis genes in *VrMC5* mutants was not conspicuously activated in response to Z-3-hexenal. That indicated that the activation of SA synthesis in *VrMC5* was mainly through cinnamic acid pathway induced by Z-3-hexenal. As expected, *PR1a* as a SA responsive gene, the expression level was enhanced in *VrMC5* compared with its three mutants (**Figure 3.9 D**). In summary, those results reflected that Z-3-hexenal activates SA signalling pathway associated to cell death in *VrMC5*.

Results

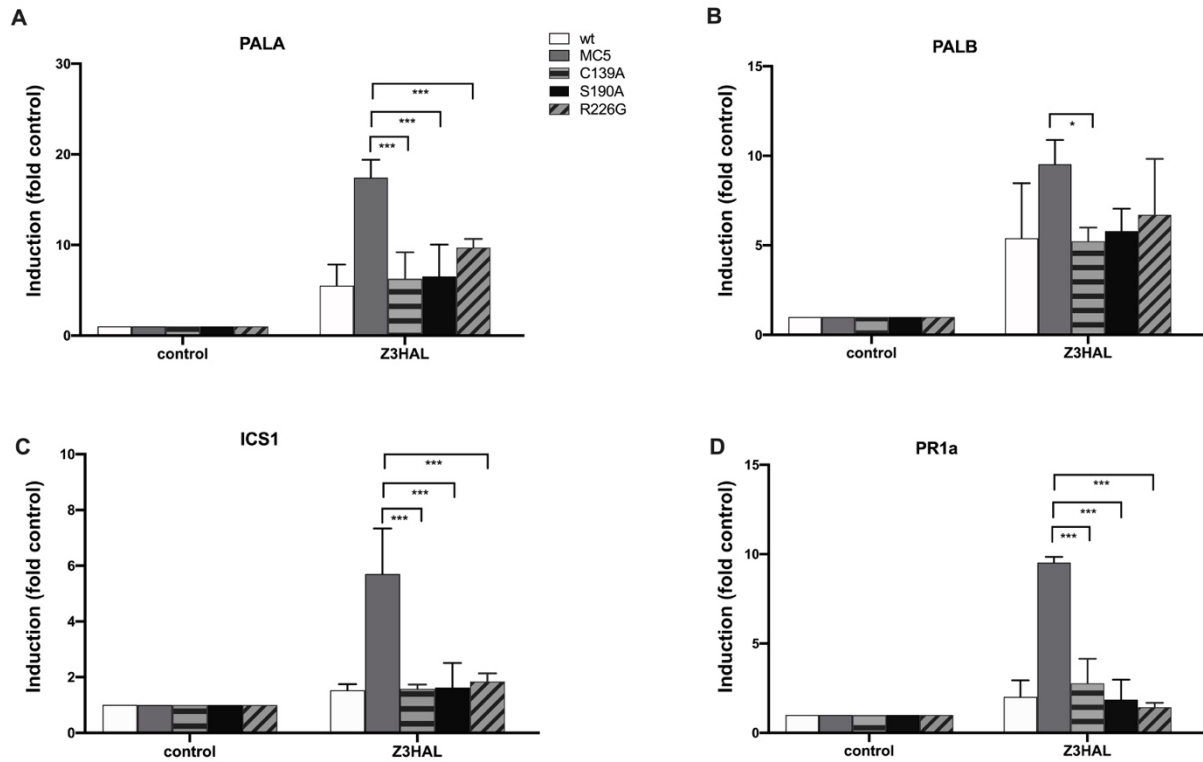


Figure 3.9 Steady-state transcription of SA-related genes in *VrMC5* and its variants induced by Z-3-hexenal. Induction levels for *phenylammonium lyase A and B* (*PALA* and *PALB*), *isochorismate synthase1* (*ICS1*), and *pathogenesis related-1a* (*PR1a*) to Z-3-hexenal treatment (12.5 μ M, 30 min) were estimated by qPCR and normalized to *EF-1 α* as the internal standard. Data represents the mean \pm standard error (SE) of three independent biological replicates, asterisks indicate significant differences with * $P < 0.05$, ** $P < 0.01$ and *** $P < 0.001$ (Student's t-test).

Harpin is a strong elicitor, which can induce intense upregulation of *PAL* which reached more than 100-fold in our experiments. As a parallel experiment, harpin showed a similar effect of transcription of SA related genes as Z-3-hexenal. Cells were collected after 6h of harpin treatment and genes induction was analyzed. *PALA* and *PALB* were greatly activated in all the *VrMC5* cell lines, no matter if wild type form or mutant form, but the induction was much higher in the mutant forms, *ICS1*

Results

was slightly induced as well. In addition, *PR1a* was upregulated almost three times in *VrMC5* variants as compared to *VrMC5* (**Figure 3.9**). Summarized, the upregulated SA-related gene expression indicates SA signalling is activated and subsequently trigger spontaneous cell death, which was consistent with cell mortality to harpin.

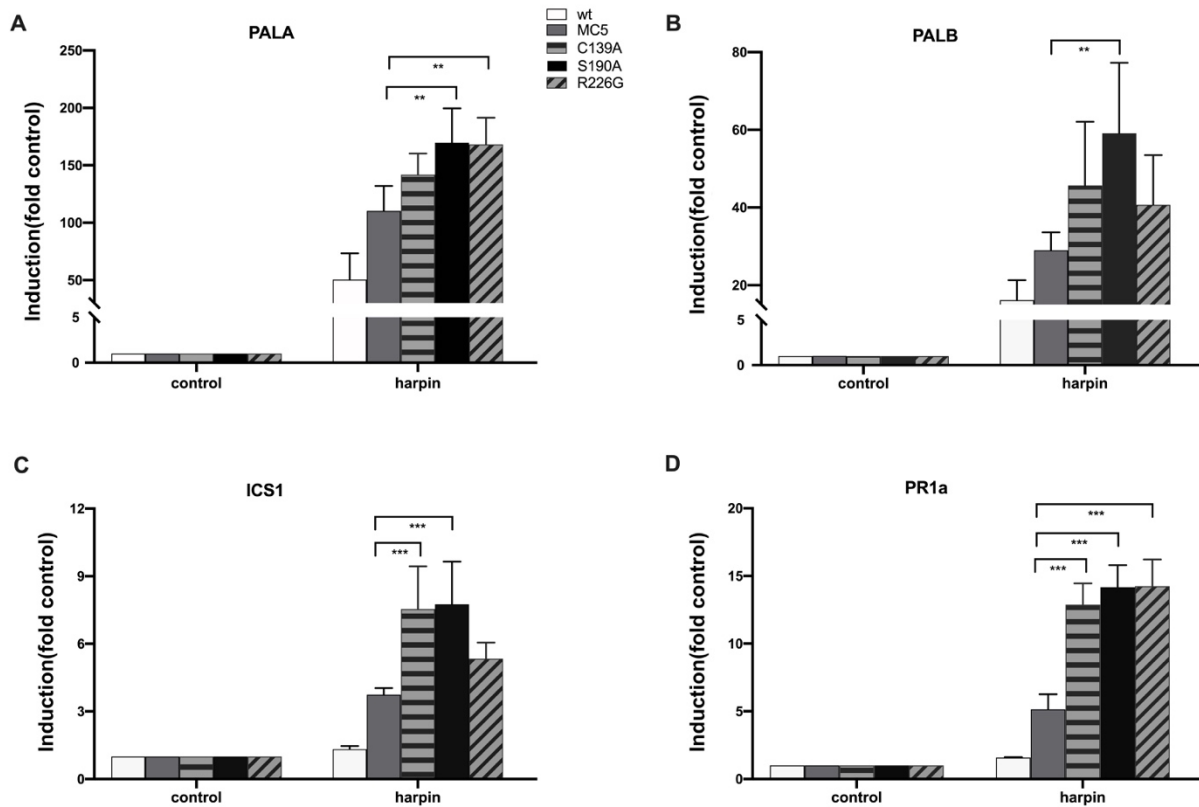


Figure 3.10 Steady-state transcription of SA-related genes in *VrMC5* and its variants induced by harpin. Induction levels for *PALA* and *PALB*, *ICS1* and *PR1a* to harpin treatment (30 μ g/ml, 6 h) were estimated by qPCR and normalized to *EF-1 α* as the internal standard. Data represents the mean \pm standard error (SE) of three independent biological replicates, asterisks indicate significant differences with ** P<0.01 and *** P<0.001 (Student's t-test).

3.1.6 JA mitigates Z-3-hexenal-triggered cell death and SA-related response

Jasmonic acid (JA) is known to activate basal immunity, and interplay between JA and SA was demonstrated in many ways. For example, JA antagonizes SA-dependent stress-induced accumulation of acidic PR proteins (Tomoya Niki, 1998) and high concentrations of JA and SA would result in a antagonistic effect on the JA- and SA-responsive genes *PDF1.2* and *PR-1*, respectively (Mur *et al.*, 2006). Besides, exogenous JA has been reported to act antagonistically to the *HPL1* overexpression to harpin response (Akaberi *et al.*, 2018). Therefore, we wondered if JA could suppress the Z-3-hexenal-induced cell death response. 100 μ M MeJA was added prior to Z-3-hexenal treatment, which remarkably inhibited the mortality caused by Z-3-hexenal in *VrMC5* (**Figure 3.11 A**), even in *VrMC5* mutants, this pretreatment reduced the low mortality to even lower level. The suppression effect of JA on cell death was more significant when it was induced by harpin (**Figure 3.11 B**).

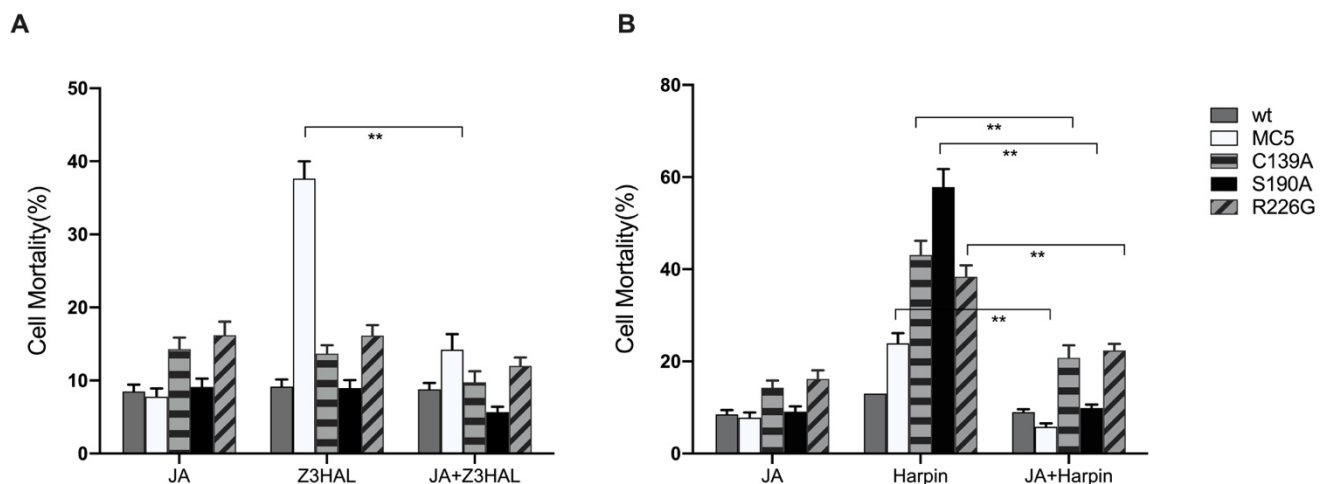


Figure 3.11 Effect of jasmonic acid (JA, 100 μ M) on cell mortality induced Z-3-hexenal and harpin. **A**, Cell mortality of *VrMC5* mutants induced by 12.5 μ M Z-3-hexenal, JA was applied into cells 30 min prior to addition of Z-3-hexenal, and mortality was scored after 15 min of treatment. **B**, Cell mortality of *VrMC5* mutants induced by 30 μ g/ml harpin, JA was applied with harpin simultaneously into cells, and mortality was scored after 48h of treatment. Data represents the mean \pm standard error (SE) of three independent biological replicates, ** indicates significant difference value $P < 0.01$ (Student's t-test).

To investigate whether inhibitory effects of MeJA on Z-3-hexenal or harpin-induced cell death accompany the inhibition of SA-defense gene activation, we analyzed the expression level of genes we test above. JA or Z-3-hexenal alone made a similar activation pattern of *PALA* or *PALB* on cells, while the combination dramatically suppressed the expression (**Figure 3.12 A, B**). On the other hand, JA did not lead to accumulation of much *ICS1* transcripts, although it downregulated *ICS1* in *VrMC5* (**Figure 3.12 C**). In the JA pretreatment group, induction of SA responsive gene *PR1a* was reduced (**Figure 3.12 D**), revealing an antagonistic function of JA for the SA-activated signalling pathway triggered by Z-3-hexenal. Like the role JA played in Z-3-hexenal-triggered pathway, the same effect was shown in harpin-induced response, there was significant expression inhibition between harpin treatment and JA-harpin combination (**Figure 3.13**).

Results

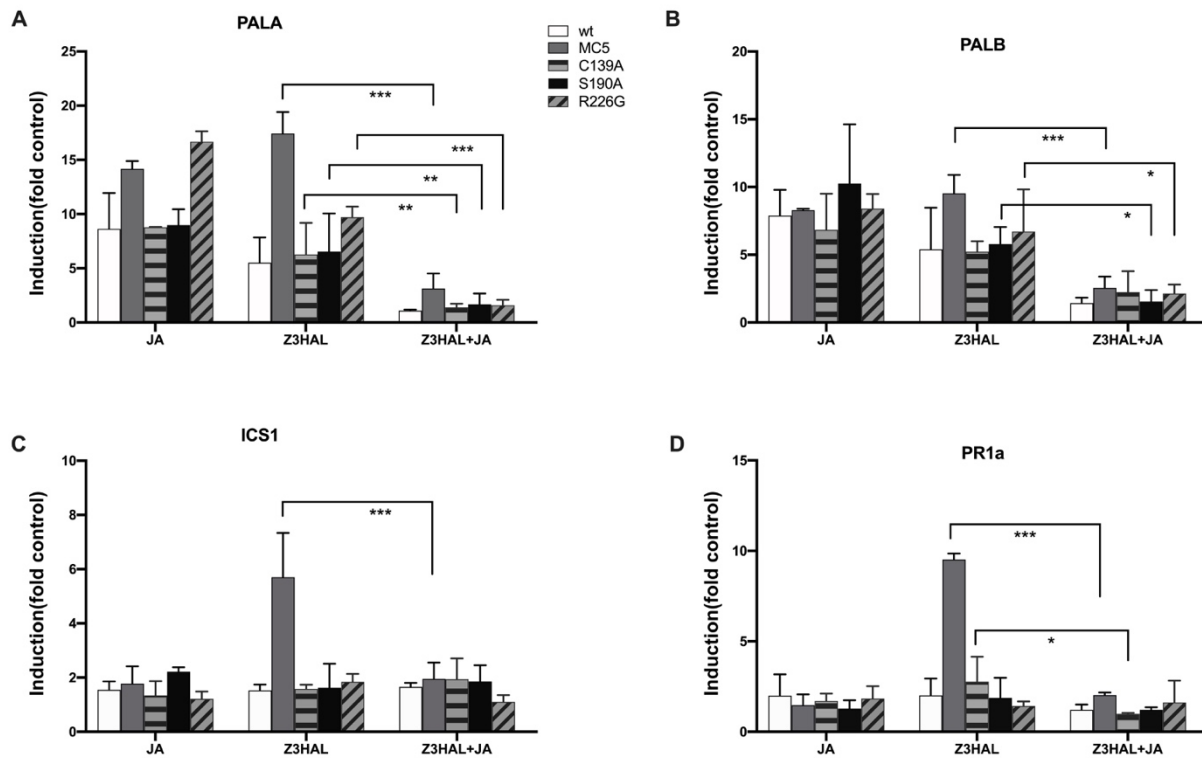


Figure 3.12 Effect of JA on transcription of SA-related genes in *VrMC5* and its variants induced by Z-3-hexenal. Induction levels for *PALA* and *PALB*, *ICS1* and *PR1* to Z-3-hexenal treatment (12.5 μ M, 30 min) with 100 μ M MeJA pretreatment for 30 min were estimated by qPCR and normalized to *EF-1 α* as the internal standard. Data represents the mean \pm standard error (SE) of three independent biological replicates, asterisks indicate significant differences with * $P < 0.05$, ** $P < 0.01$ and *** $P < 0.001$ (Student's t-test).

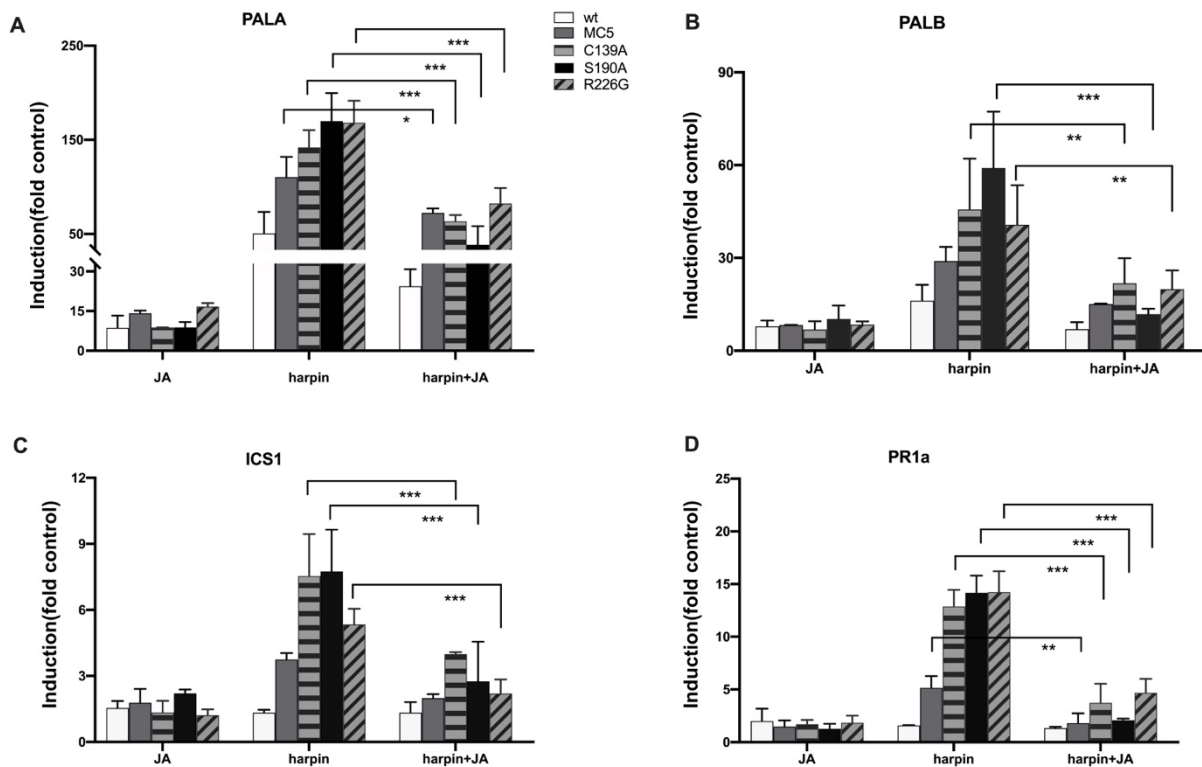


Figure 3.13 Effect of JA on transcription of SA-related genes in *VrMC5* and its variants induced by harpin. Induction levels for *PALA* and *PALB*, *ICS1* and *PR1* to harpin treatment (30 $\mu\text{g/ml}$, 6 h) with 100 μM MeJA were estimated by qPCR and normalized to *EF-1 α* as the internal standard. Data represents the mean \pm standard error (SE) of three independent biological replicates, asterisks indicate significant differences with * $P<0.05$, ** $P<0.01$ and *** $P<0.001$ (Student's t-test).

3.1.7 Ca^{2+} is required for *VrMC5* self-processing and enzymatic activity

Our experiments showed that *VrMC5* is involved in *Z*-3-hexenal induced cell death signalling and its mutant forms are deficient in self-processing *in vivo* and response to *Z*-3-hexenal. To get insight into the biochemical characterization of *VrMC5*, heterologous expression of *VrMC5* and its mutant forms in *E.coli* BL21(DE3) strain was necessary. The full-length coding sequence of *VrMC5* and mutants were cloned

Results

into pET21b vector to generate recombinant expression fused with a hexa-histidine tag at the C-terminus of the protein. Constructs used for purification are shown in **Figure 3.14 A**.

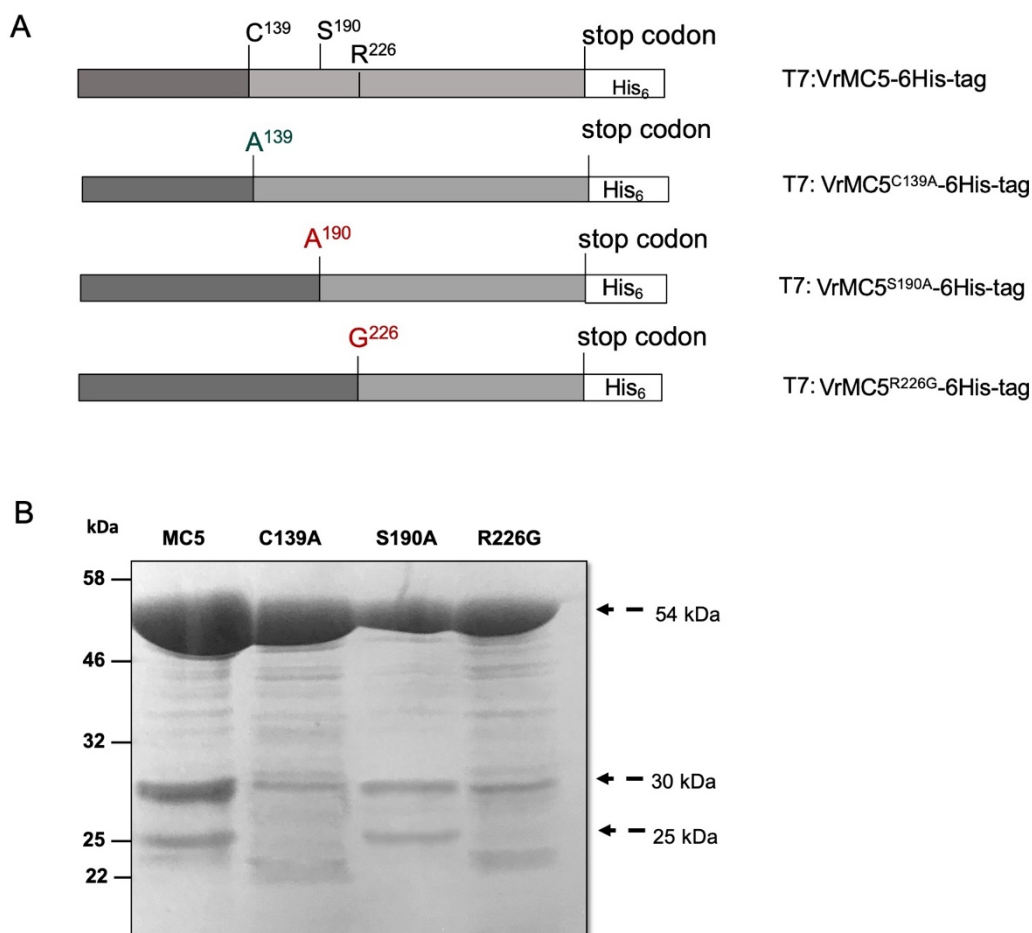


Figure 3.14 Analysis of self-processing of VrMC5 and its mutants *in vitro*. **A**, constructs for biochemical analysis of VrMC5 used in this study were shown. These four constructs have the hexa-histidine sequences at the C-terminus. **B**, 10 μ g of purified VrMC5 and its mutant forms (C139A, S190A, R226G) were separated on 12% SDS-PAGE, and bands were visualized by Coomassie Blue staining.

The recombinant proteins were purified under native conditions using Ni-NTA agarose, purified proteins were then separated through 12% SDS-PAGE. The full-

length recombinant VrMC5 with molecular weight of approximately 54 kDa, was also capable to autocleave itself. Consistent to their self-processing *in vivo*, one of major cleaved products of VrMC5 variants C139A and R226G were not detectable, approximately 25 kDa (**Figure 3.14 B**).

Previous studies showed most of Type II metacaspases required Ca^{2+} for the autoprocessing activity *in vitro*, such as *Arabidopsis* metacaspase AtMCP2d, Yca1 from *Saccharomyces cerevisiae* or MCA2 from *Trypanosoma brucei* (Watanabe & Lam, 2011b; McLuskey *et al.*, 2012; Wong *et al.*, 2012), suggesting a critical role for Ca^{2+} in the catalytic mechanism. To analyze VrMC5 Ca^{2+} dependent autolysis and activation, 10 μg purified VrMC5 was incubated in 100 μl enzyme reaction mixture with different concentration Ca^{2+} (from 1mM to 50 mM) for 20 min at room temperature. Upon incubation with Ca^{2+} , full-length VrMC5 was further processed into a few fragments. The conversion of VrMC5 to smaller fragments became increasingly more complete at higher concentration of Ca^{2+} (**Figure 3.15 A**).

We further examined whether Ca^{2+} -dependent autolysis of VrMC5 is reversible, a strong Ca^{2+} specific chelating agent EGTA was added into reaction buffer. SDS-PAGE confirmed EGTA directly inhibits Ca^{2+} -dependent self-processing by chelating Ca^{2+} , and it clearly depends on the ratio between $[\text{Ca}^{2+}]$ and $[\text{EGTA}]$ added in the reaction mixtures (**Figure 3.15 B**). This indicated that chelation of Ca^{2+} by EGTA directly blocks further self-processing of Ca^{2+} -activated VrMC5.

Boc-GRR-AMC is the preferred synthetic metacaspase substrate (Vercammen *et al.*, 2004; He *et al.*, 2008). VrMC5 theoretically was able to cleave after the arginine residue of GRR, releasing the fluorophore AMC. Therefore, we investigated the effects of Ca^{2+} concentration on VrMC5 Boc-GRR-AMC-hydrolyzing activity

(GRRase activity). The reaction was started by adding both Ca^{2+} and the substrate Boc-GRR-AMC simultaneously, 33 nM VrMC5 purified protein to catalyze the reaction. Data were monitored every min at room temperature and expressed as increase of relative fluorescence as a function of time. The enzymatic activities were recorded as nmol of substrate hydrolyzed/mg of protein/min (RFU). In the absence of Ca^{2+} or with a low concentration of Ca^{2+} (1 mM), no significant GRRase activity was detected during the reaction time, however, an intensive acceleration of the rate of AMC release was observed when Ca^{2+} concentration was more than 5 mM in the reaction. And this acceleration rapidly reached a plateau with higher Ca^{2+} concentration (**Figure 3.15 C**). Those results suggested that calcium is required not only for the autocatalytic processing of VrMC5, but also for the maintenance of its catalytic activity.

3.1.8 C139 and R226 are essential for VrMC5 self-processing and enzymatic activity

We further tested the autoprocessing and proteolytic activity of VrMC5 variants in the presence of Ca^{2+} . Same reaction condition set as described above, 10 μg purified proteins and 5 mM Ca^{2+} were added and incubated at room temperature. Neither variant C139A or R226G showed any obvious Ca^{2+} -induced processing patterns on SDS-PAGE, while variant S190A was activated by Ca^{2+} (**Figure 3.16 A**). In addition, GRRase activity assay exhibited that variant C139A and R226G showed null GRRase activity while this enzymatic activity was impaired in variant S190A (**Figure 3.16 B**). These results proved that Cys-139 and Arg-226 are critical for the self-processing and catalytic activity of VrMC5.

Results

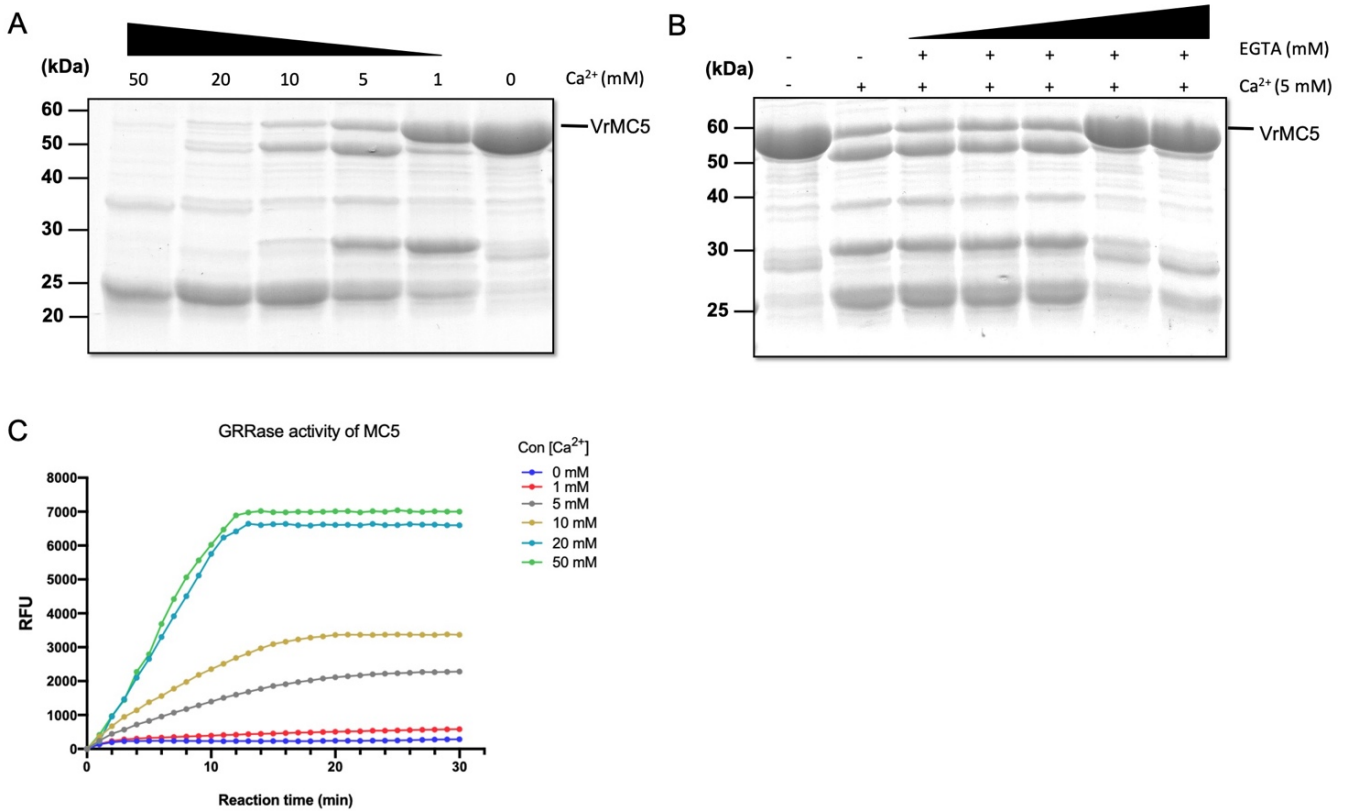


Figure 3.15 Ca^{2+} greatly facilitates the autolysis processing and GRRase activity of VrMC5. **A**, Calcium facilitates the autocatalytic processing of VrMC5 in a concentration-dependent manner. Mixtures were separated on 12% SDS-PAGE and bands were visualized by Coomassie Blue staining. **B**, Effect of EGTA on self-processing of VrMC5 in the presence of 5 mM Ca^{2+} , full-length VrMC5 bands significantly retained after sufficient EGTA addition. Mixtures were separated on 12% SDS-PAGE and bands were visualized by Coomassie Blue staining. **C**, VrMC5 GRRase activity was readout as relative fluorescence units (RFU), Ca^{2+} dependent activation profile of GRRase activity.

Results

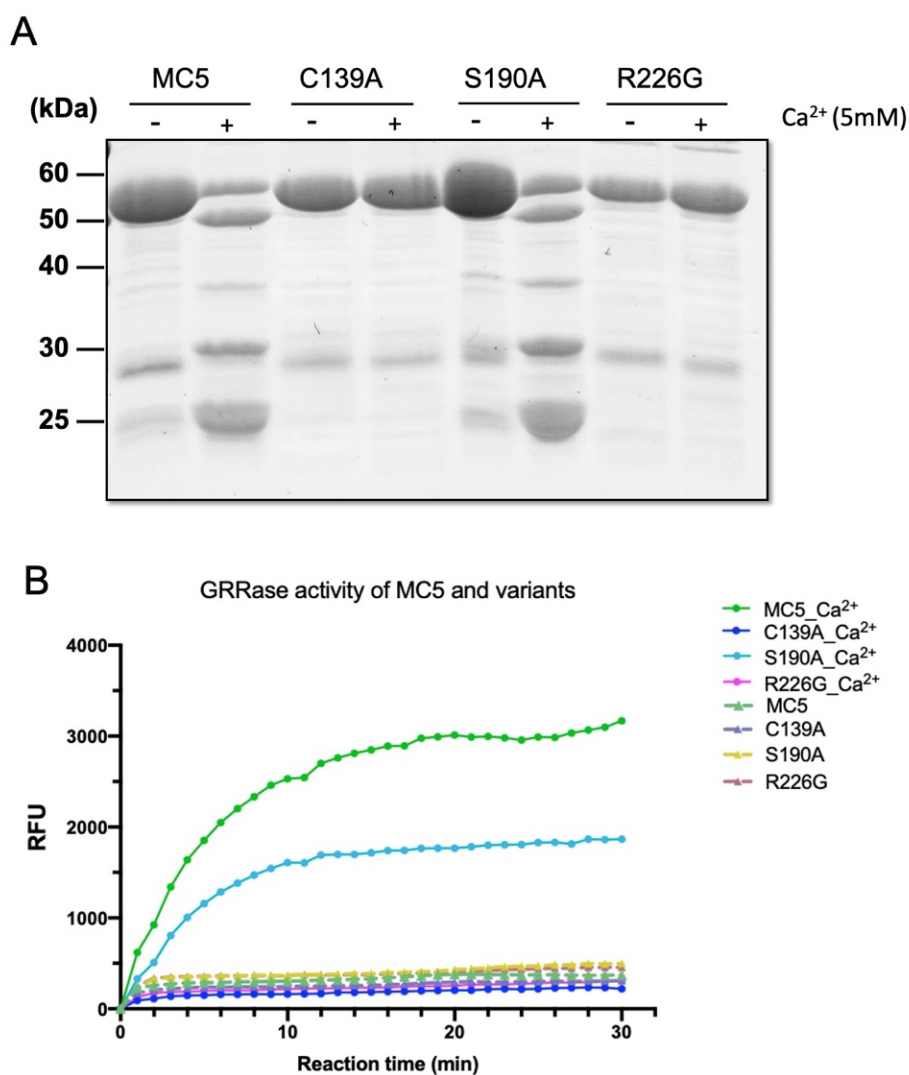


Figure 3.16 Self-processing and proteolytic activity of VrMC5 depends on site Cys-139 and Arg-226. **A**, Ca²⁺ dependent autolysis of VrMC5 variants in vitro. Mixtures were separated on 12% SDS-PAGE and bands were visualized by Coomassie Blue staining. **B**, Relative GRRase activity of each variants in the presence of 10 mM Ca²⁺, mutants C139A and R226G completely lost catalytic activity, and GRRase activity was impaired in mutant S190A. 30-40 nM purified proteins were tested in enzymatic activity assay.

3.2 Chapter 2: Cell permeating peptide inhibits VrMC5 activity.

In the previous approach, I have used overexpression of *VrMC5* are specific mutants thereof as gain of function strategy. This leads to the question, what the phenotype of a loss-of-function would be. To generate a *VrMC5* defective mutant would require a targeted knock-out. While this would be principle possible using a CRISPR-Cas strategy, for BY-2 cells, the success of this approach has remained limited, culminating in complex chimeras, which had been proposed to be a consequence of the rapid division of those cells (Mercx *et al.*, 2016). Hence, I decided to use chemical engineering as a novel strategy to control protein function. In order to deliver functional cargos into cells, cell-penetrating peptides (CPPs) serve as a vehicle to mediate the plasma membrane passage of those cargos to interact with their intracellular targets.

3.2.1 Cellular uptake of LMTP-peptide in BY-2 cell

Lipid-membrane-translocating peptide (LMTP) is one of most common and effective carriers that we used in this study. The polypeptide fragment applied in this study is derived from Apoptotic Suppressor p35, which could attack the catalytic cysteine of caspase 3 and denature it (Stefan J. Riedl, 2001; Matza-Porges *et al.*, 2003). We aimed to manipulate *Vitis* metacaspase 5 activity via delivering this LMTP-peptide (sequence: KKAAAVLLPVLLAAP-VDQMDG-amide) into BY-2 cells.

A time-course experiment was conducted with BY-2 wild type cells to gain insight into the cellular uptake aspect of LMTP-peptide. Rhodamine B conjugated with LMTP-peptide was utilized to visualize the uptake of the peptide. 3-day-old non-transformed BY-2 cells were incubated with 1 μ M Rhodamine B-LMTP-peptide and

Results

the rhodamine signal was followed by spinning disc microscopy at an excitation wavelength of 561 nm. At the early stage of uptake (15 min and 30min), signal increased slowly but rapidly accumulated after the first hour. Signal in most of cells went up saturation at 2 h after incubation (**Figure 3.17**).

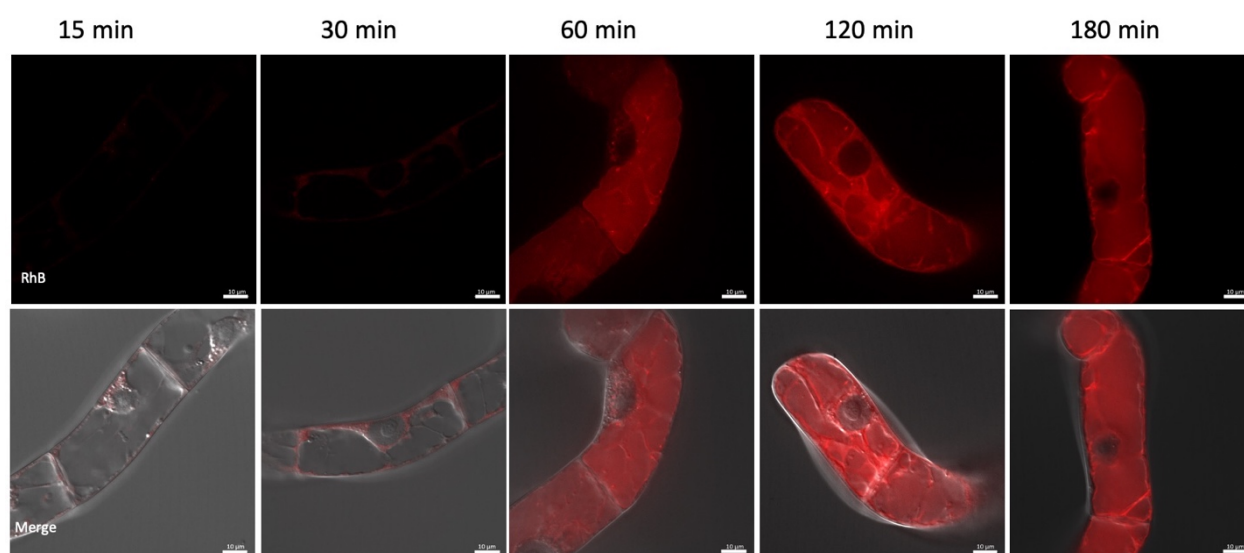


Figure 3.17. Time course for the uptake of LMTP-peptide into non-transformed BY-2 cells. 1 μ M LMTP-peptide labelled with Rhodamine B incubated with 3-day-old cells. Observations are representative of three independent experiments with a population of 100 individual cells for each biological experiment. Exposure time was fixed as 500 ms. Scale bar=10 μ m.

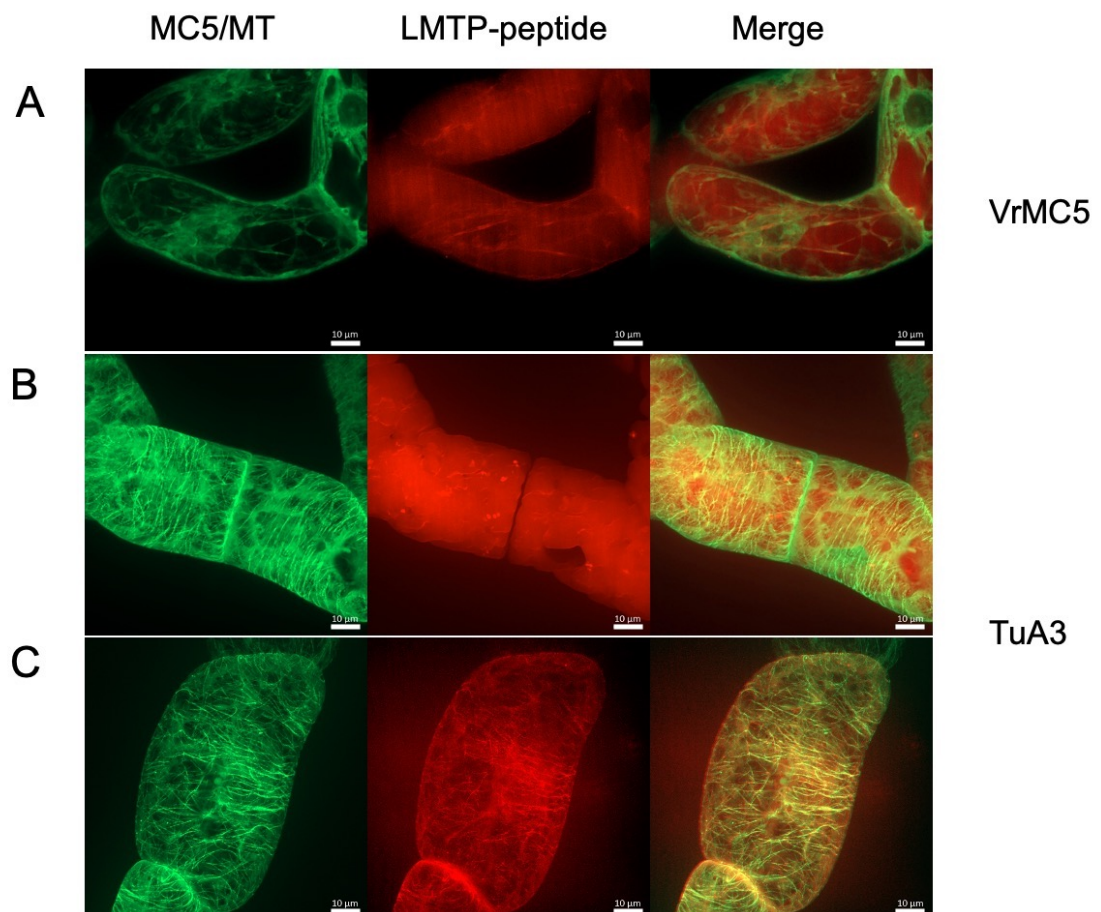
3.2.2 Subcellular localization of LMTP-peptide

The LMTP-peptide was designed to bind to metacaspase conserved catalytic site, therefore we verified the LMTP-peptide subcellular localization in *VrMC5-GFP* overexpression cells. 1 μ M Rhodamine B-LMTP-peptide was incubated in *VrMC5-GFP* for 2h and washed thoroughly, the rhodamine signal was observed throughout the cytoplasm and overlapped with filamentary structure (**Figure 3.18 A**). Moreover, there were two localization patterns in *TuA3-GFP*, one was like in *VrMC5* (**Figure**

Results

3.18 B), the other was specifically co-localized with microtubule filaments (**Figure 3.18 C**).

Since LMTP-peptide could bind to microtubules, we further investigated the peptide performance in *TuA3-GFP* during mitosis. 1 μ M LMTP-peptide coupled to Rhodamine B was incubated in active proliferation status *TuA3-GFP* cells. The clear co-localization between microtubules and LMTP-peptide was shown in **Figure 3.19**. This tight relevance was recorded in both proliferating or the stationary phases of the cell, except in cytokinesis phase. And this only was observed in *TuA3*, not in other cell lines, like wt or *GF11* (**Figure 3.17** and **Figure 3.22 A-C**).



Results

Figure 3.18 Localization of the LMTP-peptide in transformed BY-2 cells. **A**, Localization of LMTP-peptide in *VrMC5-GFP* cells. **B and C**, Localization of LMTP-peptide in *TuA3-GFP* cells. 1 μ M LMTP-peptide was incubated in cells for 2 hours. The representative cells showed merged z-stack of confocal sections from mid-plane. Scale bar=10 μ m.

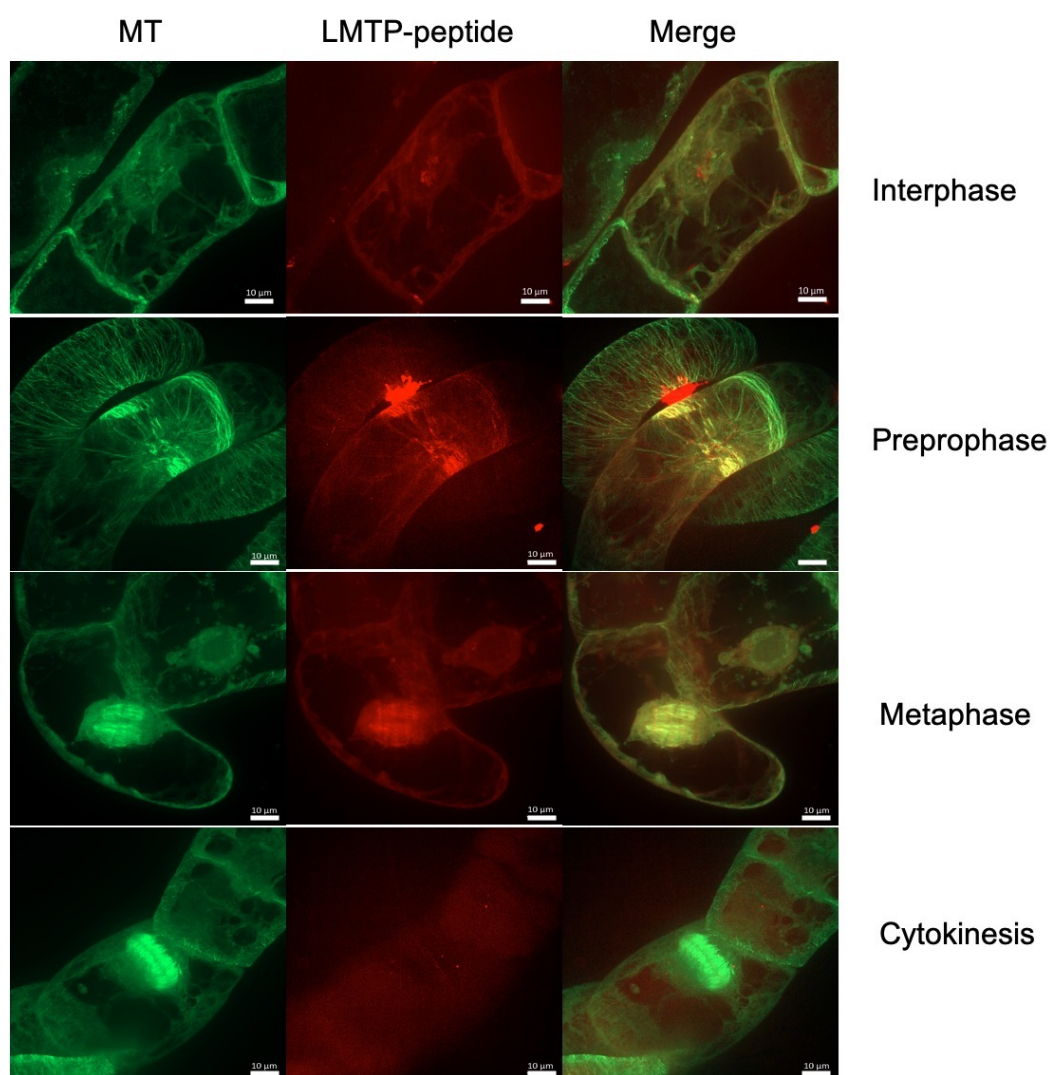


Figure 3.19 Localization of the LMTP-peptide in *TuA3-GFP* during mitosis. Peptide was visualized in 5-day-old *TuA3-GFP* cells during different phases of mitosis. 1 μ M LMTP-peptide was incubated in cells for 2 hours. The representative cells showed merged z-stack of confocal sections from mid-plane. Scale bar=10 μ m.

3.2.3 LMTP-peptide is taken up into cell through endocytosis

To find out whether endocytosis is required for cellular uptake of the peptide, we used an endocytosis inhibitor to disrupt the processing passage. Ikarugamycin (IKA) could specifically block clathrin-mediated endocytosis, but not other endocytosis pathways (Elkin *et al.*, 2016). *TuA3-GFP* cells at day 7 after subcultivation were pretreated with 10 μ M Ikarugamycin for 30 min, and further incubated with 1 μ M LMTP-peptide for additional 2 h to ensure that the peptide was fully taken up. In contrast to complete uptake of the peptide (**Figure 3.20 A-C**), pretreatment with Ikarugamycin evidently showed that the uptake of the LMTP-peptide was blocked efficiently, signal was predominantly confined in the cell wall (**Figure 3.20 D-F**). These results showed that the uptake of LMTP-peptide into cell depends on endocytosis.

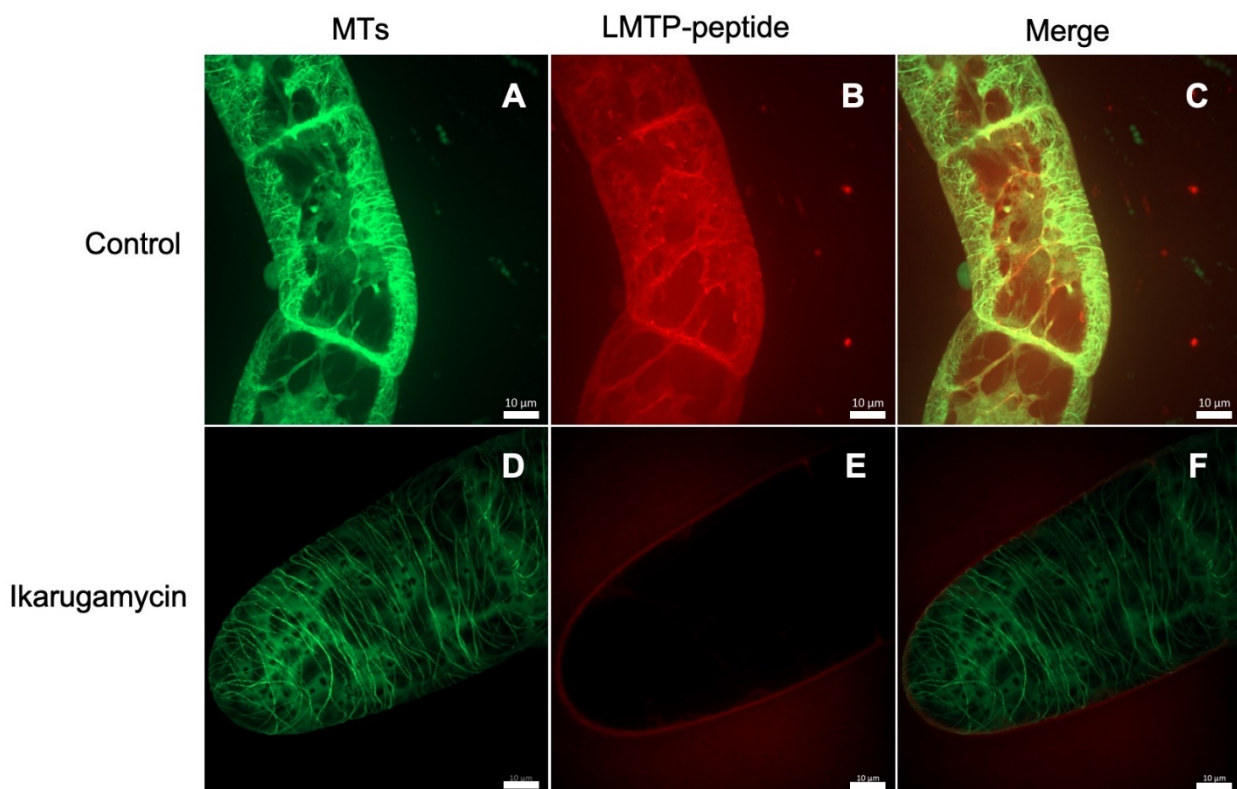


Figure 3.20 Inhibitors of endocytosis impair the cellular uptake of LMTP-peptide into *TuA3-GFP* cell. Control cells (**A-C**) showed co-localization of microtubules and LMTP-peptide, in comparison to cells that were pretreated with endocytosis inhibitor 10 μ M Ikarugamycin for 30 min (**D-F**). The GFP signal indicated tubulin (**A, D**), the rhodamine signal indicated the LMTP-peptide (**B, E**), and the merged signal (**C, F**) is shown for representative cells. The representative cells showed merged z-stack of confocal sections from mid-plane. Scale bar=10 μ m.

3.2.4 Uptake of LMTP-peptide depends on microtubules, not actin

To address the role of cytoskeleton in the cellular uptake of LMTP-peptide, *GF11* and *TuA3-GFP* were used as reporter for actin filaments and microtubules, respectively. Since this peptide could bind to microtubules, we assumed that the uptake was relevant to microtubules. *TuA3-GFP* cells were pretreated with 10 μ M oryzalin, a plant-specific inhibitor to depolymerize microtubules, for 1 h, before incubation with 1 μ M LMTP-peptide for additional 2 h. Compared to the control condition, rhodamine signal still was overlaid with tubulin despite the tubulin has been disassembled and rhodamine signal became slightly weaker (**Figure 3.21 D-F**).

However, when the *GF11* cells were pretreated for 1h with 10 μ M of Latrunculin B, a specific inhibitor that prevents actin assembly, followed by 2 h peptide incubation, actin filaments were eliminated completely (**Figure 3.22 D**). Although actin had been disintegrated by Latrunculin B, the pretreated cells were able to take up LMTP-peptide effectively as normal (**Figure 3.22 E and F**). In contrast, in the control cells rhodamine signal was distributed throughout the entire cytoplasm, highlighting a few filaments supposed to be microtubules (**Figure 3.22 B**). These observations showed that microtubules are involved in LMTP-peptide uptake, while actin not.

Results

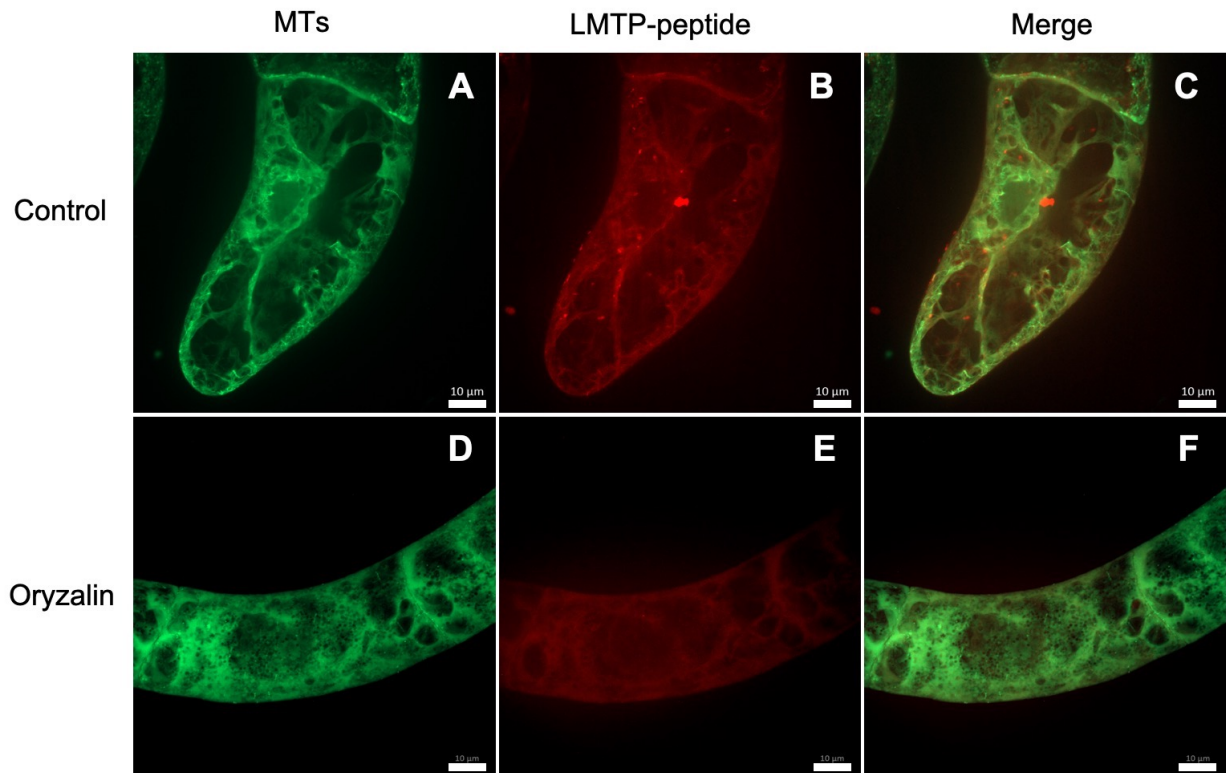


Figure 3.21 Uptake of LMTP-peptide requires microtubules. 7-day-old microtubule marker line *TuA3-GFP* cells were incubated with 1 μM of LMTP-peptide for 2h either without (**A–C**) or with (**D–F**) microtubule depolymerizing drug oryzalin (10 μM , 1h). The GFP signal indicated tubulin (**A, D**), the rhodamine signal indicated the LMTP-peptide (**B, E**), and the merged signal (**C, F**) were shown for representative cells. The representative cells showed merged z-stack of confocal sections in the mid-plane. Scale bar=10 μm .

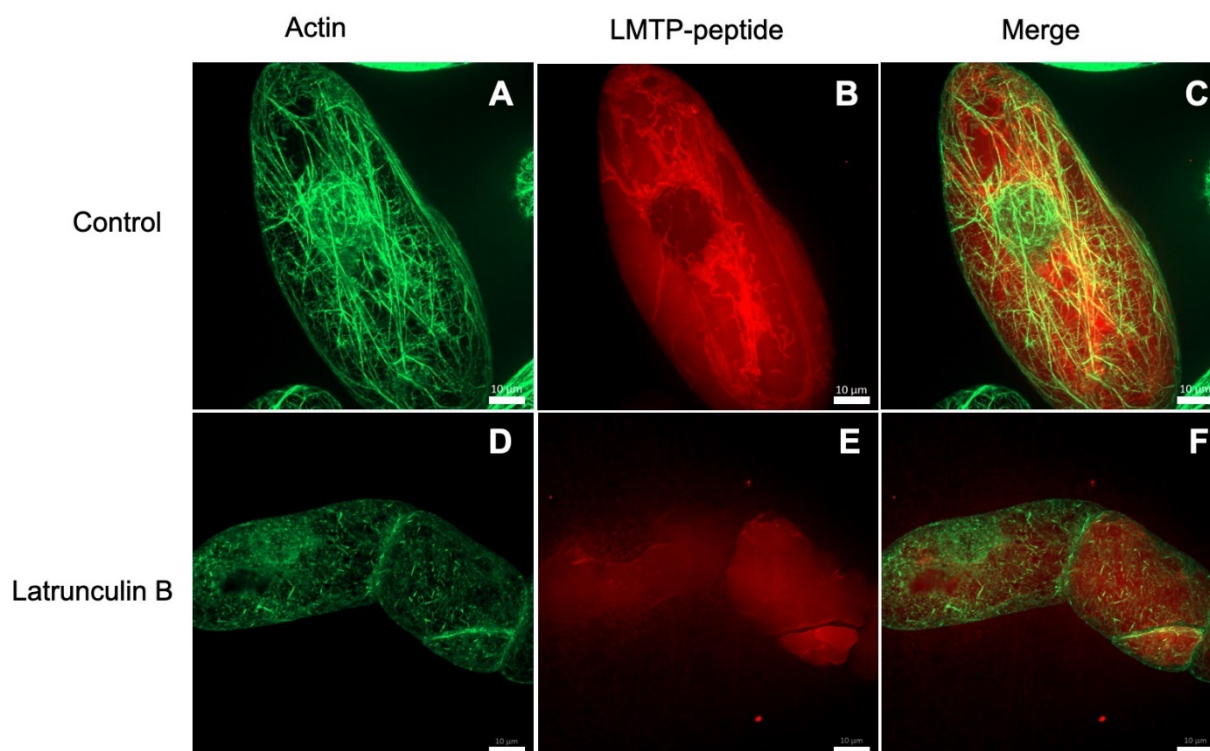


Figure 3.22 Acin filaments are not relevant for uptake of LMTP-. 3-day-old actin marker line *GF11* cells were incubated with 1 μM of LMTP-peptide for 2 h either without (A–C) or with (D–F) Latrunculin B (10 μM , 1h) to eliminate actin filaments. The GFP signal indicated actin (A, D), the rhodamine signal indicated the LMTP-peptide (B, E), and the merged signal (C, F) were shown for representative cells. The representative cells showed merged z-stack of confocal sections from the mid-plane. Scale bar=10 μm .

3.2.5 LMTP-peptide could relieve actin depolymerization to Z-3-hexenal

Since we had proved that LMTP-peptide could target to microtubules, as well as metacaspase 5, we therefore explored the potential effect of LMTP-peptide on biological changes of BY-2 cells induced by Z-3-hexenal. We already knew that Z-3-hexenal could trigger actin depolymerization and uptake of peptide did not depend on actin, we asked whether a pretreatment with LMTP-peptide could mitigate this morphological damage of actin. We followed the actin response to 3-day-old *GF11*

cells pretreated with 1 μM of LMTP-peptide for 2 h and additional 10 min incubation with 12.5 μM Z-3-hexenal. Actin filaments in a few cells remained at a semi-integrated status, exhibiting the co-existence of integrated filaments and punctate structure (**Figure 3.23 A**). The quantification of distribution of cells with different actin responses showed that only few cells with integrated actin meshwork could be observed in Z-3-hexenal treatment, while the ratio of cells along with integrated and semi-integrated actin was increased to 3.2 % and 6.3% under LMTP-peptide pretreatment condition, respectively (**Figure 3.23 B**).

3.2.6 LMTP-peptide could decrease cell death induced by Z-3-hexenal and harpin

As a tool for chemical manipulating metacaspase 5, the potential effect of LMTP-peptide on mortality in *VrMC5* cell line was examined. 1 μM LMTP-peptide was added prior to Z-3-hexenal or harpin treatment, which remarkably suppressed the mortality in *VrMC5* caused by Z-3-hexenal or harpin. Even in wild type, this pretreatment reduced the low mortality to even lower level (**Figure 3.24 A**). The suppression effect of peptide on cell death was significant when it was induced by harpin as well (**Figure 3.24 B**).

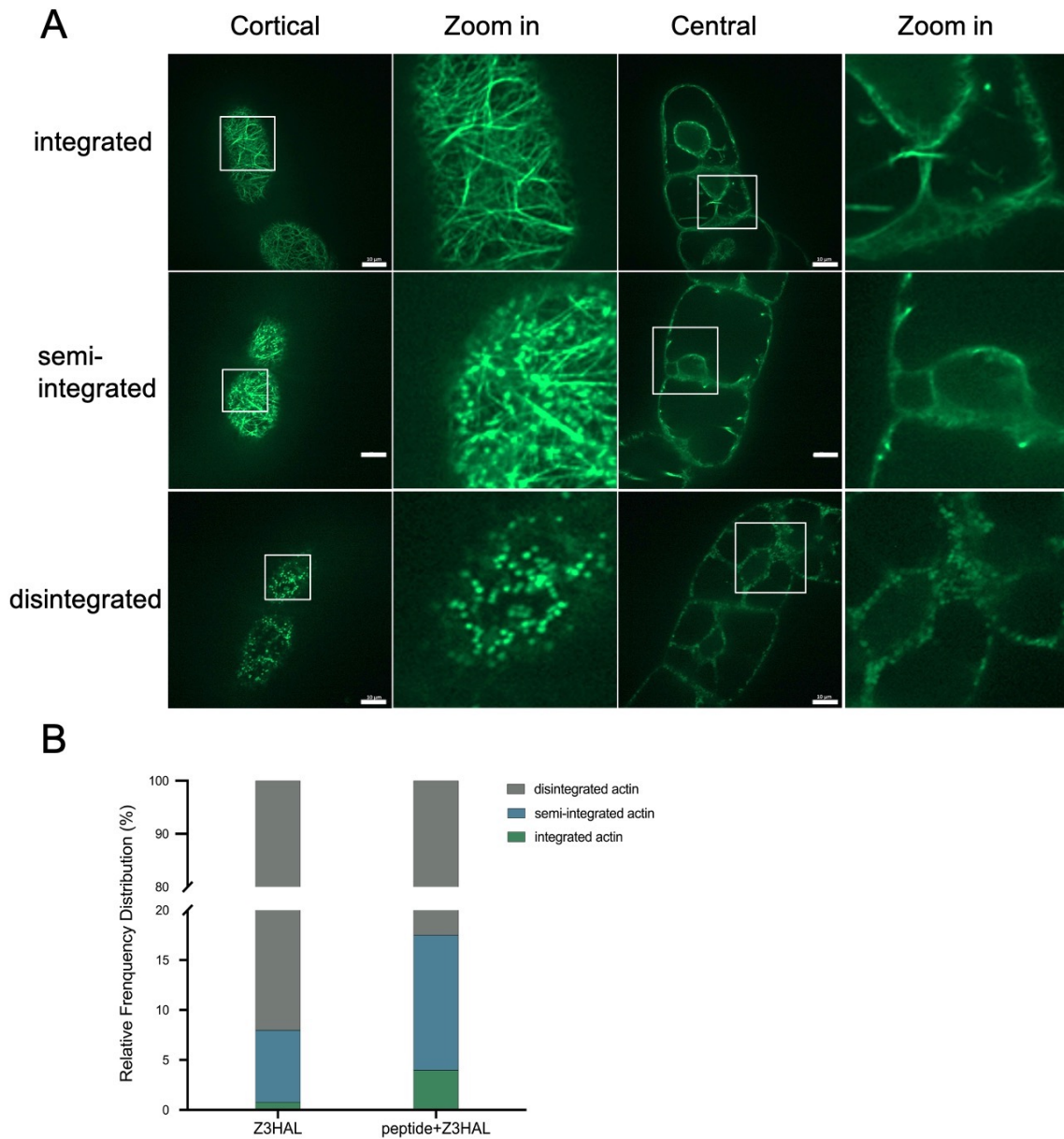


Figure 3.23 Effect of LMTP-peptide on actin depolymerization caused by Z-3-hexenal. The response of *GF11* to Z-3-hexenal with 1 μ M of LMTP-peptide pretreatment for 2 h. **A**, Representative cells showed three patterns of actin network morphology. **B**, Quantification of relative frequency distribution of cells with various actin patterns. Observations are representative of four independent experimental series with a population of 100 individual cells for each treatment. Scale bar=10 μ m.

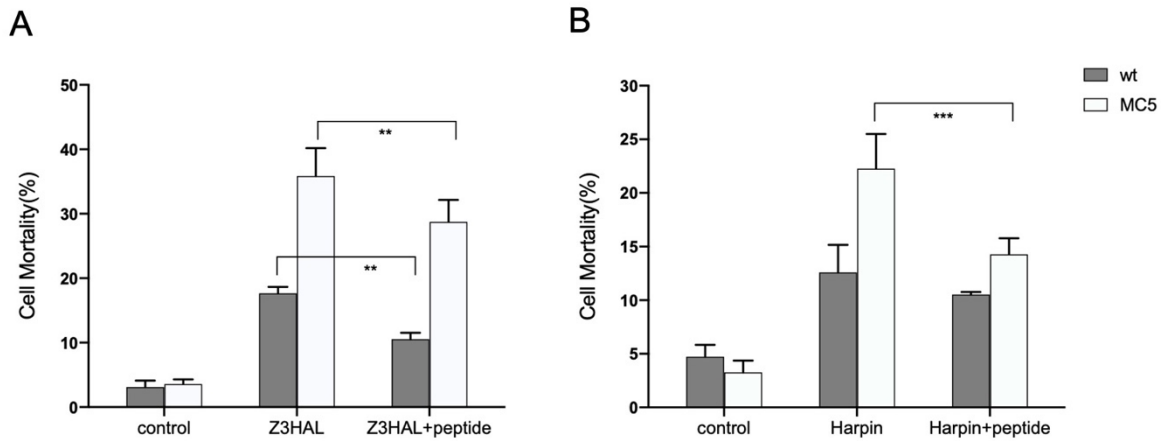


Figure 3.24 Effect of LMTP-peptide on cell death caused by Z-3-hexenal and harpin. **A**, Cell mortality of wt and *VrMC5* induced by 12.5 μ M Z-3-hexenal, peptide was applied into cells 2h prior to addition of Z-3-hexenal, and mortality was scored after 15 min of treatment. **B**, Cell mortality of wt and *VrMC5* induced by 30 μ g/ml harpin, peptide was applied with harpin simultaneously into cells, and mortality was scored after 48h of treatment. Data represents the mean \pm standard error (SE) of three independent biological replicates, asterisks indicate significant differences with** P<0.01 and *** P<0.001 (Student's t-test).

3.2.7 LMTP-peptide protects VrMC5 from autoproteolysis in the presence of Ca^{2+}

It had been proved above that cell death induced by Z-3-hexenal in *VrMC5* was relevant to VrMC5 self-processing and proteolytic activity, therefore we further tested the autoprocessing and proteolytic activity of VrMC5 in the presence of LMTP-peptide. Varying concentration LMTP-peptide was mixed with 10 μ g purified proteins for 10 min in 100 μ l reaction buffer and 1 mM Ca^{2+} was added for additional 10 min at room temperature. Upon addition of sufficient LMTP-peptide, full-length VrMC5 bands was slightly increased in the presence of Ca^{2+} , and the smaller processing fragments decreased (**Figure 3.25 A**). Moreover, GRRase activity assay of VrMC5 was revealed that 20 μ M of LMTP-peptide was able to

Results

inhibit VrMC5 catalytic activity (**Figure 3.25 B**). Those results demonstrated that LMTP-peptide protects the autolysis processing and proteolytic activity of VrMC5.

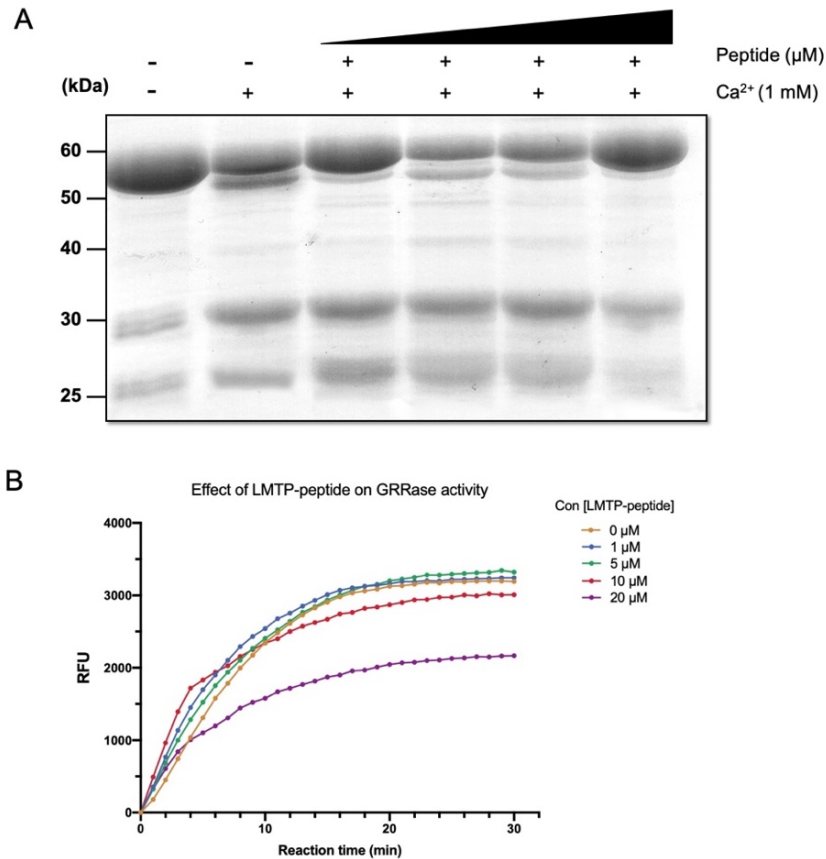


Figure 3.25 The effect of LMTP-peptide on autolysis processing and GRRase activity of VrMC5. **A**, LMTP-peptide bind to VrMC5 on the addition of 1 mM Ca^{2+} , causing a small regain of full-length VrMC5 bands and protected VrMC5 from autoproteolysis in the presence of 1 mM Ca^{2+} . The mixtures were separated on 12% SDS-PAGE and bands were visualized by Coomassie Blue staining. **B**, VrMC5 GRRase activity was suppressed with high concentration LMTP-peptide in the presence of 10 mM Ca^{2+} . 33 nM purified VrMC5 was tested in the presence of 10 mM Ca^{2+} in enzymatic activity assay.

3.3 Summary of results

In the first part of this study, we revealed some biological features of VrMC5 and how it regulates in cell death induced by Z-3-hexenal. The main findings are listed following:

- 1) The heterologous expression of VrMC5 co-localizes with microtubules.
- 2) As a type II metacaspase, VrMC5 requires self-processing for activation during the Z-3-hexenal triggered PCD.
- 3) The autolysis and enzymatic activity of VrMC5 is calcium dependency.
- 4) VrMC5 catalytic site Cys-139 and well-conserved site Arg-226 are essential for its autolysis processing and activity, while the other putative Ser-190 doesn't affect autolysis but relates to VrMC5 activity.
- 5) VrMC5 is a positive regulator in Z-3-hexenal induced cell death and positively regulate SA signalling under induction of Z-3-hexenal.

The second part described how a chemical tool, LMTP-peptide, manipulate VrMC5 activity *in vivo*. We presented the uptake mechanism of short peptide and the effect of peptide on VrMC5. The main findings are:

- 1) The uptake of LMTP-peptide is saturable and it through clathrin-dependent endocytosis to penetrate cell membrane.

Results

- 2) LMTP-peptide not only targets at cytoplasm but also specifically at microtubules.
- 3) LMTP-peptide endocytic uptake depends on microtubules but not actin filaments.
- 4) LMTP-peptide could repress the cell death and actin depolymerization caused by Z-3-hexenal and harpin in *VrMC5* overexpressor.
- 5) LMTP-peptide inhibits enzymatic activity and auto-proteolysis of *VrMC5* in the presence of Ca^{2+} .

4 Discussion

Almost every green plant could produce Green Leaf Volatiles (GLVs) to interact with their continuously changing environment. As one important group of volatile organic compounds, GLVs not only impart aromas and flavours to many natural foods but also emerge as key players in plant defence responses to pathogens or herbivores and plants priming (ul Hassan *et al.*, 2015). The importance of GLVs in the plant response to microbial pathogen attack has been studied since the early 1990s. In the last few decades, various studies have revealed the roles that GLVs play in plant physiology and defence, but the downstream signals and transduction mechanism leading to defence response remain elusive. In this study, we aim to explore the downstream molecular mechanisms in a typical GLV, Z-3-hexenal induced defence signalling.

Meanwhile, mild or severe stress might qualitatively alter plant response, either leading to stress priming and adaptation or to hypersensitive response (HR) (Niinemets, 2010). Metacaspases as important executor in regulating HR have been identified in various organisms over a few decades. VrMC5 from a family of metacaspase in grapevine has been reported as a candidate to mediate HR, we then ask what the roles of VrMC5 play in Z-3-hexenal triggered cell death?

The first half of this study, we present the cellular response and activation mechanism of VrMC5 in Z-3-hexenal induced signalling. We have shown VrMC5 positively regulates HR-related cell death and basal immunity activated by JA could mitigate this cell-death. Moreover, We also reveal a short peptide as the chemical

engineering tool manipulates VrMC5 enzymatic activity *in vitro* and uptake mechanism of the peptide.

4.1 Biological characterization of VrMC5

4.1.1 The heterologously expressed VrMC5 co-localizes with microtubules

Previous work in our lab has analyzed the secondary structure of VrMC5 and predicted VrMC5 does not target in any organelle, implying that VrMC5 protein is probably located in the cytoplasm. Microscopy observation in stable expression of VrMC5-GFP living cell showed more details, for instance the morphological change in the nucleus during mitosis. This pattern is similar to microtubules array during cell division, during which cortical microtubules arrays are gradually replaced by PPB, spindle and phragmoplast. The further study presented the co-localization between VrMC5 and microtubules, which is distinct from other reported metacaspases in high plants (**Figure 3.1**).

Features on the subcellular localization could provide potential protein-protein interactions. For example, rice metacaspase OsMC1 was exclusively localized in the nucleus, whereas OsMC3 was found to distribute both in the cytoplasm and nucleus, furthermore, OsMC1 interacted with OsLSD1 and OsLSD3 while OsMC3 only interacted with OsLSD1 (Huang *et al.*, 2015). Arabidopsis AtMC5 localized in cytosol and nucleus, interacting with AtDAD1, a transmembrane protein in the ER network surrounding the nucleus, to regulate cell death. Except for unknown substrates of VrMC5, the co-localization with microtubules of VrMC5 also led to the question, whether VrMC5 is involved in non-death pathway.

4.1.2 Interaction between VrMC5 with cytoskeleton

It has to be noted that VrMC5 fused with GFP at C-terminus and the co-localized signal of GFP might be the cleaved fusion protein due to self-processing of VrMC5. Further biochemical analysis using EPC affinity revealed that VrMC5 directly binds to α -tubulin (**Figure 3.2**), not only binds to tyrosinated α -tubulins but also detyrosinated α -tubulins, that indicates the correlation between VrMC5 and dynamic microtubules.

Associating with the role of microtubule in cell division and VrMC5 localization pattern, it has a possibility that VrMC5 might plays a function in cell proliferation. It is the first time to propose this hypothesis in plants, while in parasitic protozoa and yeast several metacaspases have been found to regulate cell proliferation (Helms, 2006; Ambit *et al.*, 2008; Cookson *et al.*, 2008). *Leishmania major*, its metacaspase LmjMCA relatively disperses throughout the cell during interphase but tends to concentrate in the kinetoplast during mitochondria segregation and it also translocates to the nucleus to associate with mitotic spindle during mitosis. Overexpression or deletion LmjMCA resulted in either growth defect with impairment of cytokinesis or inviability, suggesting this protein is essential during cell division (Ambit *et al.*, 2008).

Apart from microtubules, actin filaments also showed a connection with VrMC5. Analysis of actin in *VrMC5-GFP* cells presented the actin overlapped GFP signal of VrMC5 (**Figure S1**). During cell death, in order to achieve such dramatic morphologic changes, apoptotic cells make profound cytoskeleton reorganizations (Ndozangue-Touriguine *et al.*, 2008). On the other hand, actin as a typical substrate of caspases during apoptosis has been found among targets of *Arabidopsis* metacaspase AtMC9 (Mashima *et al.*, 1999; Tsiatsiani *et al.*, 2013). Our study also

exhibited the alteration of VrMC5 subcellular expression pattern under inducer Z-3-hexenal or harpin (**Figure 3.4 A**). Actin architecture was broke down after harpin elicitation and punctate distribution throughout the cell under Z-3-hexenal induction(**Figure 3.3 A**). Regarding microtubules response, radial microtubule elimination but cortical microtubules remained integrated caused by harpin, while Z-3-hexenal dramatically resulted in microtubules depolymerization in a spotty pattern (**Figure 3.3 B**) (Guan *et al.*, 2013). The subcellular response of VrMC5 to elicitors was highly similar to microtubules, whereas actin response had less similarity. Our results suggest VrMC5 has close interaction with the cytoskeleton, especially with microtubules, that would guide further study to explore its potential function on cell proliferation or the roles on cytoskeleton reorganization during cell death.

4.2 VrMC5 acts as a positive regulator in Z-3-hexenal triggered HR cell death

Contribution of GLVs in relation to decreasing the infection and inhibiting the growth of bacteria has been documented. There are several examples that GLVs are emitted by plants upon biotic stress caused by pathogens, some volatiles may play a role in hypersensitive response. For instance, upon *Pseudomonas* infection, Lima bean leaves release sufficient amounts of E-2-hexenal and Z-3-hexenol to inhibit bacterial growth *in vitro* (Croft *et al.*, 1993). Additionally, meta-analysis suggested that the lower conversion from Z-3-hexenal to E-2-hexenal after fungal treatment and herbivory, on the other hand, clearly increases the conversion from Z-3-hexenal to E-2-hexenal (Ameye *et al.*, 2018). The idea that volatiles can initiate plant defence responses has been confirmed since a few decades ago. Treating plants with GLVs can induce the expression of several defence-related genes and downstream

metabolites production (Kant *et al.*, 2009; Karban *et al.*, 2014; Engelberth *et al.*, 2013). Since the previous study revealed that *Z*-3-hexenal acts as cellular signal rather than as toxic executor of cell death while *E*-2-hexenal not (Akaberi *et al.*, 2018), the downstream response of this signalling is worth to investigate.

Although the metacaspase family of grapevine has been previously characterized (Zhang *et al.*, 2013), few of the family members has been studied for the biological function in plant hypersensitive response (HR) by analysing their induction fold under infection (Gong *et al.*, 2019). Our molecular and genetic studies provided evidence that VrMC5 is involved in facilitating cell-death induction upon treatment with *Z*-3-hexenal and bacterial elicitor harpin. Phenotypic studies revealed that overexpression of VrMC5 results in a significantly increased mortality and disperses throughout cell along with the disintegration of cytoskeleton under *Z*-3-hexenal (**Figure 3.4 A and B**). These data supported the function of VrMC5 as a positive mediator of cell death triggered by biotic types of cell-death inducers. That is similar to the phenotypes of *VrMC5* and *VrMC2* overexpressors to harpin-induced cell death.

As *VrMC5* overexpressor was sensitive to *Z*-3-hexenal, our biochemical analysis using anti-GFP antibody revealed that VrMC5 degraded in multiple forms with various molecular masses, including proenzyme and processed degraded forms (**Figure 3.4 C**). It was noted that degradation or processing of VrMC5 is apparently dependent on treatment time and sensitive to *Z*-3-hexenal. The drawback here was the antibody used to detect the accumulation of degraded forms of VrMC5. Unlike the antibody targeting to the specific region of metacaspase (for example, anti-AtMCP2d antibody), the anti-GFP was limited to detect the fragments with C-terminal, that explained why the accumulation pattern of degraded VrMC5 is inconsistent with AtMC4 (Watanabe & Lam, 2011a). Although *VrMC5*

overexpressor showed the increased sensitivity of cell-death to harpin, the elicitor did not affect the processing of VrMC5 (**Figure S2**). It is intriguing that the self-processing of AtMC4 was highly correlated with the induction of a PCD-inducing mycotoxin FB1 and pathogen-induced cell death (Watanabe & Lam, 2011a).

In plants, one of the prominent molecular events that lead to HR is the accumulation of SA, changes in transcriptional reprogramming, intracellular calcium levels and production of antimicrobial compounds. In addition, the disruption of actin filaments leads to the induction of the SA pathway in *Arabidopsis* and tobacco (Kobayashi & Kobayashi, 2007; Matoušková *et al.*, 2014). Therefore, the signalling pathway induced by Z-3-hexenal, resulting in actin depolymerization and cell death, is supposed to be associated with SA signalling. Thus, we found by quantitative RT-PCR analysis that center genes for SA synthesis *PALA*, *PALB* and *ICS1* significantly upregulated than during Z-3-hexenal-induced cell death (**Figure 3.9 A-C**) in *VrMC5* overexpressor than wt, representing two branches of SA synthesis, phenylalanine ammonia lyase (PAL) pathway and isochorismate synthase (ICS) pathway are highly activated and *VrMC5* could enhance the activation. Meanwhile, the expression of a defence-related SA marker gene *PR-1* (*pathogenesis-related 1*) was investigated, suggesting Z-3-hexenal could induce the activation of the SA signalling and *VrMC5* positively upregulated SA response (**Figure 3.9 D**). Thus, it demonstrated that *VrMC5* plays a positive role in SA signalling pathway triggered by Z-3-hexenal.

If Z-3-hexenal induced cell-death related signalling, activation of jasmonic acid (JA) signalling should produce an antagonistic effect. Exogenous application of JA is known to elevate basal immunity level to promote the resistance to necrotrophic pathogens, whereas the HR to biotrophic pathogens is often suppressed by JA (Yan & Xie, 2015). As expected, exogenous JA pretreatment could repress the Z-3-

hexenal-induced mortality in the *VrMC5* overexpressor (**Figure 3.11 A**), which meant *Z*-3-hexenal causes cell-death related signalling that *VrMC5* acts in, and JA as a signal to activate basal immunity mitigate cell death in the *VrMC5* overexpressor.

4.3 Self-processing is essential for *VrMC5* activation during cell death

VrMC5 as a typical type II metacaspase requires cleavage within linker region to be activated. In this thesis, we provided evidence that its autolysis processing and endopeptidase activities of *VrMC5* are strictly Ca^{2+} -dependent, and identified the catalytic site Cys-139 and cleaved site Arg-226 are essential for its activation and biological function during cell death.

Previous studies on the mechanism of autolysis processing of AtMC4 and AtMC9 indicated that cleavage at site Arg-183 and Lys-225 are required for their endopeptidase activity (Vercammen *et al.*, 2004; Watanabe & Lam, 2011a). Additionally, it is noted that Lys-225 of AtMCP4 and catalytic site Cys-139 located at a highly conserved region in all reported type II metacaspase (Klemencic & Funk, 2019). Analysis of catalytically inactive and autolysically inactive forms of *VrMC5* expressed in BY-2 cells indicated that fully functional *VrMC5* largely depends on its self-processing and specific cleavage at Arg-226 and its catalytic activity are prerequisite for the self-processing (**Figure 3.6 B, Figure 3.8 A and B**). This is consistent with the observed behavior of recombinant *VrMC5* variant proteins *in vitro* that specific processing at Arg-226 of *VrMC5* and its catalytic site Cys-139 are indispensable for Ca^{2+} -induced enzymatic activation and self-processing (**Figure 3.14 B and Figure 3.16**). Those observations suggested that *VrMC5* processing is necessary for the enzyme to be active and tight control of activation mechanism for *VrMC5* is critical for maintaining proper activation during PCD.

Ca²⁺ is one of the most important signals in most aspects of growth and development, as well as responses to biotic and abiotic stresses. Our biochemical characterized VrMC5 is a Ca²⁺-activated protease. Low concentration of Ca²⁺ (1 mM) could induce autocatalytic processing of VrMC5 (**Figure 3.15 A**), whereas the low concentration Ca²⁺ only stimulate a weak level of the VrMC5 GRRase activity, the enzymatic activity of VrMC5 can be stimulated much more strongly by a higher concentration of Ca²⁺ in a range of 10–50 mM (**Figure 3.15 C**). The one explanation for the increased Ca²⁺ concentrations requirement might because of low binding affinity for Ca²⁺. On the other hand, it has been proved intermolecular processing of recombinant AtMC4 can occur only at a minor level *in vitro* assay condition, and Ca²⁺ predominantly facilitates further intramolecular processing mediated by initial activation of AtMC4 (Watanabe & Lam, 2011b).

4.4 Cell penetrating peptide manipulates VrMC5 activity

In classical genetic research, overexpression and gene loss-of-function is the general tool to manipulate protein function. In the present study, we have generated overexpression *VrMC5* mutants to demonstrate the features and role of *VrMC5*. On the other hand, a loss-of-function of *VrMC5* remains elusive, to generate a *VrMC5* defective mutant, the effective approach CRISPR-Cas9 could be used. However, in suspension cells, the efficiency of this approach was limited because of complex chimeras (Mercx *et al.*, 2016), thus the chemical engineering was used as a novel strategy to control protein function. In direct analogy to classical genetics, reverse chemical genetic approaches are ideal for identification of a known protein target. Like the use of knock-out in classical genetics, the overexpression of target protein is inhibited by the screened small molecule that modulates the function of the protein

and elucidates the phenotypic consequences of altering the function of the target protein in a cellular context (Blackwell and Zhao, 2003).

In this study we demonstrated expression of a functional short peptide (LMTP-peptide) containing the DQMD core sequence target to metacaspase and the subsequent alteration of cellular phenotype to PCD resistance. The sequence of metacaspase inhibitory peptide is inspired by the caspase inhibitor P35 protein. P35 is capable of binding to the active site of caspases through its pseudo-substrate motif DQMD and inhibits the activity of caspases (Zhou *et al.*, 1998). Several studies have indicated that synthetic peptide harboring the DQMD served as efficient targets for several caspases and may inhibit a wide range of caspases (Talanian *et al.*, 1997; Ekert, 1999; Matza-Porges *et al.*, 2003).

4.4.1 Cellular uptake mechanism of metacaspase inhibitory peptide

Uptake process of a cell-penetrating peptide involves interaction with the target site, saturability and internalization mechanism. Considering that multiple metacaspases are expected to be targets for LMTP-peptide, the uptake should be saturable. Monitoring the cellular uptake of LMTP-peptide over 3 hours, we found that the uptake was increased over time and clearly was saturable (**Figure 3.17**). This CPP carrier LMTP exhibits high efficiency in translocating cargo peptide due to its amphipathicity. The previous work also compared the cell-penetrating ability of different variety of CPPs to deliver GFP into cells. It revealed that the more hydrophobic, amphipathic CPP transporter was found to be the most efficient CPP for delivering an organic fluorophore into mammalian cells among their candidates (Patel *et al.*, 2019).

To prove the predicted inhibition to metacaspase of the peptide, we colocalized the LMTP-peptide with stable VrMC5 overexpression line *VrMC5-GFP* and microtubules marker line *TuA3-GFP*. The localization of peptide varies in the different cell line. It was shown that LMTP-peptide not only distributes throughout the cytosol but also targets to microtubules, especially during mitosis in *TuA3*, that is consistent with VrMC5 localization pattern (**Figure 3.18** and **Figure 3.19**). However, in actin marker cell line *GF11*, LMTP-peptide only disperses within the cytoplasm. It could be understood that LMTP-peptide tends to target to VrMC5 than other endogenous metacaspases in VrMC5 overexpression cells, in which case, LMTP-peptide localized in correspondence to the VrMC5.

In order to gain the mechanism of the internalization of LMTP-peptide, we used Ikarugamycin (inhibitor of clathrin-dependent endocytosis) to pretreat the cells. In the presence of inhibitors, the observed patterns were significantly different: after treatment only few residual signals could be seen at the periphery of cell walls (**Figure 3.20 E and F**). The mode of action of Ikarugamycin has been demonstrated that IKA appears to block the maturation and pinching off of clathrin-coated pits (CCPs) and disrupts Golgi morphology in a disorganized and vesiculated form (Elkin *et al.*, 2016). This suggests that the LMTP-peptide is taken up by endocytosis, and this endocytosis is clathrin-dependent.

In plants, microtubules and actin filaments provide force to deform and assist in the scission of membranes, the spatial organisation of endocytic trafficking requires actin and microtubule cytoskeletons to facilitate endosomal sorting and recycling (Granger *et al.*, 2014). Our data indicated when we disintegrated actin using Latrunculin B, the LMTP-peptide was still taken up in the same manner as in the controls, where actin meshwork was intact (**Figure 3.22**). However, pretreatment

with microtubule inhibitor Oryzalin, leaving weaker and punctate signals overlaid with depolymerized microtubules (**Figure 3.21 D-F**). Since vesicular trafficking is dependent on the microtubules network, we assumed that Oryzalin eliminates this membrane-associated, highly dynamic population of microtubules, which will disrupt the internalization process. This concept has been established that the integrity of the MT cytoskeleton is necessary to control exo-endocytosis events in the tip. MT depolymerization in the apex and shank induce endosome misallocation (Idilli *et al.*, 2013).

4.4.2 LMTP-peptide efficiently alleviates cellular stress responses

The target of peptide delivery in the current study to is aimed at blocking PCD mediated by metacaspase. We analyzed the ability of this short peptide to inhibit mortality or cell death-related cellular response induced by two inducers Z-3-hexenal and harpin.

When the cellular effect of Z-3-hexenal on a GFP actin marker cell line with LMTP-peptide pretreatment was tested, a growth of the percentage of cells with integrated and semi-integrated cortical actin for Z-3-hexenal was observed (**Figure 3.23 B**). Actin depolymerization is a hallmark for programmed cell death (Doncel *et al.*, 2017), the suppression of actin response implied the peptide might contribute to the resistance of PCD.

Since described above VrMC5 is a positive effector metacaspase of PCD pathways, the inhibition of VrMC5 was investigated by different experimental methods, including inhibition of cell death in VrMC5 overexpression cells or inhibition of cleavage processing and activity of VrMC5 *in vitro*. As shown by measuring cell

viability after treatment with these two PCD inducers (**Figures 3.24**), the LMTP-peptide abrogates PCD through death receptor pathway pathways. Interestingly, insertion of the core DQMD sequence into a heterogeneous scaffold polypeptide CrmA would change its specificity to inhibit caspase (Ekert, 1999). And both free DQMD peptide and the pDQMD vector was demonstrated similar activities in blocking apoptosis, in both the transient and the stable expression systems (Matza-Porges *et al.*, 2003; Matza-Porges *et al.*, 2005).

On the other hand, the reason that LMTP-peptide could mitigate cell death could be attributed to the suppression effect on the activity of VrMC5. The finding that high concentration of LMTP-peptide would to some extent prevent autolysis of VrMC5 and inhibit VrMC5 GRRase activity (**Figures 3.25**). Both results suggest that the LMTP-peptide is capable of manipulating VrMC5 function no matter it is *in vivo* or *in vitro*, similar to the anti-apoptotic peptide DQMD (Matza-Porges *et al.*, 2005).

4.5 Conclusion

In this study, we understand the biological function and activation mechanism of VrMC5 in Z-3-hexenal triggered HR cell death, and reveal part of molecular and cellular events underlying the response. The VrMC5 not only localizes in cytoplasm and nucleus but specifically co-localized with microtubules. In the simplified signalling model, Z-3-hexenal drives VrMC5 activation by cleaving at site Arg226 in the Ca²⁺-dependent manner. The experiments *in vitro* indicate the catalytic site Cys139 is also essential for VrMC5 auto-cleavage and enzymatic activity. The inducer Z-3-hexenal is able to upregulate SA synthesize related genes and SA responsive gene expression so that activate SA signalling and induce HR cell death, while this upregulation and cell death could be repressed by exogenous JA. Inactive

proenzyme form of VrMC5 undergoes self-processing into active form then directly and positively regulates SA signalling pathway and HR cell death (**Figure 4.1**).

Meantime, we generate a chemical tool for manipulation of VrMC5 activity. A short peptide with metacaspase functional inhibition suppresses the HR cell death induced by harpin and Z-3-hexenal, furthermore, peptide effectively inhibits the VrMC5 GRRase activity *in vitro* experiment. In addition, the uptake mechanism of this peptide is revealed that it penetrates through the plasma membrane via clathrin-dependent endocytosis. And microtubules are indispensable for its endocytic uptake while actin is optional.

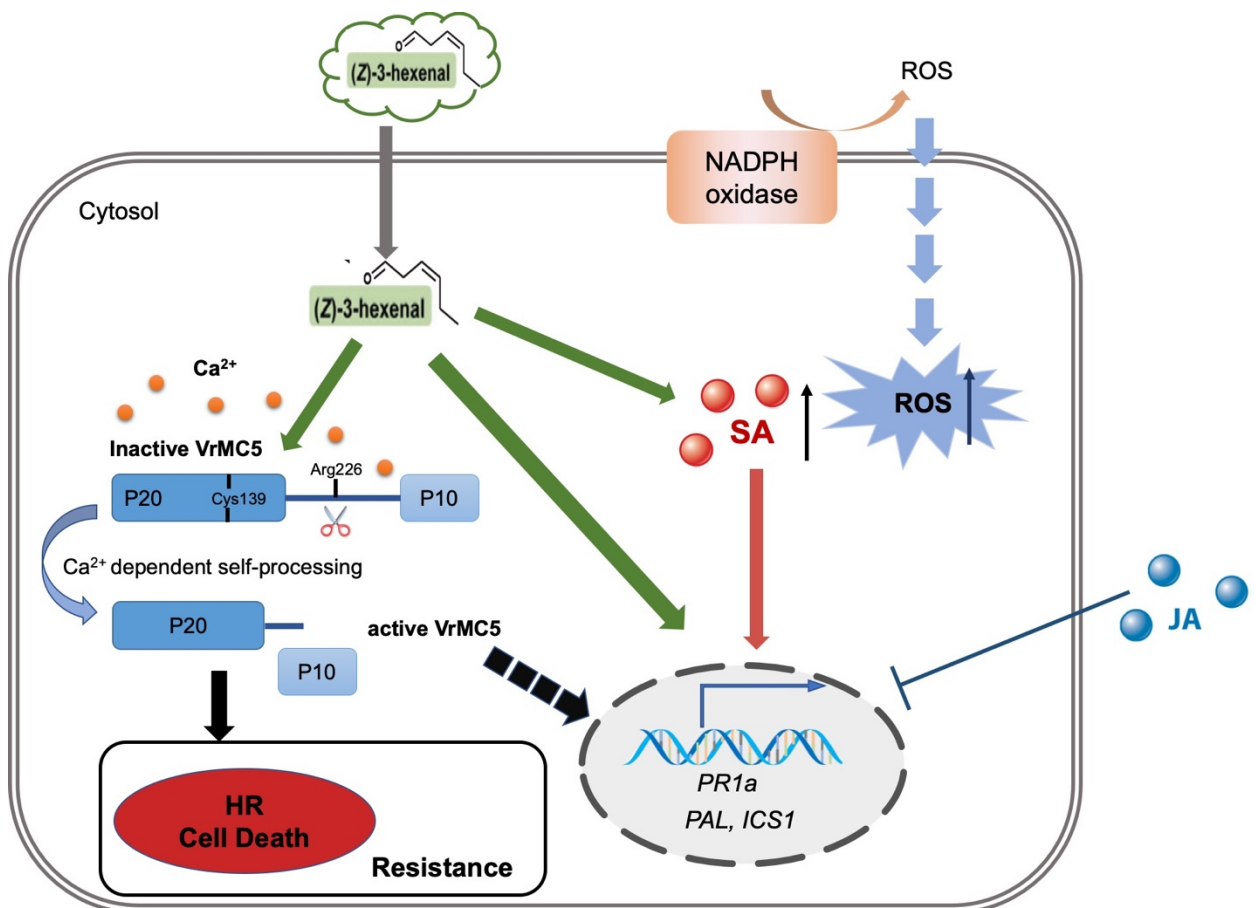


Figure 4.1 Simplified model of VrMC5-mediated cell-death related signalling induced by Z-3-hexenal. The diagram represents some of the characteristic features of VrMC5-mediated HR cell death that could occur in response to a green leaf volatile Z-3-hexenal in plants. Details are explained in the discussion. ROS: reactive oxygen species; SA: salicylic acid; JA: jasmonic acid; PAL: phenylalanine ammonia lyase; ICS1: isochorismate synthase; PR1: pathogenesis related 1; VrMC5: *Vitis rupestris* metacaspase 5; HR: hypersensitive response.

4.6 Outlook

4.6.1 Hunting the specific downstream events of Z-3-hexenal signal pathway

The previous study has described either the actin response or increased cell death was not seen for Z-3-hexenal isomer, E-2-hexenal. When a biological response is elicited by a molecule, but not by its isomer, the effect cannot be caused by a general chemical effect, but by specific molecule interaction. The first possible explanation for the isomer specificity would be that this response is activated by a receptor. A competition experiment was conducted to testify whether Z-3-hexenal signalling is initiated by a certain receptor. The combination of Z-3-hexenal and E-2-hexenal caused an increased burst of cell death, even when E-2-hexenal in a low concentration (**Figure S3**). This combination effect of those isomers was similar to a synergistic effect, where multiple molecular mechanisms underlie it. They might target at the same event but different sites with direct contact and agonist site, or have different targets of the same pathways that regulate the same downstream component (Jia *et al.*, 2009). Currently, most of the ongoing research on GLVs are limited to the roles they play in tri-trophic interactions and plant-plant communication, but the molecular mechanisms driving these processes are not clear. For example, what types of plant receptors can receive airborne signals? As the long-

distance signals, how are the signals transmitted through receiver plants, and how do they induce a priming defence response? To understand the signalling mechanisms of these pathways at the genetic and molecular levels, the systematic approach or the genetic engineering tools and advanced biochemical strategies, such as epigenetic alterations, could be used for further study. For instance, previous research took a transcriptomics approach to screen genes that are only induced by *E*-2-hexenal and identified WRKY6 and 40 act as important players transducing *E*-2-hexenal perception (Mirabella *et al.*, 2015).

4.6.2 Functional features of VrMC5 in PCD

In the present study, we described VrMC5 is indispensable in regulating PCD, and its activation requires self-processing cleaved at site Arginine 226 during cell death. The studies in the other organism revealed the broad range of pathways that metacaspases may regulate. For example, Type I MCs in the parasite *Leishmania major* also control the cell cycle and proliferation (Ambit *et al.*, 2008). In addition to the biochemical approaches that have revealed the close interaction of VrMC5 and microtubules. Thus, whether these functions are conserved in VrMC5 would be interesting to explore.

So far, the only substrates known for metacaspases are the TSN (Tudor staphylococcal nuclease) protein by mII-Pa in spruce (Sundström *et al.*, 2009), the GAPDH enzyme by Yca1p in yeast (Silva *et al.*, 2011) and AtDAD1 (Defender against Apoptotic Death-1) by AtMC5 in *Arabidopsis*. Mass spectrometry or mRNA-display techniques could be used to approach for screen biological substrates for metacaspase family on a proteome-wide scale (Ju *et al.*, 2007). Further peptide mapping could identify other functional cleavages sites that contribute to enzyme

activity and putative bystander sites that are cleaved following metacaspase activation (Lam & Zhang, 2012).

5 Appendix

5.1 Suspension BY-2 cell used in this study and its cultivation conditions

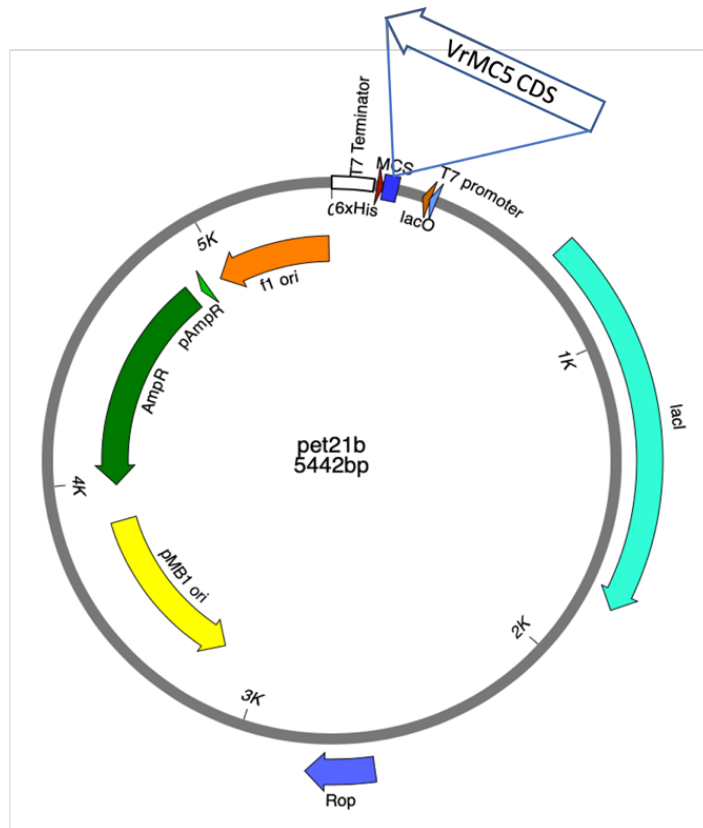
Name of the cell line	Antibiotics	Sources
wild type	none	Nagata <i>et al.</i> , 1992
GF11	Hygromycin 30 µg/ml	Sano <i>et al.</i> , 2005
TuA3	Kanamycin 25 µg/ml	Kumagai <i>et al.</i> , 2001
VrMC5	Hygromycin 30 µg/ml	This work
VrMC5 ^{C139A}	Hygromycin 30 µg/ml	This work
VrMC5 ^{S190A}	Hygromycin 30 µg/ml	This work
VrMC5 ^{R226G}	Hygromycin 30 µg/ml	This work

5.2 Primers used for construction variants

Table 5.1 List of primers used for VrMC5 overexpressor variants construction.

Primers name	Sequences (5'- 3')
VrMC5_C139A_F	TACGATAGTGTTCGGATTTCGGCCCCACAGCGGTGGCCTGAT
VrMC5_C139A_R	ATCAGGCCACCGCTGTGGGCCGAATCCGACACTATCGTA
VrMC5_S190A_F	GGAATTCAGCTCCCTGCGGCCTTGCAACACC
VrMC5_S190A_R	GGTGTGCAAGGCCGCAGGGAGCTGAATTCC
VrMC5_R225G_F	GCGGCTATGTGAAGAGCGGATCTCTGCCGCTTTC
VrMC5_R225G_R	GAAAGCGGCAGAGATCCGCTCTTCACATAGCCGC

5.3 Vector used for recombinant expression of VrMC5 and its variants



5.4 Primers used for real-time qPCR analysis

Table 5.2 List of primers used for expression analysis by qPCR.

Gene name	Sequence (5'-3')
EF1α	Forward: TGAGATGCACCACGAAGCTCTTC Reverse: GCTGAAGCACCCATTGCTGGG
PALA	Forward: TTGACAGTGGCTCAAGTTGC Reverse: CACCACCATTCTTGGTCCTC
PALB	Forward: TGCTAATGGTGAACCTTCATCCA Reverse: TGACATTCTTCTCACTTTCACCA
ICS1	Forward: TTGCTATAGTACGGGAGTGC Reverse: TCATCTTCAGTCTGGAGTCT
PR1a	Forward: GGATGCCATAACACAGCTC Reverse: GCTAGGTTTTTCGCCGTATTG

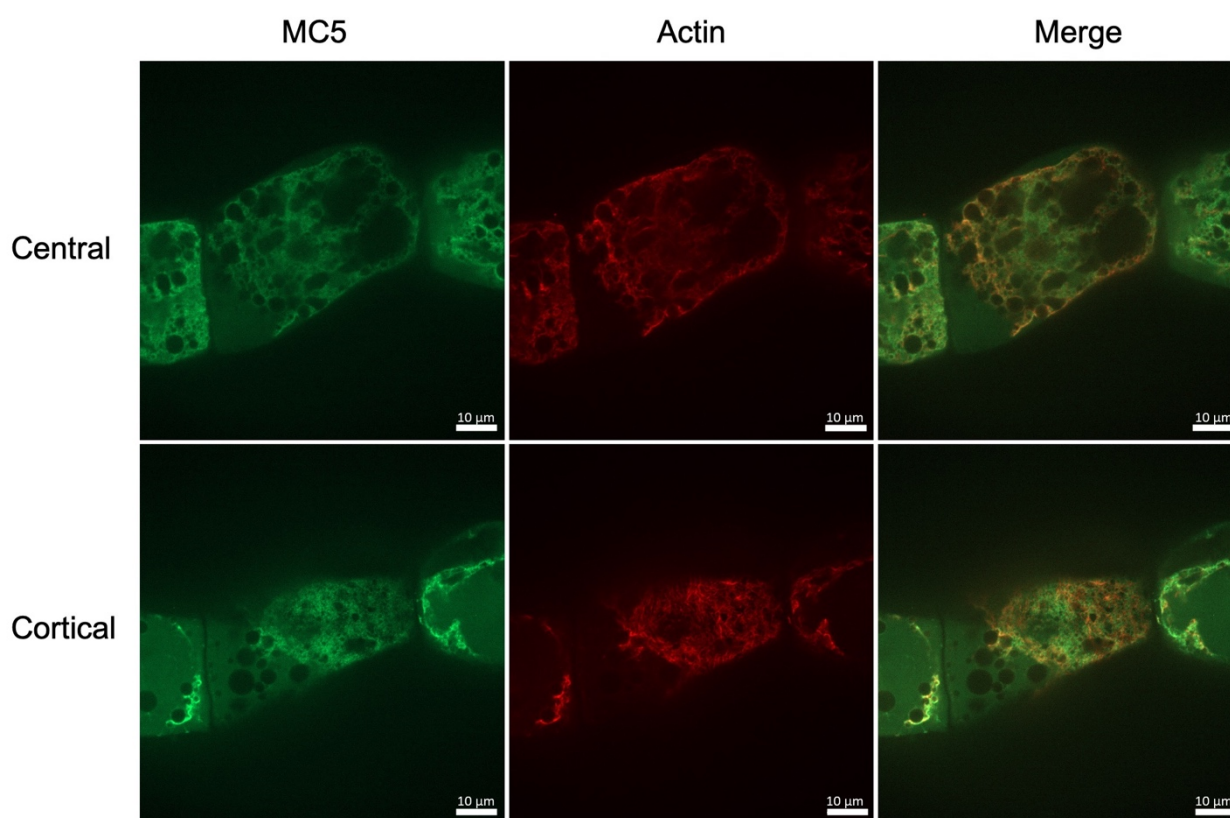


Figure S1. Actin filaments staining in *VrMC5-GFP* tobacco cell lines. Central and cortical actin filaments were visualized in *VrMC5-GFP*. Actin filaments are labelled using TRITC. Cells 3 days after subcultivation were stained. Scale bar=10 μm.

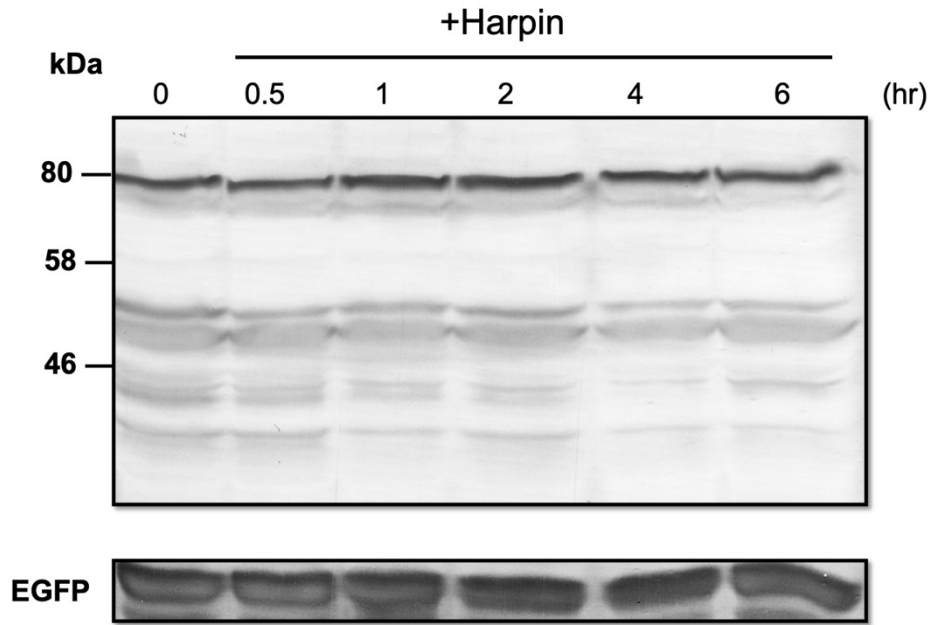


Figure S2. Self-processing of VrMC5 proteins during harpin-induced cell death. Cells after subcultivation were treated with 30 $\mu\text{g}/\text{ml}$ harpin and samples were collected at time point after incubation, immunoblot analysis using anti-GFP antibody.

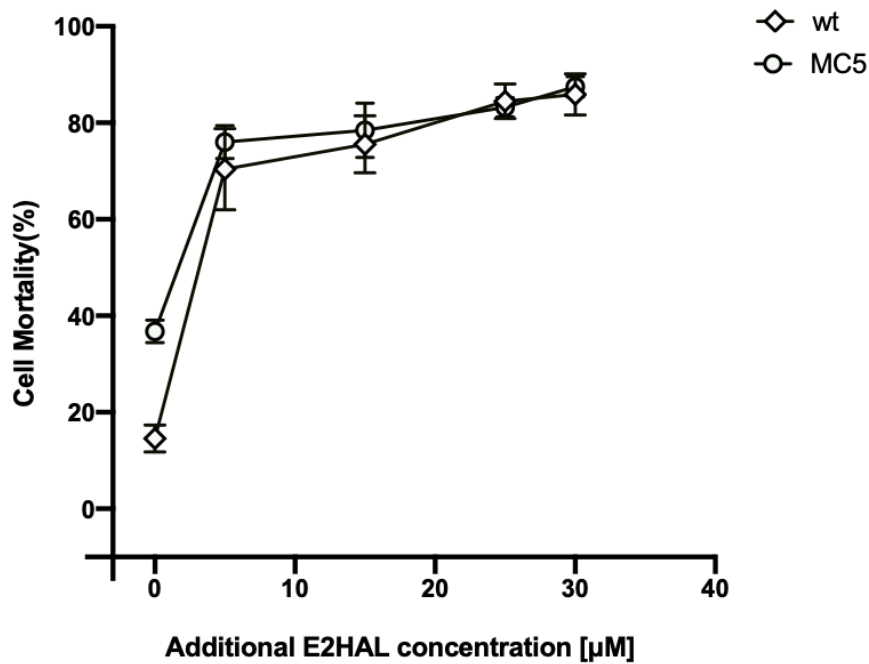


Figure S3. Dose response of E2HAL combined with Z3HAL on cell mortality. Cell mortality of *VrMC5* and wt challenged with combination of Z3HAL (12.5 µM) and various concentration E2HAL treatment. Data represents the mean \pm standard error (SE) of three independent biological replicates.

Reference

- Abramovitch RB, Anderson JC, Martin GB. 2006.** Bacterial elicitation and evasion of plant innate immunity. *Nature Reviews Molecular Cell Biology* **7**(8): 601-611.
- Adrain C, Martin SJ. 2001.** The mitochondrial apoptosome: a killer unleashed by the cytochrome seas. *Trends in Biochemical Sciences* **26**(6): 390-397.
- Akaberi S, Wang H, Claudel P, Riemann M, Hause B, Hugueney P, Nick P. 2018.** Grapevine fatty acid hydroperoxide lyase generates actin-disrupting volatiles and promotes defence-related cell death. *J Exp Bot* **69**(12): 2883-2896.
- Allmann S, Baldwin IT. 2010.** Insects betray themselves in nature to predators by rapid isomerization of green leaf volatiles. *Science* **329**(5995): 1075-1078.
- Ambit A, Fasel N, Coombs GH, Mottram JC. 2008.** An essential role for the *Leishmania* major metacaspase in cell cycle progression. *Cell Death Differ* **15**(1): 113-122.
- Ameye M, Allmann S, Verwaeren J, Smagghe G, Haesaert G, Schuurink RC, Audenaert K. 2018.** Green leaf volatile production by plants: a meta-analysis. *New Phytologist* **220**(3): 666-683.
- Arimura G-i, Ozawa R, Horiuchi J-i, Nishioka T, Takabayashi J. 2001.** Plant-plant interactions mediated by volatiles emitted from plants infested by spider mites. *Biochemical Systematics and Ecology* **29**(10): 1049-1061.
- Ausubel FM. 2005.** Are innate immune signalling pathways in plants and animals conserved? *Nat Immunol* **6**(10): 973-979.
- Bari R, Jones JD. 2009.** Role of plant hormones in plant defense responses. *Plant Mol Biol* **69**(4): 473-488.
- Belenghi B, Romero-Puertas MC, Vercammen D, Brackeenier A, Inzé D, Delledonne M, Van Breusegem F. 2007.** Metacaspase Activity of *Arabidopsis thaliana* Is Regulated by S-Nitrosylation of a Critical Cysteine Residue. *Journal of Biological Chemistry* **282**(2): 1352-1358.

- Bensadoun A, Weinstein D. 1976.** Assay of proteins in the presence of interfering materials. *Anal Biochem* **70**(1): 241-250.
- Blackwell, H.E. and Zhao, Y. 2003.** Chemical genetic approaches to plant biology. *Plant Physiol.* **133**, 448–455
- Bollhoner B, Zhang B, Stael S, Denance N, Overmyer K, Goffner D, Van Breusegem F, Tuominen H. 2013.** Post mortem function of AtMC9 in xylem vessel elements. *New Phytol* **200**(2): 498-510.
- Borrelli A, Tornesello A, Tornesello M, Buonaguro F. 2018.** Cell Penetrating Peptides as Molecular Carriers for Anti-Cancer Agents. *Molecules* **23**(2).
- Bozhkov PV, Suarez MF, Filonova LH, Daniel G, Zamyatnin AA, Rodriguez-Nieto S, Zhivotovsky B, Smertenko A. 2005.** Cysteine protease mCII-Pa executes programmed cell death during plant embryogenesis. *Proceedings of the National Academy of Sciences* **102**(40): 14463-14468.
- Brennan MA, Cookson BT. 2000.** Salmonella induces macrophage death by caspase-1-dependent necrosis. *Mol Microbiol* **38**(1): 31-40.
- Buschmann H, Green P, Sambade A, Doonan JH, Lloyd CW. 2011.** Cytoskeletal dynamics in interphase, mitosis and cytokinesis analysed through Agrobacterium-mediated transient transformation of tobacco BY-2 cells. *New Phytol* **190**(1): 258-267.
- Chen Z, Zheng Z, Huang J, Lai Z, Fan B. 2009.** Biosynthesis of salicylic acid in plants. *Plant Signal Behav* **4**(6): 493-496.
- Chichkova NV, Shaw J, Galiullina RA, Drury GE, Tuzhikov AI, Kim SH, Kalkum M, Hong TB, Gorshkova EN, Torrance L, et al. 2010.** Phytaspase, a relocalisable cell death promoting plant protease with caspase specificity. *The EMBO Journal* **29**(6): 1149-1161.
- Cohen GM. 1997.** Caspases: the executioners of apoptosis. *Biochemical Journal* **326**(1): 1-16.
- Coll NS, Epple P, Dangl JL. 2011.** Programmed cell death in the plant immune system. *Cell Death Differ* **18**(8): 1247-1256.

- Coll NS, Smidler A, Puigvert M, Popa C, Valls M, Dangl JL. 2014.** The plant metacaspase AtMC1 in pathogen-triggered programmed cell death and aging: functional linkage with autophagy. *Cell Death & Differentiation* **21**(9): 1399-1408.
- Coll NS, Vercammen D, Smidler A, Clover C, Van Breusegem F, Dangl JL, Epple P. 2010.** Arabidopsis type I metacaspases control cell death. *Science* **330**(6009): 1393-1397.
- Colombo M, Mizzotti C, Masiero S, Kater MM, Pesaresi P. 2015.** Peptide aptamers: The versatile role of specific protein function inhibitors in plant biotechnology. *J Integr Plant Biol* **57**(11): 892-901.
- Cook DE, Mesarich CH, Thomma BPHJ. 2015.** Understanding Plant Immunity as a Surveillance System to Detect Invasion. *Annual Review of Phytopathology* **53**(1): 541-563.
- Cookson MR, Lee REC, Puente LG, Kærn M, Megeney LA. 2008.** A Non-Death Role of the Yeast Metacaspase: Yca1p Alters Cell Cycle Dynamics. *PLoS One* **3**(8).
- Croft KPC, Juttner F, Slusarenko AJ. 1993.** Volatile Products of the Lipoxygenase Pathway Evolved from *Phaseolus vulgaris* (L.) Leaves Inoculated with *Pseudomonas syringae* pv *phaseolicola*. *Plant Physiology* **101**(1): 13-24.
- D.F.Gaff, O.Okong'O-Ogola. 1971.** The Use of Non-permeating Pigments for Testing the Survival of Cells. *Journal of Experimental Botany* **22**(7): 758-758.
- D'Auria JC, Pichersky E, Schaub A, Hansel A, Gershenzon J. 2007.** Characterization of a BAHD acyltransferase responsible for producing the green leaf volatile (Z)-3-hexen-1-yl acetate in *Arabidopsis thaliana*. *Plant J* **49**(2): 194-207.
- De Rybel B, Audenaert D, Vert G, Rozhon W, Mayerhofer J, Peelman F, Coutuer S, Denayer T, Jansen L, Nguyen L, et al. 2009.** Chemical Inhibition of a Subset of *Arabidopsis thaliana* GSK3-like Kinases Activates Brassinosteroid Signalling. *Chemistry & Biology* **16**(6): 594-604.
- De Vos M, Van Oosten VR, Van Poecke RM, Van Pelt JA, Pozo MJ, Mueller MJ, Buchala AJ, Metraux JP, Van Loon LC, Dicke M, et al. 2005.** Signal signature and transcriptome changes of *Arabidopsis* during pathogen and insect attack. *Mol Plant Microbe Interact* **18**(9): 923-937.

Degterev A, Huang Z, Boyce M, Li Y, Jagtap P, Mizushima N, Cuny GD, Mitchison TJ, Moskowitz MA, Yuan J. 2005. Chemical inhibitor of nonapoptotic cell death with therapeutic potential for ischemic brain injury. *Nat Chem Biol* **1**(2): 112-119.

Dietrich L, Rathmer B, Ewan K, Bange T, Heinrichs S, Dale TC, Schade D, Grossmann TN. 2017. Cell Permeable Stapled Peptide Inhibitor of Wnt Signalling that Targets β -Catenin Protein-Protein Interactions. *Cell Chemical Biology* **24**(8): 958-968.e955.

Diezel C, von Dahl CC, Gaquerel E, Baldwin IT. 2009. Different lepidopteran elicitors account for cross-talk in herbivory-induced phytohormone signalling. *Plant Physiol* **150**(3): 1576-1586.

Dodds PN, Rathjen JP. 2010. Plant immunity: towards an integrated view of plant-pathogen interactions. *Nat Rev Genet* **11**(8): 539-548.

Doncel JP, Ojeda PdC, OropesaÁvila M, Paz MV, Lavera ID, Mata MDL, Córdoba MÁ, Hidalgo RL, Rivero JMS, Cotán D, et al. 2017. Cytoskeleton Rearrangements during the Execution Phase of Apoptosis. *Cytoskeleton - Structure, Dynamics, Function and Disease*.

Dong X. 2004. NPR1, all things considered. *Current Opinion in Plant Biology* **7**(5): 547-552.

Ekert PG. 1999. Inhibition of apoptosis and clonogenic survival of cells expressing crmA variants: optimal caspase substrates are not necessarily optimal inhibitors. *The EMBO Journal* **18**(2): 330-338.

Elkin SR, Oswald NW, Reed DK, Mettlen M, MacMillan JB, Schmid SL. 2016. Ikarugamycin: A Natural Product Inhibitor of Clathrin-Mediated Endocytosis. *Traffic* **17**(10): 1139-1149.

Engelberth J, Alborn HT, Schmelz EA, Tumlinson JH. 2004. Airborne signals prime plants against insect herbivore attack. *Proc Natl Acad Sci U S A* **101**(6): 1781-1785.

Engelberth J, Contreras CF, Dalvi C, Li T, Engelberth M. 2013. Early transcriptome analyses of Z-3-hexenol-treated Zea mays revealed distinct

transcriptional networks and anti-herbivore defense potential of green leaf volatiles. *PLoS ONE* 8: e77465.

Flor HH. 1971. Current Status of the Gene-For-Gene Concept. *Annual Review of Phytopathology* 9(1): 275-296.

Fonseca S, Chini A, Hamberg M, Adie B, Porzel A, Kramell R, Miersch O, Wasternack C, Solano R. 2009. (+)-7-iso-Jasmonoyl-L-isoleucine is the endogenous bioactive jasmonate. *Nature Chemical Biology* 5(5): 344-350.

Fyans JK, Altowairish MS, Li Y, Bignell DR. 2015. Characterization of the Coronatine-Like Phytotoxins Produced by the Common Scab Pathogen *Streptomyces scabies*. *Mol Plant Microbe Interact* 28(4): 443-454.

Garcion C, Métraux J-P 2007. Salicylic Acid. *Annual Plant Reviews Volume 24: Plant Hormone Signalling*, 229-255.

Gilio JM, Marcondes MF, Ferrari D, Juliano MA, Juliano L, Oliveira V, Machado MFM. 2017. Processing of metacaspase 2 from *Trypanosoma brucei* (TbMCA2) broadens its substrate specificity. *Biochim Biophys Acta Proteins Proteom* 1865(4): 388-394.

Gimenez-Ibanez S, Boter M, Fernandez-Barbero G, Chini A, Rathjen JP, Solano R. 2014. The bacterial effector HopX1 targets JAZ transcriptional repressors to activate jasmonate signalling and promote infection in *Arabidopsis*. *PLoS Biol* 12(2): e1001792.

Glazebrook J. 2005. Contrasting mechanisms of defense against biotrophic and necrotrophic pathogens. *Annu Rev Phytopathol* 43: 205-227.

Gong P, Riemann M, Dong D, Stoeffler N, Gross B, Markel A, Nick P. 2019. Two grapevine metacaspase genes mediate ETI-like cell death in grapevine defence against infection of *Plasmopara viticola*. *Protoplasma* 256(4): 951-969.

Granger E, McNee G, Allan V, Woodman P. 2014. The role of the cytoskeleton and molecular motors in endosomal dynamics. *Seminars in Cell & Developmental Biology* 31: 20-29.

Greenberg JT, Yao N. 2004. The role and regulation of programmed cell death in plant-pathogen interactions. *Cell Microbiol* 6(3): 201-211.

Guan X, Buchholz G, Nick P. 2013. The cytoskeleton is disrupted by the bacterial effector HrpZ, but not by the bacterial PAMP flg22, in tobacco BY-2 cells. *J Exp Bot* **64**(7): 1805-1816.

Halitschke R, Stenberg JA, Kessler D, Kessler A, Baldwin IT. 2007. Shared signals – ‘alarm calls’ from plants increase apparency to herbivores and their enemies in nature. *Ecology Letters* **0**(0): 071026235140001-???

Hatsugai N, Iwasaki S, Tamura K, Kondo M, Fuji K, Ogasawara K, Nishimura M, Hara-Nishimura I. 2009. A novel membrane fusion-mediated plant immunity against bacterial pathogens. *Genes Dev* **23**(21): 2496-2506.

Hatsugai N, Kuroyanagi M, Nishimura M, Hara-Nishimura I. 2006. A cellular suicide strategy of plants: vacuole-mediated cell death. *Apoptosis* **11**(6): 905-911.

Hatsugai N, Kuroyanagi M, Yamada K, Meshi T, Tsuda S, Kondo M, Nishimura M, Hara-Nishimura I. 2004. A plant vacuolar protease, VPE, mediates virus-induced hypersensitive cell death. *Science* **305**(5685): 855-858.

He R, Drury GE, Rotari VI, Gordon A, Willer M, Farzaneh T, Woltering EJ, Gallois P. 2008. Metacaspase-8 modulates programmed cell death induced by ultraviolet light and H₂O₂ in Arabidopsis. *J Biol Chem* **283**(2): 774-783.

Heil M, Engelberth J, Contreras CF, Dalvi C, Li T, Engelberth M. 2013. Early Transcriptome Analyses of Z-3-Hexenol-Treated Zea mays Revealed Distinct Transcriptional Networks and Anti-Herbivore Defense Potential of Green Leaf Volatiles. *PLoS One* **8**(10).

Heitz F, Morris MC, Divita G. 2009. Twenty years of cell-penetrating peptides: from molecular mechanisms to therapeutics. *British Journal of Pharmacology* **157**(2): 195-206.

Helms MJ. 2006. Bloodstream form Trypanosoma brucei depend upon multiple metacaspases associated with RAB11-positive endosomes. *Journal of Cell Science* **119**(6): 1105-1117.

Higaki T, Kurusu T, Hasezawa S, Kuchitsu K. 2011. Dynamic intracellular reorganization of cytoskeletons and the vacuole in defense responses and hypersensitive cell death in plants. *J Plant Res* **124**(3): 315-324.

- Hildebrand DF, Brown GC, Jackson DM, Hamilton-Kemp TR. 1993.** Effects of some leaf-emitted volatile compounds on aphid population increase. *Journal of Chemical Ecology* **19**(9): 1875-1887.
- Huang L, Zhang H, Hong Y, Liu S, Li D, Song F. 2015.** Stress-Responsive Expression, Subcellular Localization and Protein–Protein Interactions of the Rice Metacaspase Family. *International Journal of Molecular Sciences* **16**(7): 16216-16241.
- Idilli AI, Morandini P, Onelli E, Rodighiero S, Caccianiga M, Moscatelli A. 2013.** Microtubule Depolymerization Affects Endocytosis and Exocytosis in the Tip and Influences Endosome Movement in Tobacco Pollen Tubes. *Molecular Plant* **6**(4): 1109-1130.
- Jia J, Zhu F, Ma X, Cao ZW, Li YX, Chen YZ. 2009.** Mechanisms of drug combinations: interaction and network perspectives. *Nature Reviews Drug Discovery* **8**(2): 111-128.
- Jiang Q, Qin S, Wu QY. 2010.** Genome-wide comparative analysis of metacaspases in unicellular and filamentous cyanobacteria. *BMC Genomics* **11**: 198.
- Jones AM. 2001.** Programmed Cell Death in Development and Defense: Fig. 1. *Plant Physiology* **125**(1): 94-97.
- Jones JD, Dangl JL. 2006.** The plant immune system. *Nature* **444**(7117): 323-329.
- Ju W, Valencia CA, Pang H, Ke Y, Gao W, Dong B, Liu R. 2007.** Proteome-wide identification of family member-specific natural substrate repertoire of caspases. *Proceedings of the National Academy of Sciences* **104**(36): 14294-14299.
- Kaksonen M, Roux A. 2018.** Mechanisms of clathrin-mediated endocytosis. *Nature Reviews Molecular Cell Biology* **19**(5): 313-326.
- Kant MR, Bleeker PM, Wijk MV, Schuurink RC, Haring MA. 2009.** Chapter 14. Plant volatiles in defence. In: Loon LCV, ed. *Advances in botanical research*. Amsterdam, the Netherlands: Academic Press, 613–666.
- Karban R, Baldwin IT, Baxter KJ, Laue G, Felton GW. 2000.** Communication between plants: induced resistance in wild tobacco plants following clipping of neighboring sagebrush. *Oecologia* **125**(1): 66-71.

- Karban R, Yang LH, Edwards KF. 2014.** Volatile communication between plants that affects herbivory: a meta-analysis. *Ecology Letters* 17: 44–52.
- Katsir L, Schilmiller AL, Staswick PE, He SY, Howe GA. 2008.** COI1 is a critical component of a receptor for jasmonate and the bacterial virulence factor coronatine. *Proceedings of the National Academy of Sciences* 105(19): 7100-7105.
- Kauffman WB, Fuselier T, He J, Wimley WC. 2015.** Mechanism Matters: A Taxonomy of Cell Penetrating Peptides. *Trends in Biochemical Sciences* 40(12): 749-764.
- Kessler A, Halitschke R, Diezel C, Baldwin IT. 2006.** Priming of plant defense responses in nature by airborne signalling between *Artemisia tridentata* and *Nicotiana attenuata*. *Oecologia* 148(2): 280-292.
- Klemencic M, Funk C. 2019.** Evolution and structural diversity of metacaspases. *J Exp Bot* 70(7): 2039-2047.
- Kobayashi I, Kobayashi Y, AR H. 1994.** Dynamic reorganization of microtubules and microfilaments in flax cells during the resistance response to flax rust infection. *Planta*(195): 237–247.
- Kobayashi Y, Kobayashi I. 2007.** Depolymerization of the actin cytoskeleton induces defense responses in tobacco plants. *Journal of General Plant Pathology* 73(5): 360-364.
- Koichi MIZUNO MK, and Hiroh SHIBAOKA. 1981.** Isolation of plant tubulin from adzuki bean epicotyls by ethyl N-phenylcarbamate-Sepharose affinity chromatography.pdf>. *Journal of Biological Chemistry*.
- Kombrink E. 2012.** Chemical and genetic exploration of jasmonate biosynthesis and signalling paths. *Planta* 236(5): 1351-1366.
- Koornneef A, Pieterse CM. 2008.** Cross talk in defense signalling. *Plant Physiol* 146(3): 839-844.
- Kumagai F, Yoneda A, Tomida T, Sano T, Nagata T, Hasezawa S. 2001.** Fate of nascent microtubules organized at the M/G1 interface, as visualized by synchronized tobacco BY-2 cells stably expressing GFP-tubulin: time-sequence observations of

the reorganization of cortical microtubules in living plant cells. *Plant Cell Physiol* **42**(7): 723-732.

Kunishima M, Yamauchi Y, Mizutani M, Kuse M, Takikawa H, Sugimoto Y. 2016. Identification of (Z)-3:(E)-2-Hexenal Isomerases Essential to the Production of the Leaf Aldehyde in Plants. *J Biol Chem* **291**(27): 14023-14033.

Lam E, Zhang Y. 2012. Regulating the reapers: activating metacaspases for programmed cell death. *Trends Plant Sci* **17**(8): 487-494.

Le PU, Nabi IR. 2003. Caveolae/raft-dependent endocytosis. *Journal of Cell Biology* **161**(4): 673-677.

Lequeu J, Simon-Plas F, Fromentin J, Etienne P, Petitot A-S, Blein J-P, Suty L. 2005. Proteasome comprising a β 1 inducible subunit acts as a negative regulator of NADPH oxidase during elicitation of plant defense reactions. *FEBS Letters* **579**(21): 4879-4886.

Levine A, Pennell RI, Alvarez ME, Palmer R, Lamb C. 1996. Calcium-mediated apoptosis in a plant hypersensitive disease resistance response. *Curr Biol* **6**(4): 427-437.

Lim JP, Gleeson PA. 2011. Macropinocytosis: an endocytic pathway for internalising large gulps. *Immunology & Cell Biology* **89**(8): 836-843.

Lockshin RA, Zakeri Z. 2004. Apoptosis, autophagy, and more. *The International Journal of Biochemistry & Cell Biology* **36**(12): 2405-2419.

Machado MF, Marcondes MF, Juliano MA, McLuskey K, Mottram JC, Moss CX, Juliano L, Oliveira V. 2013. Substrate specificity and the effect of calcium on *Trypanosoma brucei* metacaspase 2. *FEBS J* **280**(11): 2608-2621.

Mashima T, Naito M, Tsuruo T. 1999. Caspase-mediated cleavage of cytoskeletal actin plays a positive role in the process of morphological apoptosis. *Oncogene* **18**(15): 2423-2430.

Matoušková J, Janda M, Fišer R, Šašek V, Kocourková D, Burketová L, Dušková J, Martinec J, Valentová O. 2014. Changes in actin dynamics are involved in salicylic acid signalling pathway. *Plant Science* **223**: 36-44.

- Matsui K, Kurishita S, Hisamitsu A, Kajiwara T. 2000.** A lipid-hydrolysing activity involved in hexenal formation. *Biochem Soc Trans* **28**(6): 857-860.
- Matsui K. 2006.** Green leaf volatiles: hydroperoxide lyase pathway of oxylipin metabolism. *Curr Opin Plant Biol* **9**(3): 274-280.
- Matza-Porges S, Horresh I, Tavor E, Panet A, Honigman A. 2005.** Expression of an anti apoptotic recombinant short peptide in mammalian cells. *Apoptosis* **10**(5): 987-996.
- Matza-Porges S, Tavor E, Panet A, Honigman A. 2003.** Intracellular expression of a functional short peptide confers resistance to apoptosis. *Experimental Cell Research* **290**(1): 60-67.
- McLuskey K, Rudolf J, Proto WR, Isaacs NW, Coombs GH, Moss CX, Mottram JC. 2012.** Crystal structure of a Trypanosoma brucei metacaspase. *Proc Natl Acad Sci U S A* **109**(19): 7469-7474.
- Milletti F. 2012.** Cell-penetrating peptides: classes, origin, and current landscape. *Drug Discovery Today* **17**(15-16): 850-860.
- Mirabella R, Rauwerda H, Allmann S, Scala A, Spyropoulou EA, de Vries M, Boersma MR, Breit TM, Haring MA, Schuurink RC. 2015.** WRKY40 and WRKY6 act downstream of the green leaf volatile E-2-hexenal in Arabidopsis. *Plant J* **83**(6): 1082-1096.
- Mittler R, Simon L, Lam E. 1997.** Pathogen-induced programmed cell death in tobacco. *J Cell Sci* **110** (Pt 11): 1333-1344.
- Moore JW, Loake GJ, Spoel SH. 2011.** Transcription dynamics in plant immunity. *Plant Cell* **23**(8): 2809-2820.
- Moss CX, Westrop GD, Juliano L, Coombs GH, Mottram JC. 2007.** Metacaspase 2 of Trypanosoma brucei is a calcium-dependent cysteine peptidase active without processing. *FEBS Letters* **581**(29): 5635-5639.
- Mur LA, Kenton P, Atzorn R, Miersch O, Wasternack C. 2006.** The outcomes of concentration-specific interactions between salicylate and jasmonate signalling include synergy, antagonism, and oxidative stress leading to cell death. *Plant Physiol* **140**(1): 249-262.

Mur LAJ, Kenton P, Lloyd AJ, Ougham H, Prats E. 2008. The hypersensitive response; the centenary is upon us but how much do we know? *Journal of Experimental Botany* **59**(3): 501-520.

Nakamura S, Hatanaka A. 2002. Green-Leaf-Derived C6-Aroma Compounds with Potent Antibacterial Action That Act on Both Gram-Negative and Gram-Positive Bacteria. *Journal of Agricultural and Food Chemistry* **50**(26): 7639-7644.

Nakashima A, von Reuss SH, Tasaka H, Nomura M, Mochizuki S, Iijima Y, Aoki K, Shibata D, Boland W, Takabayashi J, et al. 2013. Traumatins- and Dinortraumatins-containing Galactolipids in *Arabidopsis*. *Journal of Biological Chemistry* **288**(36): 26078-26088.

Ndozangue-Touriguine O, Hamelin J, Breard J. 2008. Cytoskeleton and apoptosis. *Biochem Pharmacol* **76**(1): 11-18.

Niinemets Ü. 2010. Mild versus severe stress and BVOCs: thresholds, priming and consequences. *Trends in Plant Science* **15**(3): 145-153.

Park SY, Fung P, Nishimura N, Jensen DR, Fujii H, Zhao Y, Lumba S, Santiago J, Rodrigues A, Chow TF, et al. 2009. Abscisic acid inhibits type 2C protein phosphatases via the PYR/PYL family of START proteins. *Science* **324**(5930): 1068-1071.

Patel SG, Sayers EJ, He L, Narayan R, Williams TL, Mills EM, Allemann RK, Luk LYP, Jones AT, Tsai YH. 2019. Cell-penetrating peptide sequence and modification dependent uptake and subcellular distribution of green fluorescent protein in different cell lines. *Sci Rep* **9**(1): 6298.

Pooga M, Langel Ü 2015. Classes of Cell-Penetrating Peptides. *Cell-Penetrating Peptides*, 3-28.

Qiang X, Zechmann B, Reitz MU, Kogel KH, Schafer P. 2012. The mutualistic fungus *Piriformospora indica* colonizes *Arabidopsis* roots by inducing an endoplasmic reticulum stress-triggered caspase-dependent cell death. *Plant Cell* **24**(2): 794-809.

Ragin AD, Morgan RA, Chmielewski J. 2002. Cellular Import Mediated by Nuclear Localization Signal Peptide Sequences. *Chemistry & Biology* **9**(8): 943-948.

Reddy GVP, Guerrero A. 2004. Interactions of insect pheromones and plant semiochemicals. *Trends in Plant Science* **9**(5): 253-261.

Riviere MP, Marais A, Ponchet M, Willats W, Galiana E. 2008. Silencing of acidic pathogenesis-related PR-1 genes increases extracellular beta-(1->3)-glucanase activity at the onset of tobacco defence reactions. *J Exp Bot* **59**(6): 1225-1239.

Robert S, Chary SN, Drakakaki G, Li S, Yang Z, Raikhel NV, Hicks GR. 2008. Endosidin1 defines a compartment involved in endocytosis of the brassinosteroid receptor BRI1 and the auxin transporters PIN2 and AUX1. *Proceedings of the National Academy of Sciences* **105**(24): 8464-8469.

Robert-Seilaniantz A, Grant M, Jones JDG. 2011. Hormone Crosstalk in Plant Disease and Defense: More Than Just JASMONATE-SALICYLATE Antagonism. *Annual Review of Phytopathology* **49**(1): 317-343.

Ruther J, Kleier S. 2005. Plant-Plant Signalling: Ethylene Synergizes Volatile Emission In Zea mays Induced by Exposure to (Z)-3-Hexen-1-ol. *Journal of Chemical Ecology* **31**(9): 2217-2222.

Sano T, Higaki T, Oda Y, Hayashi T, Hasezawa S. 2005. Appearance of actin microfilament 'twin peaks' in mitosis and their function in cell plate formation, as visualized in tobacco BY-2 cells expressing GFP-fimbrin. *Plant J* **44**(4): 595-605.

Scala A, Allmann S, Mirabella R, Haring MA, Schuurink RC. 2013a. Green leaf volatiles: a plant's multifunctional weapon against herbivores and pathogens. *Int J Mol Sci* **14**(9): 17781-17811.

Scala A, Mirabella R, Mugo C, Matsui K, Haring MA, Schuurink RC. 2013b. E-2-hexenal promotes susceptibility to *Pseudomonas syringae* by activating jasmonic acid pathways in *Arabidopsis*. *Front Plant Sci* **4**: 74.

Seo HS, Song JT, Cheong JJ, Lee YH, Lee YW, Hwang I, Lee JS, Choi YD. 2001. Jasmonic acid carboxyl methyltransferase: a key enzyme for jasmonate-regulated plant responses. *Proc Natl Acad Sci U S A* **98**(8): 4788-4793.

Seybold H, Trempel F, Ranf S, Scheel D, Romeis T, Lee J. 2014. Ca²⁺ signalling in plant immune response: from pattern recognition receptors to Ca²⁺ decoding mechanisms. *New Phytol* **204**(4): 782-790.

Shai Y. 1999. Mechanism of the binding, insertion and destabilization of phospholipid bilayer membranes by α -helical antimicrobial and cell non-selective membrane-lytic peptides. *Biochimica et Biophysica Acta (BBA) - Biomembranes* **1462**(1-2): 55-70.

Shiojiri K, Kishimoto K, Ozawa R, Kugimiya S, Urashimo S, Arimura G, Horiuchi J, Nishioka T, Matsui K, Takabayashi J. 2006. Changing green leaf volatile biosynthesis in plants: an approach for improving plant resistance against both herbivores and pathogens. *Proc Natl Acad Sci U S A* **103**(45): 16672-16676.

Silva A, Almeida B, Sampaio-Marques B, Reis MIR, Ohlmeier S, Rodrigues F, Vale Ad, Ludovico P. 2011. Glyceraldehyde-3-phosphate dehydrogenase (GAPDH) is a specific substrate of yeast metacaspase. *Biochimica et Biophysica Acta (BBA) - Molecular Cell Research* **1813**(12): 2044-2049.

Stefan J. Riedl MR, Scott J. Snipas, and Guy S. Salvesen. 2001. Mechanism-Based Inactivation of Caspases by the Apoptotic Suppressor p35. *Biochemistry* **40**: 13274-13280.

Sundström JF, Vaculova A, Smertenko AP, Savenkov EI, Golovko A, Minina E, Tiwari BS, Rodriguez-Nieto S, Zamyatnin AA, Välineva T, et al. 2009. Tudor staphylococcal nuclease is an evolutionarily conserved component of the programmed cell death degradome. *Nature Cell Biology* **11**(11): 1347-1354.

Tada Y, Spoel SH, Pajerowska-Mukhtar K, Mou Z, Song J, Wang C, Zuo J, Dong X. 2008. Plant Immunity Requires Conformational Changes of NPR1 via S-Nitrosylation and Thioredoxins. *Science* **321**(5891): 952-956.

Takemoto D, Jones DA, Hardham AR. 2006. Re-organization of the cytoskeleton and endoplasmic reticulum in the Arabidopsis pen1-1 mutant inoculated with the non-adapted powdery mildew pathogen, *Blumeria graminis* f. sp. *hordei*. *Mol Plant Pathol* **7**(6): 553-563.

Talanian RV, Quinlan C, Trautz S, Hackett MC, Mankovich JA, Banach D, Ghayur T, Brady KD, Wong WW. 1997. Substrate specificities of caspase family proteases. *J Biol Chem* **272**(15): 9677-9682.

Tomoya Niki IM, Shigemi Seo, Norihiro Ohtsubo and Yuko Ohashi. 1998. Antagonistic effect of salicylic acid and jasmonic acid on the expression of

pathogenesis- related (PR) protein genes in wounded mature tobacco leaves. *Plant Cell Physiol* **39**(5): 500-507.

Torres MA, Jones JD, Dangl JL. 2005. Pathogen-induced, NADPH oxidase-derived reactive oxygen intermediates suppress spread of cell death in *Arabidopsis thaliana*. *Nat Genet* **37**(10): 1130-1134.

Tóth R, van der Hoorn RAL. 2010. Emerging principles in plant chemical genetics. *Trends in Plant Science* **15**(2): 81-88.

Truman W, Zabala MT, Grant M. 2006. Type III effectors orchestrate a complex interplay between transcriptional networks to modify basal defense responses during pathogenesis and resistance. *The Plant Journal* **46**(1): 14-33.

Tsiatsiani L, Timmerman E, De Bock PJ, Vercammen D, Stael S, van de Cotte B, Staes A, Goethals M, Beunens T, Van Damme P, et al. 2013. The *Arabidopsis* metacaspase9 degradome. *Plant Cell* **25**(8): 2831-2847.

Tsiatsiani L, Van Breusegem F, Gallois P, Zavialov A, Lam E, Bozhkov PV. 2011. Metacaspases. *Cell Death & Differentiation* **18**(8): 1279-1288.

Tsuda K, Sato M, Stoddard T, Glazebrook J, Katagiri F. 2009. Network properties of robust immunity in plants. *PLoS Genet* **5**(12): e1000772.

ul Hassan MN, Zainal Z, Ismail I. 2015. Green leaf volatiles: biosynthesis, biological functions and their applications in biotechnology. *Plant Biotechnol J* **13**(6): 727-739.

Uren A. 2000. Identification of Paracaspases and Metacaspases Two Ancient Families of Caspase-like Proteins, one of which Plays a Key Role in MALT Lymphoma. *Molecular Cell* **6**(4): 961-967.

Van der Does D, Leon-Reyes A, Koornneef A, Van Verk MC, Rodenburg N, Pauwels L, Goossens A, Korbes AP, Memelink J, Ritsema T, et al. 2013. Salicylic acid suppresses jasmonic acid signalling downstream of SCFCO11-JAZ by targeting GCC promoter motifs via transcription factor ORA59. *Plant Cell* **25**(2): 744-761.

van Doorn WG. 2011. Classes of programmed cell death in plants, compared to those in animals. *Journal of Experimental Botany* **62**(14): 4749-4761.

Vercammen D, van de Cotte B, De Jaeger G, Eeckhout D, Casteels P, Vandepoele K, Vandenberghe I, Van Beeumen J, Inze D, Van Breusegem F. 2004. Type II metacaspases Atmc4 and Atmc9 of *Arabidopsis thaliana* cleave substrates after arginine and lysine. *J Biol Chem* **279**(44): 45329-45336.

Vlot AC, Dempsey DA, Klessig DF. 2009. Salicylic Acid, a multifaceted hormone to combat disease. *Annu Rev Phytopathol* **47**: 177-206.

War AR, Paulraj MG, Ahmad T, Buhroo AA, Hussain B, Ignacimuthu S, Sharma HC. 2014. Mechanisms of plant defense against insect herbivores. *Plant Signalling & Behavior* **7**(10): 1306-1320.

Watanabe N, Lam E. 2005. Two *Arabidopsis* metacaspases AtMCP1b and AtMCP2b are arginine/lysine-specific cysteine proteases and activate apoptosis-like cell death in yeast. *J Biol Chem* **280**(15): 14691-14699.

Watanabe N, Lam E. 2011a. *Arabidopsis* metacaspase 2d is a positive mediator of cell death induced during biotic and abiotic stresses. *Plant J* **66**(6): 969-982.

Watanabe N, Lam E. 2011b. Calcium-dependent activation and autolysis of *Arabidopsis* metacaspase 2d. *J Biol Chem* **286**(12): 10027-10040.

Wong AH, Yan C, Shi Y. 2012. Crystal structure of the yeast metacaspase Yca1. *J Biol Chem* **287**(35): 29251-29259.

Yan C, Xie D. 2015. Jasmonate in plant defence: sentinel or double agent? *Plant Biotechnol J* **13**(9): 1233-1240.

Yan S, Dong X. 2014. Perception of the plant immune signal salicylic acid. *Current Opinion in Plant Biology* **20**: 64-68.

Zeringue HJ, McCormick SP. 1989. Relationships between cotton leaf-derived volatiles and growth of *Aspergillus flavus*. *Journal of the American Oil Chemists' Society* **66**(4): 581-585.

Zhang C, Gong P, Wei R, Li S, Zhang X, Yu Y, Wang Y. 2013. The metacaspase gene family of *Vitis vinifera* L.: characterization and differential expression during ovule abortion in stenopermocarpic seedless grapes. *Gene* **528**(2): 267-276.

Zhao, Hong Xia, et al. 2003. Structural and charge requirements for antimicrobial peptide insertion into biological and model membranes. *Pore Forming Peptides and Protein Toxins*: 151-177.

Zhou Q, Krebs JF, Snipas SJ, Price A, Alnemri ES, Tomaselli KJ, Salvesen GS. 1998. Interaction of the baculovirus anti-apoptotic protein p35 with caspases. Specificity, kinetics, and characterization of the caspase/p35 complex. *Biochemistry* **37**(30): 10757-10765.

Zipfel C, Felix G. 2005. Plants and animals: a different taste for microbes? *Curr Opin Plant Biol* **8**(4): 353-360.